

10. TABLE OF CONTENTS

10. TABLE OF CONTENTS.....	10-i
10. THERMAL CONTROL SYSTEM.....	10-1
10.1 Introduction.....	10-1
10.1.1 Thermal Systems Design Drivers	10-1
10.2 Spartnik Thermal Systems Analysis and Design.....	10-4
10.2.1 Thermal Environments.....	10-5
10.2.2 Orbital Thermal Environments	10-9
10.2.3 Surface Thermal-Optical Properties.....	10-18
10.2.4 Spartnik Bulk Temperature Analysis.....	10-18
10.2.5 Spartnik Biot Number.....	10-18
10.2.6 Orbit-Average Temperatures.....	10-20
10.2.7 Spartnik Component Thermal Design Analysis.....	10-23
10.2.8 Temperature Sensor Design and Placement.....	10-25
10.2.9 SINDA Analysis.....	10-29
10.3 Construction And Assembly	10-33
10.4 TCS Testing.....	10-34
10.4.1 Thermal Control Systems Testing Industry Standards.....	10-35
10.4.2 TCS Testing Schedule	10-38
10.4.3 TCS Test Plan.....	10-39
10.4.4 San Jose State Thermal Vacuum Chamber.....	10-40
10.4.5 Thermal Transducer Testing.....	10-40
10.5 Operations	10-40
10.6 Safety.....	10-41
10.7 Conclusions	10-41
10.8 Reference List.....	10-41
10.9 Appendices.....	10-42
10.9.1 Discussion of Thermodynamic and Heat Transfer Theory Used in Analysis.	10-42
10.9.2 Heat Transfer Analysis Methods	10-56
10.9.3 Panel-Wise Heat Rate Calculations.....	10-56
10.9.4 SINDA Analysis.....	10-66
10.9.5 SINDA 3D Analysis	10-82
10.9.6 Thermal Transducer Test Results	10-85
10.9.7 Glossary of Thermal Control Systems Terms and Acronyms:	10-95
10.9.8 Materials and Company Contact Information.....	10-99

10. THERMAL CONTROL SYSTEM

10.1 Introduction

The Spartnik Thermal Control Systems (TCS) will maintain the temperatures of all of Spartnik's components within acceptable ranges for the life of the spacecraft. TCS will insure that the design will function with minimum modifications in all possible thermal environments. Additional design drivers include data acquisition requirements, launch and ascent environments, and operational conditions.

Temperature variances in variable-angle orbits can be minimized, but not eliminated without resorting to active thermal control methods. These orbits represent the extreme operating envelope of the thermal control system. Although Spartnik is designed with maximum orbital flexibility, some orbits will exceed operating thermal limits.

Guidance was sought from Lockheed Martin in performing adequate thermal analysis. Lockheed Martin provided results for numerical calculations that were beyond the resources of the undergraduate Spartnik project. Lockheed Martin project mentors also provided TCS personnel with extensive training specific to spacecraft thermal control systems. The remainder of the calculations and all documentation were subsequently completed by TCS personnel.

10.1.1 Thermal Systems Design Drivers

The thermal design of Spartnik must consider five categories of design drivers. Design drivers include temperature constraints on components, data acquisition requirements, orbital environments, launch and ascent environments, and operational conditions. Each category is discussed here separately in detail.

10.1.1.1 Temperature Constraints on Components

The following temperature constraints were specified for each component (Table 10-1 and figure 10-1). The respective subsystem teams provided these constraints.

Each set of constraints contains an upper and a lower bound on absolute operating temperature. The component may neither be operated nor stored outside of these temperature ranges without damage to the component. Spartnik's thermal design must not allow any component to exceed absolute operating temperature ranges.

Component temperature constraints also contain an upper and a lower bound of each component's preferred operating temperature range. Components operate most efficiently and effectively when preferred operating temperatures are maintained. In addition, component life span will be degraded by either operating or storing the component outside of its preferred temperature range. Therefore, in order to maximize the mission life of each component, Spartnik's thermal design must keep all components operating temperature within preferred temperature ranges. In addition, components must be stored within preferred operating temperatures whenever it is both possible and reasonable to do so.

The two notable component temperature constraints are on the battery and the camera. The camera is neither space-rated nor mil-spec. The camera is designed to operate at standard

atmospheric conditions and may be damaged by operation or storage at lower temperatures. The battery must be maintained in absolute temperature ranges at all times.

Table 10-1 lists temperature ranges for representative Spartnik’s components. Figure 10-1 plots these same temperature ranges graphically.

Further reference to Spartnik’s thermal design “operating” will refer to maintaining all component temperatures within each component’s required temperature range listed below.

Table 10-1 Spartnik Component Temperature Limits

<i>System</i>	<i>Equipment</i>	<i>Temperature Limits in Celsius</i>			
		Absolute Lower	Desired Lower	Desired Upper	Absolute Upper
Power	Battery Cell	-5	0	10	25
	Solar Array	-100	-10	25	100
	Regulator	0	0	25	25
Payload	Kodak CCD Camera	-20	0	40	60
	MMID	-40	-20	30	80
Communications	Receiver Board	-40	-20	30	90
	Antenna	-40	-20	30	90
ADAC	Horizon Sensor	-30	-20	30	50
	Bar Magnets	-40	-20	30	50
	Nutation Damper	-40	-20	30	50
	Hysteresis Rods	-100	-20	30	100
	Solar Paddles	-100	-20	30	100
Computer	Computer Board	-40	-20	30	85
Structures	Aluminum 6061 T4	-100	-30	30	100

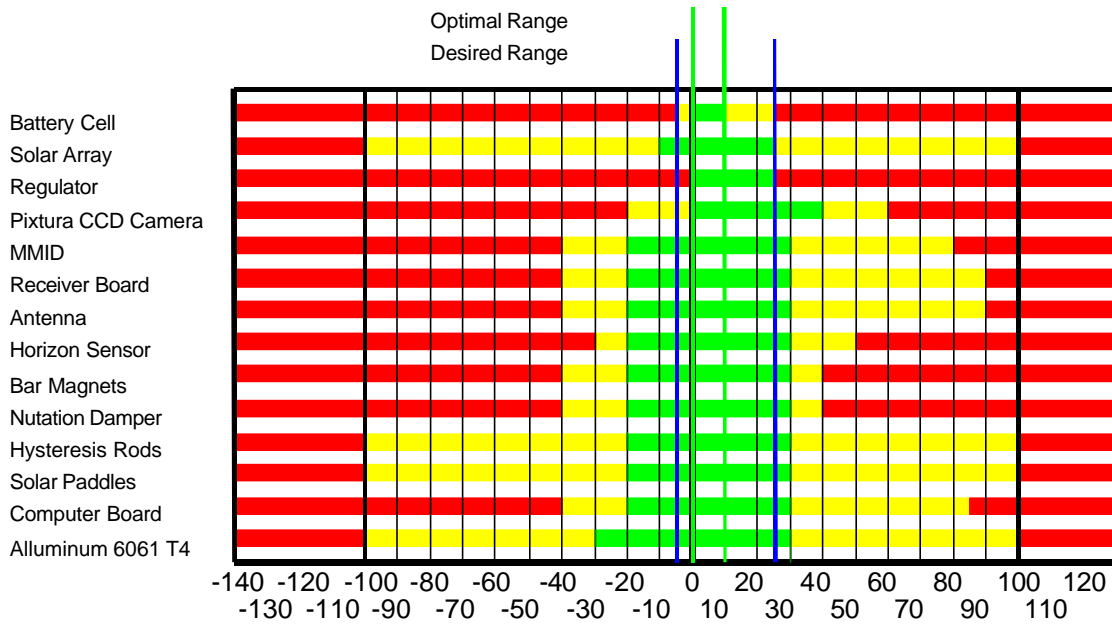


Figure 10-1 Spartnik Component Temperature Limits

10.1.1.2 Thermal Systems Data Acquisition Requirements

The following thermal data acquisition tasks will be required:

- Temperature-voltage data on orbit from Spartnik’s batteries.
- Operational temperature data as deemed necessary for thermal maintenance of the spacecraft.
- Experimental temperature data as deemed appropriate by TCS.

10.1.1.3 Orbital Environments

Spartnik will be launched on a donated or sponsored flight. The design team may not rely on a single launch provider. Therefore Spartnik must be able to function thermally in the widest possible range of orbits with minimum modification to the spacecraft.

For each orbit condition, Spartnik must operate within the above specified component temperature ranges. Spacecraft heat loads must be calculated for each orbit. Primary terms of the heat load will include solar incident, albedo, and Earth generated thermal radiation.

10.1.1.4 Pre-Orbital Environments

Spartnik's thermal design must ensure mission integrity in pre-orbital environments. Pre-orbital environments include spacecraft manufacture, assembly, storage, testing, transport, fairing mounting, ascent, and deployment.

TCS must review all manufacturing assembly instructions to ensure no procedures will be used that would thermally damage spacecraft components. TCS must also review all questionable storage facilities, shipping methods, testing procedures, and payload fairing mountings for excessive thermal environments. TCS must also insure spacecraft survivability of the ascent and deployment phase of each prospective launch vehicle and primary payload arrangement.

10.1.1.5 Operational Conditions

Spartnik's thermal design must operate under a variety of internal power allocation modes. Some possible modes are listed in Table 10-2. For purposes of thermal analysis, all energy allocated to a component is assumed to be converted perfectly into heat unless the energy is radiated as through the communications antennas.

Table 10-2 Maximum Heat Generation by Powered Systems

Powered System	Maximum Operational Heat Load in Watts
Kodak CCD Camera	1 per picture
Micro-Meteorite Impact (MMI) Board	1
Communications Transponder	0.055
Computer Board	1
Battery Pack	6

10.2 Spartnik Thermal Systems Analysis and Design.

The design and analysis section of this report proceeds through three phases:

1. Consideration will be given to the thermal environments Spartnik will encounter.
2. Bulk thermal design and analysis results of Spartnik will be presented.
3. Thermal analysis and design of Spartnik's components will be discussed.

These design phases will be presented in the sections to follow.

10.2.1 Thermal Environments

The spacecraft will encounter many thermal environments during its lifetime. These include but are not limited to manufacturing, storage, shipping, testing, launch-vehicle installation, ascent, deployment, orbital operations, orbit decay, and re-entry. Each environment and its matters of concern to TCS is discussed separately below.

10.2.1.1 *Manufacturing*

During manufacturing, Spartnik and its components will experience thermal environments consisting of various machine shops, labs and suppliers. Spartnik currently carries no equipment or materials that would be damaged by exposure to standard atmospheric temperatures or pressures. It is assumed that the various machine shops, laboratories and suppliers are equipped to properly handle materials with respect to thermal environments. Part sources and maintenance history will be tracked.

10.2.1.2 *Storage*

It is assumed that most of Spartnik's components will be stored at room temperature, an environment deemed thermally safe for most systems. TCS is aware of several materials used in manufacture that require refrigerated or frozen storage. Table 10-3 lists thermally volatile materials and their recommended storage temperatures.

Table 10-3 Thermally Volatile Materials and Storage Temperatures

Material	Storage Temperature
LOCKIT 411	33-40 deg F
Batteries (Flight Set)	0-10 deg C

10.2.1.3 *Shipping*

The required thermal shipping environment for each material is observed and documented upon receipt of the material from the manufacturer or supplier. Currently, the Spartnik project possesses no known materials that are sensitive to exposure to standard atmospheric pressures and temperatures on shipping.

Therefore, shipment of an assembled spacecraft or any sub-assembly must be done as to not expose the assembly to temperatures outside of a -32 degree F to 90 degree F temperature range.

10.2.1.4 *Testing*

Thermal Control Systems reviewed the thermal environment for Structures' shake test and EPS's battery temperature-voltage calibration test. The shake test was found to take place in standard atmospheric conditions, with substitute masses used for all temperature sensitive equipment. Battery testing thermal analysis is presented below.

Further TCS-specific tests are scheduled in the TCS Testing section below for the spring semester. Testing procedures and thermal analysis will be included in this section for these tests as test planning and analysis is completed.

10.2.1.5 Launch Vehicle Payload Fairing Installation

It has been concluded from a survey of launch vehicle handbooks that all payload fairings are air-conditioned to between 70 and 90 degrees F. When flight-ready, Spartnik will contain no materials that are subject to damage from exposure to these temperature ranges.

10.2.1.6 Ascent

Ascent will expose Spartnik to three environmental factors:

- A sudden disappearance of atmosphere, and resulting non-constant pressure transient convection.
- Radiation exchange with internal fairing components operating around 400 degrees Celsius.
- Free-molecular heating from the upper atmosphere, following payload fairing jettison.

Calculations involving variable pressure transient conduction will not be performed. It is assumed that the atmosphere and the spacecraft will be in relative thermal equilibrium during the ascent. Under these conditions, the venting of atmosphere will reduce the spacecraft's thermal mass without affecting the spacecraft temperature.

The following payload fairing temperature histories were provided for the Atlas launch vehicle family¹. The fairing is heated during ascent by aerodynamic friction, thermally loading the spacecraft within the first 200 seconds of flight. Around 200 seconds flight time, the fairing is jettisoned, introducing free molecular heating. This heat load pattern is considered typical for most launch vehicles and is shown in Figure 10-2 below.

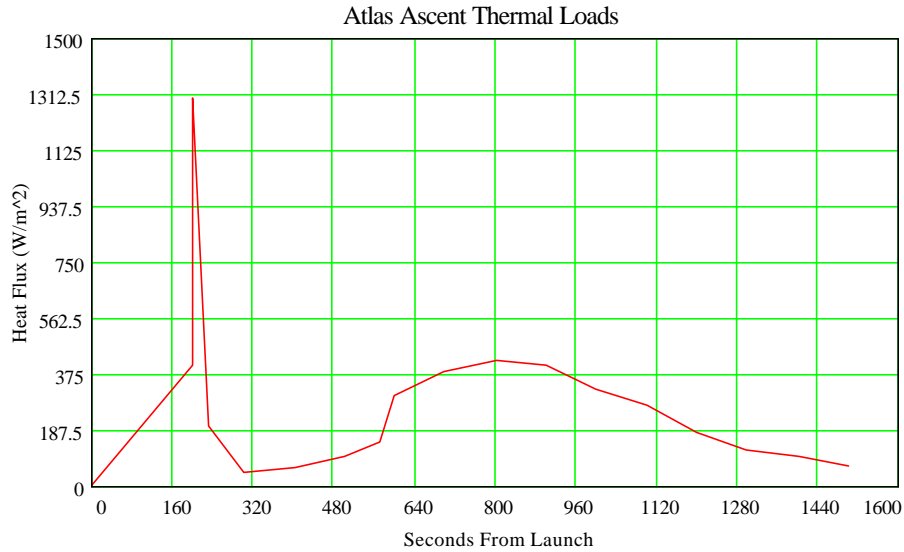


Figure 10-2 Ascent Thermal Loads Ascent

10.2.1.7 *Deployment*

During deployment, Spartnik may experience at most a three-day spinning-up period. Magnetic lock will occur relatively quickly, providing full tumble at launch vehicle separation. However, in a non-spinning case, one face may still be continuously exposed to the Sun, possibly generating a hot spot, or cold spot on space-exposed sides.

The following calculation, shown in Figure 10-3, estimates solar panel temperature as a function of percentage of time exposure to direct sunlight. No earthshine or internal power heat loads are used. A 10 degree rise is therefore expected between these numbers and the real temperatures. Operational spin rates of one rotation every two minutes give temperatures of 20-30 degrees in a subsequent analysis. This spin rate corresponds to 1/8 time exposure for any one panel. Maximum panel temperatures are reached at five times this exposure, placing required minimum spin rates at one rotation every ten minutes.

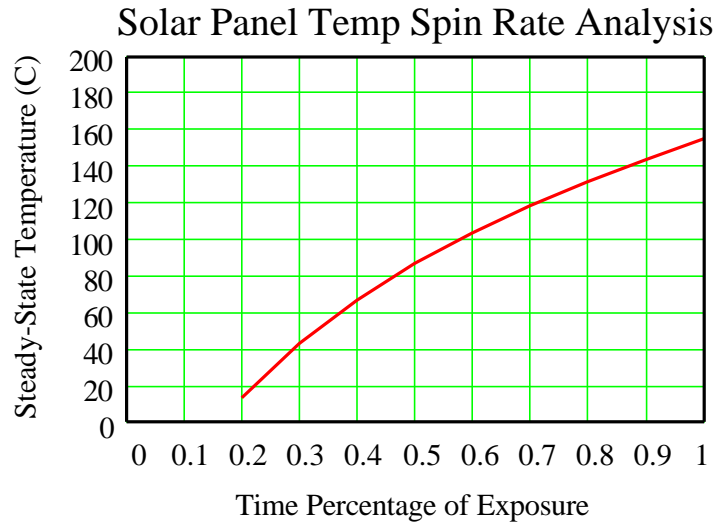


Figure 10-3 Solar Panel Time Exposure vs. Temperature

10.2.1.8 *Orbital Decay*

Without station-keeping propulsion systems, Spartnik’s orbit may decay due to atmospheric drag. This process will be used as the de-orbit mechanism for Spartnik since no propulsion system will be carried aboard.

As calculated below under Attitude Determination and Control Hardware analysis, Section 10.2.7.2, orbit decay atmospheric drag produces negligible heat loading on the outer surfaces of the spacecraft. Spartnik will therefore be able to operate normally within a two-year nominal orbit as per mission requirements.

Spartnik will be launched with a set-size Flexible Optical Solar Reflector (FOSR) radiator scaled to a two-year nominal orbit. Orbit decay into lower than design orbits will include:

- An increase in Earth-infrared heating calculated in section.
- Negligible effect on solar radiation heat loads.
- An increase in external atmospheric drag.
- A decrease in FOSR radiator effectiveness.

The result of these effects will be that Spartnik will run hotter and with stronger transient thermal fluctuations after its two year mission.

10.2.1.9 *Reentry*

As Spartnik’s orbit decays, it will begin a skip-reentry. The most thermally vulnerable component to atmospheric damage is the deployed communications antennas. Depending on the condition of the antennas, experiments may be conducted on the high-atmosphere behavior of the remainder of Spartnik’s passive thermal control system. It is recommended that these experiments be defined based on the orbit-decay performance of Spartnik and its components.

When Spartnik's orbit finally reenters the atmosphere, deployed communications antennas will be incinerated. No contact with the remaining craft will be possible.

10.2.2 Orbital Thermal Environments

The final orbit of Spartnik is not known at this time. Parametric studies were done on a range of possible orbits to determine thermal environmental loading. Three major loads were considered: direct solar radiation, Earth-reflected solar radiation, and Earth-generated radiation.

The following heat transfer modes and sources were considered negligible in this calculation:

- incoming radio signals
- moon albedo
- moonshine
- solar wind (positive charged particles)
- atmospheric drag
- starlight
- background thermal radiation @ 7 Kelvin (cosmic)
- cosmic rays (gamma)
- micrometeoroids
- material outgassing
- thermal radiation exchange with other orbiting objects
- eddy-current structural and electronic component heating
- charged particle heating

Resources permitting, calculations quantifying each of these heat load sources will be done to prove that these sources can be neglected. In addition, it is assumed that Spartnik:

- orbits in a circular LEO orbit for all cases
- experiences constant spin rate of two minutes per revolution
- experiences a constant tumble rate of two tumbles every orbit

Figure 10-4 illustrates these assumptions. Near circular orbits are required in LEO for obvious reasons. Spin rate is realistically constant at the stated rate, based on Attitude Determination and Control system design's predictions. Constant tumbling of the spacecraft is based on the influence of the bar magnets. Actual tumble rates will vary.

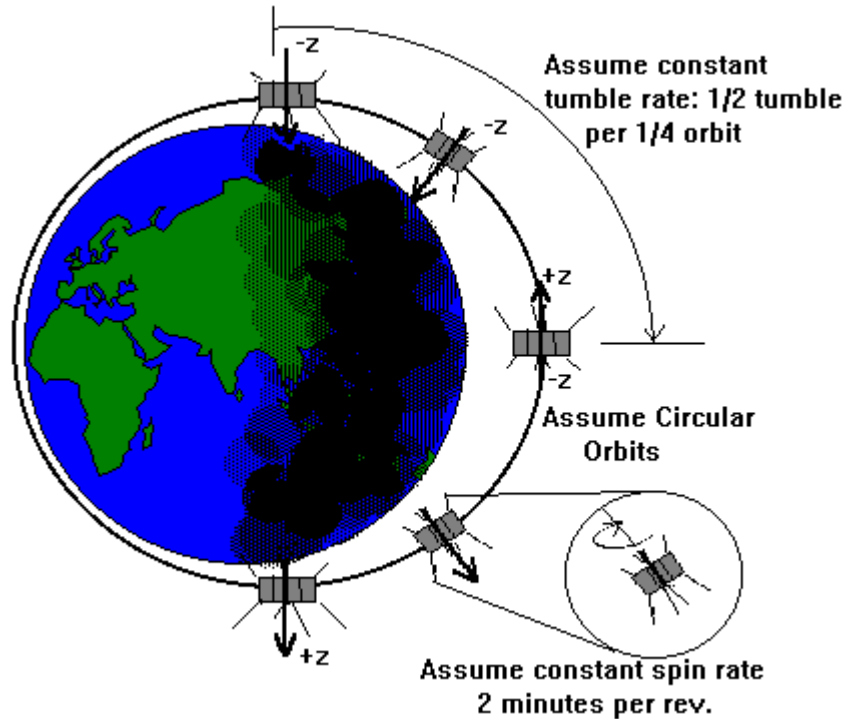


Figure 10-4 Orbit Thermal Analysis Attitude Assumptions

In accordance with these assumptions, heat load calculation results may be simplified without sacrificing information. It is assumed that Spartnik's spin rate is much faster than its tumble rate. This allows for the heat loads of the non-spinning panels to be averaged or mapped to the actual heat loads of the spinning model. Calculation time intervals will be set to equal the time required for one side panel to rotate to the next panel.

In addition to assumptions made about the heat transfer modes and orbit orientation, simplifying assumptions were made about the spacecraft geometry. For a first calculation, it is assumed that the deployed antenna array is both thermally isolated and does not cause radiation heat transfer interference or interaction with the rest of the spacecraft. Time permitting, these view factors will be calculated and shown to be negligible.

Figure 10-5 displays the surface panel model and panel numbering. Side panels are numbered 10 to 80 by 10. Positive and negative z-axis panels are numbered 200 and 100 respectively. Room was allowed in the numbering scheme for future discretizations of the model into more numerous, smaller panels. Panels 200 and 100 map to standard Spartnik side labeling scheme sides 9 and 10 respectively.

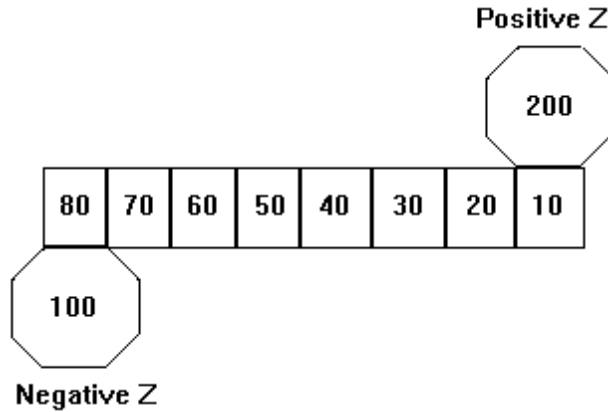


Figure 10-5 Heat Rate Calculation Panel Geometry and Numbering

No simplifying assumptions were made regarding incident orbital heat rates. Figure 10-6 shows the three orbital heat loads calculated.

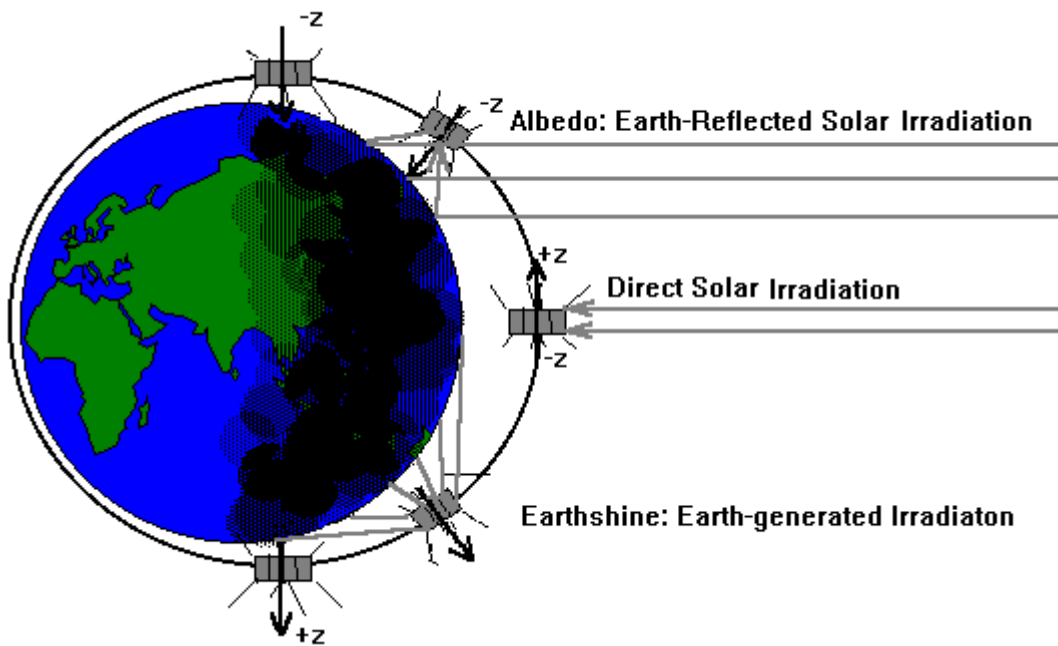


Figure 10-6 Earth-Orbit Heat Loads

Solar radiation is considered collimated outside the Earth's atmosphere. Solar radiation fluctuates throughout the year with the orbital radius of the Earth. An average value of 1350 W/m^2 was used in the calculations.

Earth-generated thermal radiation, Earthshine, is non-collimated, originating from a large solid angle view from the spacecraft. To find the total Earthshine heat loading on a surface, differential surface contribution to Earthshine must be integrated over the entire surface of the Earth facing the sun. Because of the directional nature of Earthshine, this integration must be done

separately for each face of the spacecraft for each orientation at each point on the orbit. Figure 10-7 illustrates the discretizations used to perform this integration numerically.

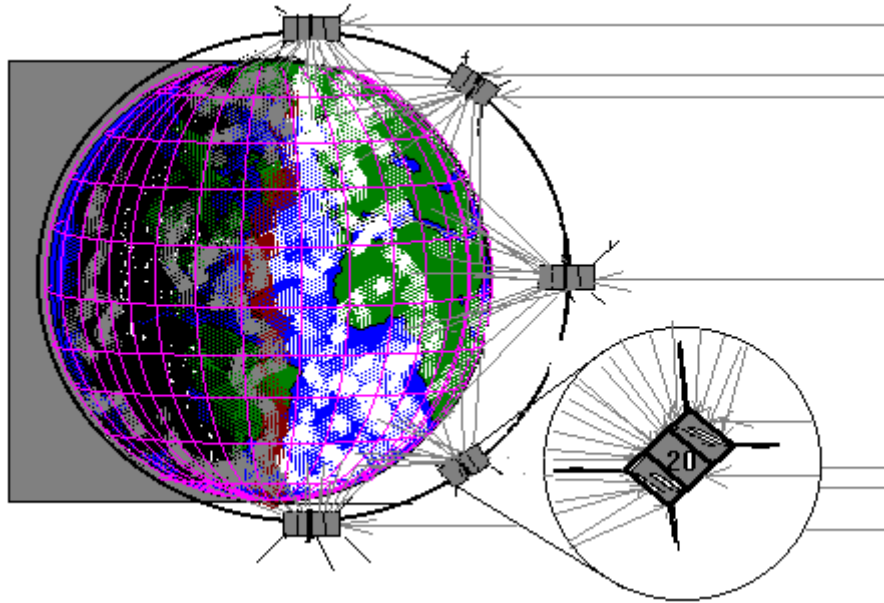


Figure 10-7 Discretization of Model

Direct solar radiation, the largest orbital heat load, is the primary concern when classifying orbits according to their thermal characteristics. Orbital beta-angle, a new orbital element, is introduced to help classify orbits, both for thermal and for power generation concerns. The beta-angle of an orbit is the minimum angle measured from the solar vector to the orbit plane. The beta angle, together with altitude, primarily characterizes the Earth-shadowing time periods of missions in orbit. For low beta-angle orbits, the spacecraft will experience the maximum Earth-shadowing on every orbit. These low-beta orbits are termed ‘cold’ orbits because they have the lowest average solar heat loading. For high-beta-angle orbits, the spacecraft may experience little or no Earth-shadowing. These higher beta angles are termed ‘hot’ orbits because they have the highest average solar heat loading. Variations of beta angle vary the time periods of the solar lit and shadowed portions of the orbit. “Critical beta angle” refers to the beta angle at which the orbit just grazes the umbra. Figure 10-8 illustrates several beta angles and their geometric relationship to Earth-shadowing.

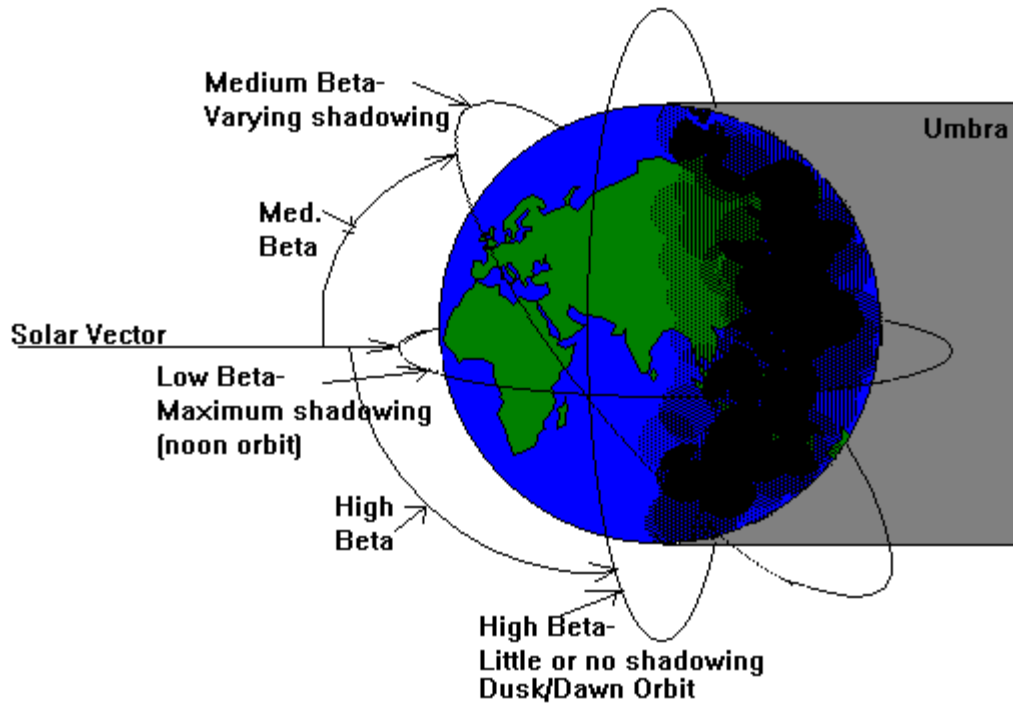


Figure 10-8 Beta-Angles and Earth Shadowing

Beta-angles are limited by orbit inclination. Higher beta angles are not possible with lower inclination orbits. For Spartnik's ability to fly in an unspecified orbit, the entire range of beta-angles must be studied. Calculations were then made at altitudes of 300 and 700 kilometers to bracket expected orbit altitudes.

At each altitude, calculations were performed for 0, 30, 60, and 90 degrees beta angle. In addition, calculations were performed at critical beta angle. It is expected that the orbital elements for a given launch can be mapped to these beta angle ranges.

Figure 10-9 displays the results of one of the panel-wise orbit heat rate calculations. The raw data used for the calculations was provided by Lockheed Martin. The entire set of graphs can be found in Appendix 10.9.3.

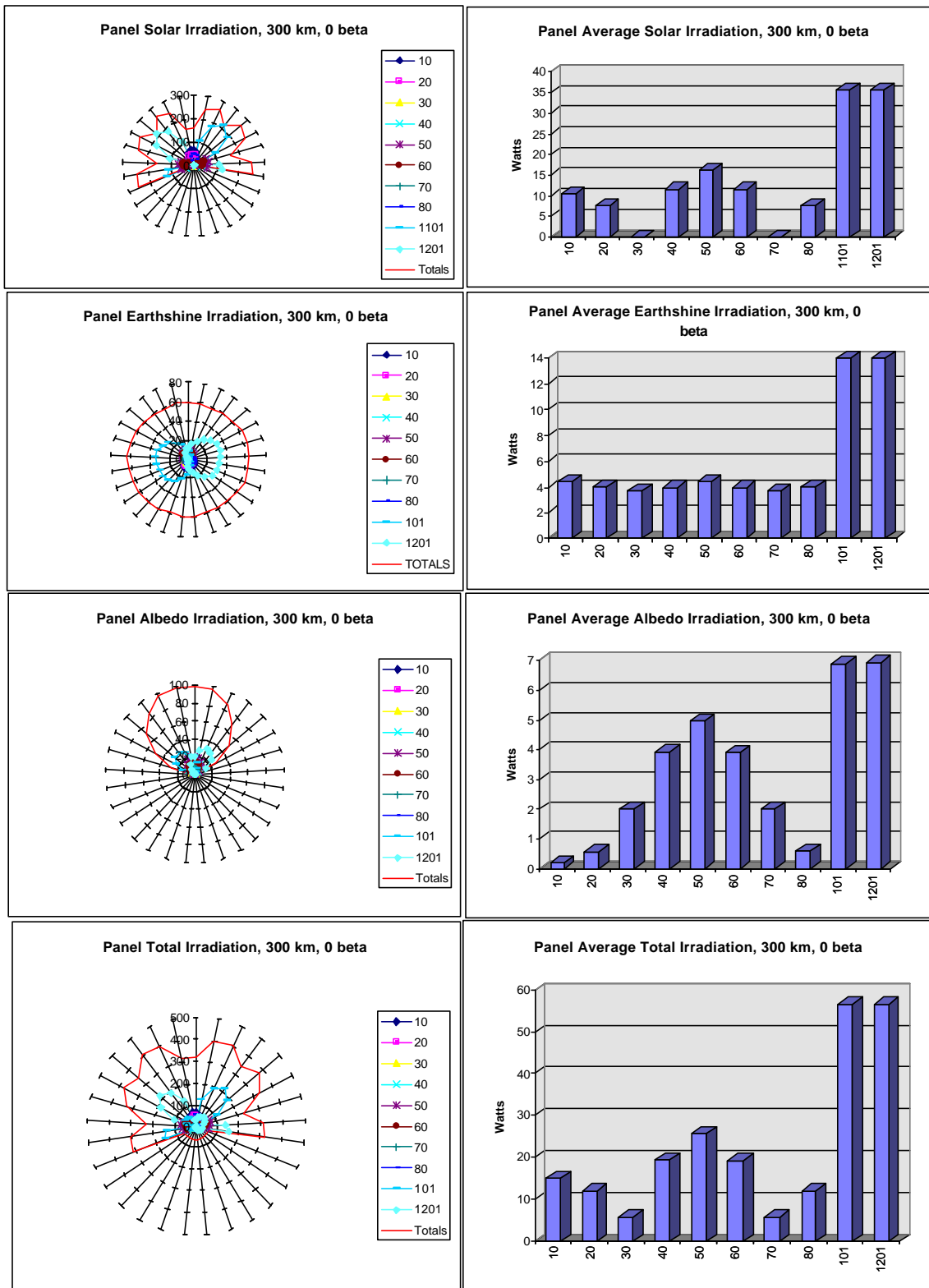


Figure 10-9 Orbit Heat Rates by Panel Number, 300 km, 0 deg beta

Several conclusions affecting Spartnik's thermal design can be drawn from these graphs:

- Top and bottom decks receive the bulk of all types of irradiation. This is due to the relative surface areas of the panels and decks. As a further conclusion drawn from these plots, the location of any thermal surface property design should be the upper and lower decks. Attempting to modify the side panels for thermal purposes would not yield satisfactory results.
- Solar irradiation is extremely variable.
 1. As Spartnik tumbles, it exposes a variable projected surface area to the Sun, creating variable total solar irradiation, even when traveling through the lit side of the orbit.
 2. As Spartnik travels around the orbit, it encounters the umbra on low beta angle orbits. This introduces a step-function into solar irradiation vs. time.
 3. The umbra characteristics of the orbit change drastically with increasing beta angle. At 90 degrees beta angle, the spacecraft encounters nearly constant solar irradiation.
- Earthshine irradiation is a constant source of heat. Radiation coupling Spartnik with the Earth would provide the most stable temperatures. Earthshine is of smaller magnitude than solar radiation.
- Albedo is nearly negligible. Albedo should therefore be considered part of solar radiation, as they are of the same wavelength.

Values for 500 km altitude orbits may be safely linearly interpolated between the 300 km and the 700 km altitude orbits provided by Lockheed Martin.

In order to expose further trends in the data, additional plots are presented. The following two figures, Figures 10-10 and 10-11, plot all irradiation loads and combinations of irradiation loads as a function of beta angle. Symmetry of the orbits was used to generate the entire range of beta angles. Only average values were used, to study trends of irradiation sources with varying beta angles.

Beta Angle (deg)	Average Bulk (W)- 300 km Orbits				
	Solar	Albedo	Earthshine	Total	Solar/Albedo
0	136.0372	31.9598	60.3091	228.3061	167.997
30	146.6662	27.5706	60.3016	234.5384	174.2368
60	158.0891	16.09967	60.2655	234.4543	174.18877
73	205.1052	9.591058	60.268	274.9643	214.696258
90	161.578	2.28025	60.1937	224.052	163.85825
108	205.1052	9.591058	60.268	274.9643	214.696258
120	158.0891	16.09967	60.2655	234.4543	174.18877
150	146.6662	27.5706	60.3016	234.5384	174.2368
180	136.0372	31.9598	60.3091	228.3061	167.997
210	146.6662	27.5706	60.3016	234.5384	174.2368
240	158.0891	16.09967	60.2655	234.4543	174.18877
252	205.1052	9.591058	60.268	274.9643	214.696258
270	161.578	2.28025	60.1937	224.052	163.85825
288	205.1052	9.591058	60.268	274.9643	214.696258
300	158.0891	16.09967	60.2655	234.4543	174.18877
330	146.6662	27.5706	60.3016	234.5384	174.2368

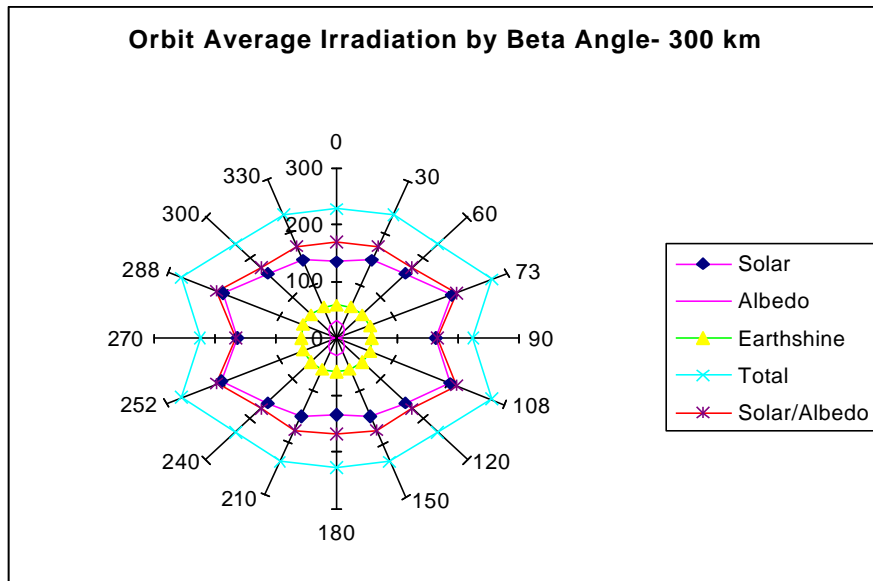


Figure 10-10 Avg. Irradiation Sources as Function of Beta Angle- 300 km Circular LEO Orbits

Although these plots were not generated to angular scale, they highlight various important trends in orbital thermal environments.

These plots show orbits passing through the umbra as relatively constant, relatively cool orbits overall. On these orbits, high solar irradiation on the lit side is balanced with time in the umbra.

Beta Angle (deg)	Average Bulk (W)-700 km Orbits				
	Solar	Albedo	Earthshine	Total	Solar/Albedo
0	145.7786	25.1954	48.0115	218.9855	170.974
30	158.9916	21.9239	48.0369	228.9524	180.9155
60	188.9073	12.93433	48.0159	249.8575	201.841632
64	219.6072	11.10916	48.6882	279.4046	230.716358
90	161.578	3.361258	48.0579	212.9972	164.939258
116	219.6072	11.10916	48.6882	279.4046	230.716358
120	188.9073	12.93433	48.0159	249.8575	201.841632
150	158.9916	21.9239	48.0369	228.9524	180.9155
180	145.7786	25.1954	48.0115	218.9855	170.974
210	158.9916	21.9239	48.0369	228.9524	180.9155
240	188.9073	12.93433	48.0159	249.8575	201.841632
244	219.6072	11.10916	48.6882	279.4046	230.716358
270	161.578	3.361258	48.0579	212.9972	164.939258
296	219.6072	11.10916	48.6882	279.4046	230.716358
300	188.9073	12.93433	48.0159	249.8575	201.841632
330	158.9916	21.9239	48.0369	228.9524	180.9155

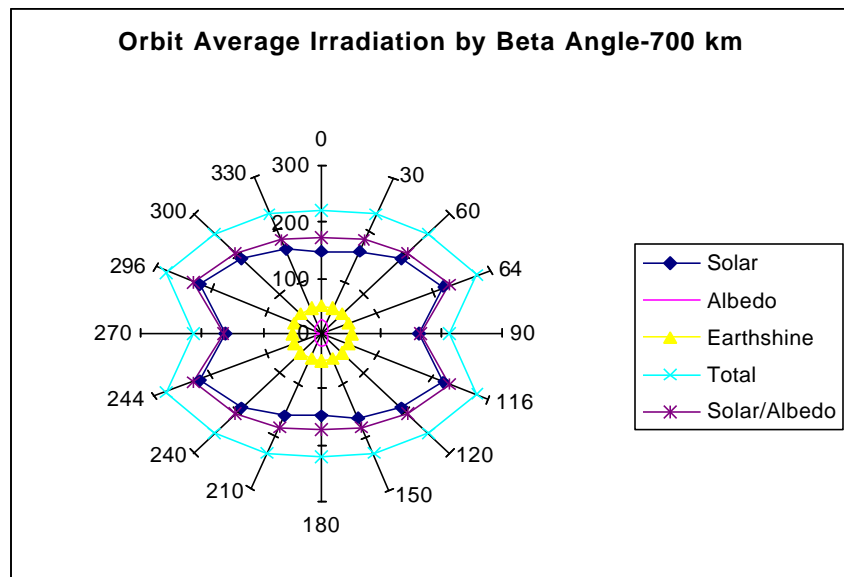


Figure 10-11 Avg. Irradiation Sources as Function of Beta Angle- 700 km Circular LEO Orbits

Normally, 90 degree beta angle orbits (dusk-dawn orbits) are considered the hottest orbits. However, due to the “tuna-can” shape of Spartnik, being edge-on and exposing minimum area to the Sun, dusk-dawn orbits may be as cool as umbra-passing orbits. Statically, these are the best orbits for Spartnik, giving continuous illumination of Spartnik’s solar cells with minimum solar heat loading.

These plots also show overall average irradiation remains relatively constant, with the exception of orbits approaching and including the critical beta angle. Near-critical beta angle LEO orbits experience as much as a 10% increase in solar wavelength irradiation. At critical beta angle, Spartnik has lost its “tuna-can” edge experienced at 90 degree beta orbits. The critical beta angle orbit exposes the spacecraft to solar loading at all points of the orbit. These factors combine to produce the hottest orbits for Spartnik.

It should also be noted here that Spartnik is expected to experience as much as ten degrees of nutation while on orbit. This nutation will expose portions of the top and bottom surfaces in dusk-dawn orbits, negating the “tuna-can” effect. These orbits should therefore be thermally considered as the average of surrounding beta-angle orbits.

10.2.3 Surface Thermal-Optical Properties

The next step in determining Spartnik’s orbital operating temperatures is to determine thermal optical surface properties. In spacecraft thermal control, two properties dominate the calculation: solar absorption, and infra-red emittance. Solar absorption determines the fraction of incident solar irradiation that is absorbed by the surface. The Stefan-Boltzmann law dictates that radiative heat exchange with the environment is dominated by the emmissivity of the surface in question.

Planck’s black body radiation spectral distribution states that solar radiation is necessarily shifted lower in wavelength than normal temperature. Because many thermal-optical surface properties are functions of wavelength, it becomes possible to selectively absorb or reject either solar irradiation or Earthshine, respectively.

“In spacecraft thermal design, wavelength-dependent thermal control coatings are used for various purposes. Solar reflectors such as second-surface mirrors and white paints or silver-or aluminum- backed Teflon are used to minimize absorbed solar energy, yet emit energy almost like an ideal black body. To minimize both the absorbed solar energy and infrared emission, polished metal such as aluminum fowl or gold plating is used. On the interior of the vehicle, if it is desired to exchange energy with the compartment and/or other equipment, black paint is commonly used. Thus, the existing state of the art uses a rather wide variety of wavelength-dependent coatings. The problems of in-space stability, outgassing, and mechanical adhesion to the substrate are all problems that have been resolved for most coatings. There are many fully qualified coatings, so development and qualification of a new coating for a new design is normally unnecessary.”²

10.2.4 Spartnik Bulk Temperature Analysis.

As a first step in the analysis of Spartnik, bulk steady-state on-orbit temperatures will be calculated. A Biot number, defined below, is first calculated for the spacecraft to validate the use of bulk temperatures.

10.2.5 Spartnik Biot Number

In heat transfer analysis, it would be expedient to consider the spacecraft as an isothermal body. To validate this assumption, the Biot number will be approximated.

The Biot number is a ratio of the object’s ability to conduct heat to the rate at which heat can be transmitted into or out of the object’s surface. Biot number calculation is dependent on the object’s material composition, size and construction. Biot numbers are also dependent on the heat transfer ability of the environment/object interface.

The heat transfer abilities of the object/environment interface are a function of the temperature gradient between the object and the environment. However, the environment in heat transfer problems is usually considered large and capable of providing or absorbing unlimited quantities of heat at a constant temperature. Therefore, the object/environment interface heat transfer ability is reduced to a function of only the object's bulk (same as surface with the isothermal assumption) temperature. In conclusion, Biot numbers will vary with the temperature of the object in question.

It is generally considered appropriate to consider objects as isothermal for Biot numbers less than 0.1. Objects with these Biot numbers can equalize internal temperatures by conduction an order of magnitude faster than local temperatures can be increased by heat transfer with the environment.

Because Spartnik is a microsatellite, small by comparison to most commercial or military satellites, it is presumed that the Biot number will be below the 0.1 required to validate the isothermal assumptions. The environments TCS is concerned about future transient temperature calculations are in atmosphere, during ground testing and installation; and on orbit. Thermal calculations in the ascent environment will be assumed to be bound at either end by these two atmospheric extremes.

Figure 10-13 displays the results of an actual calculation of Spartnik's Biot numbers. The first graph displays Biot numbers in the atmospheric environment, with conduction present. The second graph displays Biot numbers in the orbital environment, with radiation exchange, but no conduction. The following temperature assumptions were made for these calculations:

$T_{sur.pad} = 300\text{-K}$	Temperature of the surroundings on pad
$T_{sur.asc} = 500\text{-K}$	Temperature of surroundings on ascent
$T_{sur.space} = 4\text{-K}$	Temperature of surroundings on orbit

Figure 10-12 Temperature Assumptions

Temperature of the spacecraft was varied from 200 K to 400 K as shown on the x-axis of both graphs. Surface radiation emissive properties were varied from 0 to 1 as shown on the y-axis of both graphs.

Biot numbers on both graphs are an additional order of magnitude lower than required to validate isothermal structure assumptions. Only under conditions of small temperature differences in atmosphere does the Biot number approach 0.1. These results strongly support the validity of bulk temperature analysis for the steady-state case and lumped capacitance methods for transient analysis, both for ground and on-orbit environments.

It must be noted that these results are valid for the *structure* of Spartnik. Electronic components and payloads mounted on stand-offs from the structure will require additional analysis to determine temperatures.

Significant gains in component temperature calculation simplification have still been made by Biot number support. The batteries may be assumed to be operating at spacecraft bulk temperatures because the battery box is strongly coupled with the structure and accounts for a large fraction of the spacecraft's total thermal mass. During the temperature calculations for components

mounted with stand-offs, spacecraft bulk temperatures may be assumed to be present at the base of all stand-offs and in any solid aluminum housings.

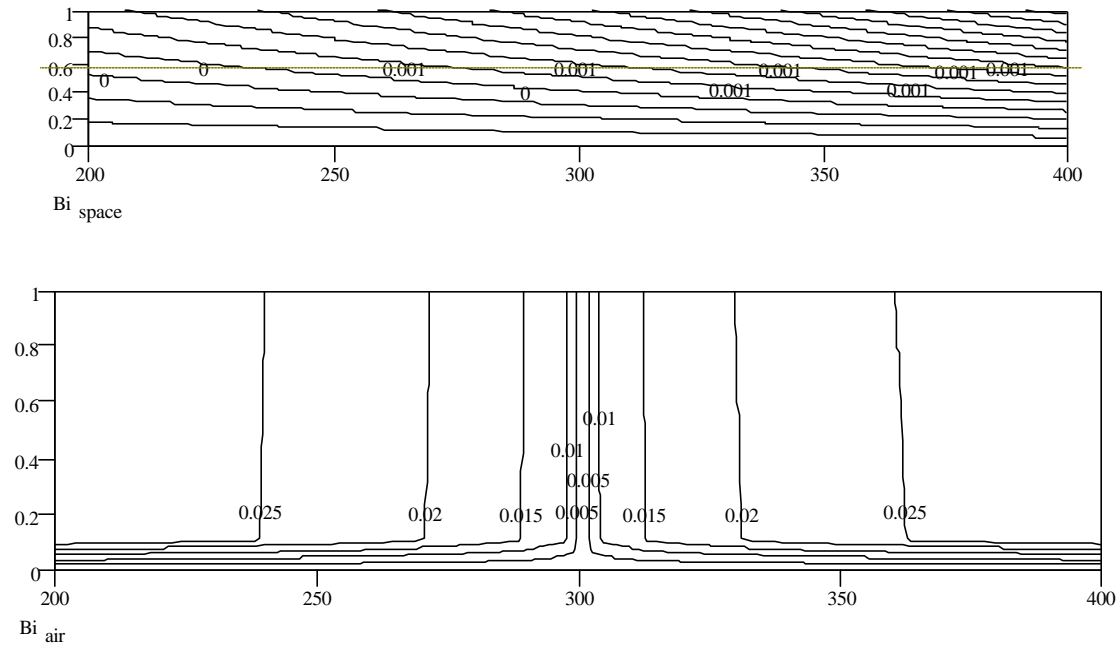


Figure 10-13 Spatnik Biot Number Results

10.2.6 Orbit-Average Temperatures

A steady-state bulk-temperature analysis was performed on the Spatnik as a first approximation of spacecraft orbit temperatures. In this calculation it is assumed that the spacecraft:

- Has no ability to store heat (steady-state)
- Is isothermal.

Figure 10-14 illustrates the consequences of these assumptions. Together these assumptions state that the transient temperature effects of entering and exiting the umbra are negligible or can be averaged out. In a continuation of the stated isothermal assumption, the top and bottom z-faces are assumed to be isothermal. Future models will discretize these faces to allow for slightly different properties due to the presence of payloads.

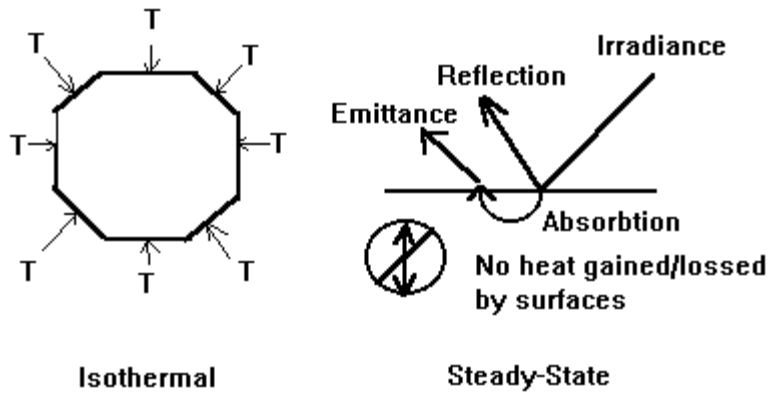


Figure 10-14 Orbit Average Temperature Spacecraft Assumptions

Accordingly, an energy balance is done on the surface of the spacecraft. It is possible to solve for the temperature of the spacecraft because heat transfer rates at the surface of the spacecraft are dependent on surface (equal to bulk in isothermal analysis) temperature.

Data from the above orbital thermal environment heat loading calculations, Section 10-2.2, were used as the input to this calculation.

Table 10-4 lists surface properties used in the model. Surface areas covered by the various materials were used to form a weighted average solar emmissivity and Earth infrared absorbtivity over the entire spacecraft surface. Both hot and cold cases were used on each studied orbit.

Table 10-4 Surface Property Estimates

Material	Worst Cold Absortivity	Absortivity BOL	Absortivity EOL	Emmissivity
Ag-FOSR, 5 mil	0.06	0.09	0.13	0.8
Al-FOSR, 5 mil	0.11	0.14	0.19	0.8
Diffuse Al-FOSR				0.8
Al tape	0.12	0.13	0.17	0.04
Flat Black Silicone Paint CV 1146	0.95	0.97	0.95	0.89
Bare Al		0.20~0.28	0.20~0.33	
Flat White Silicone Paint S13G/LO	0.2	0.24	0.4	0.88
Solar Array (GaAs)				
Not Producing Power	0.87	0.87	0.87	0.81
Producing Power	0.71	0.71	0.8	0.88
Black-Anodized Al			0.8	0.88

In order to provide information for subsequent microsatellite design, parametric studies were done on Spartnik geometry with 0-100% FOSR coverage. However, only about 20% of Spartnik's surface area is actually available for this use. The results of this calculation are given in Figure 10-15 on the following pages.

percent FOSR	TEMPERATURE (°C)								
	300 Km $\beta=83.5$	300 Km $\beta=0$	300 Km $\beta=-36$	500 Km $\beta=83.5$	500 Km $\beta=0$	500 Km $\beta=-36$	700 Km $\beta=83.5$	700 Km $\beta=0$	700 Km $\beta=-36$
0	30.88	2.18	25.69	29.36	0.13	24.09	28.71	-0.76	23.40
10	25.58	-2.23	20.57	23.98	-4.38	18.89	23.29	-5.32	18.16
20	19.97	-6.87	15.16	18.28	-9.15	13.38	17.55	-10.13	12.61
30	14.01	-11.79	9.41	12.20	-14.20	7.52	11.42	-15.24	6.69
40	7.63	-17.02	3.27	5.69	-19.57	1.25	4.86	-20.69	0.37
50	0.76	-22.60	-3.32	-1.32	-25.33	-5.50	-2.23	-26.53	-6.45
60	-6.68	-28.59	-10.46	-8.95	-31.54	-12.82	-9.93	-32.83	-13.85
70	-14.83	-35.08	-18.25	-17.32	-38.28	-20.84	-18.41	-39.69	-21.97
80	-23.85	-42.16	-26.84	-26.63	-45.68	-29.73	-27.85	-47.23	-30.99
90	-34.00	-49.99	-36.48	-37.16	-53.90	-39.74	-38.55	-55.63	-41.17
100	-45.68	-58.76	-47.49	-49.36	-63.19	-51.26	-50.99	-65.17	-52.94

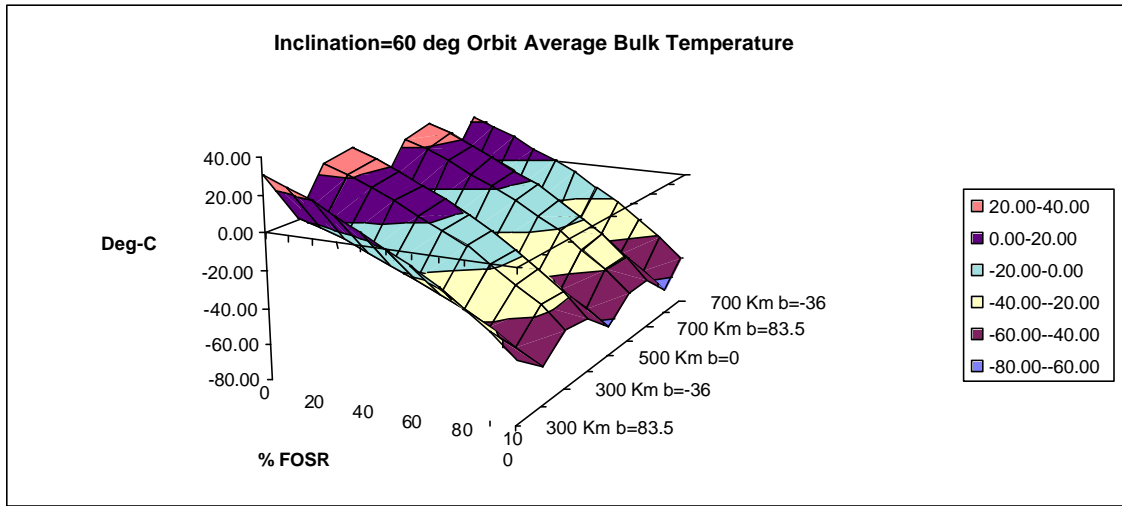


Figure 10-15 Inclination = 60 deg Orbit Average Bulk Temperature

In conclusion, from the orbit-averaged bulk temperature calculations, it is possible to choose a possible surface covering of FOSR to accommodate component temperature limits (0-20 deg C) for most orbits. Therefore, all subsequent thermal control system design will be focused on supporting the conclusions drawn from this calculation. Specifically:

- Temperature gradients within the spacecraft must be limited as much as possible by adequately linking all components with high conduction thermal paths.
- Transient temperature swings must be limited by increasing the thermal mass around critical components, such as the battery.
- Orbits that have varying beta angles must be avoided whenever possible.

10.2.7 Spartnik Component Thermal Design Analysis

The results of calculations done on each component in Spartnik's design are discussed here. Each component was analyzed to ensure adequate heat conduction and coupling to adjacent components.

10.2.7.1 Pending Calculations

The camera will be analyzed thermally in future editions of this report. There is a problem concerning the heat generating components of the camera, which were designed to be cooled by convection with the atmosphere, but will be thermally isolated in the vacuum of space. A few possible solutions are being considered at this time including using a copper braid bonded to the transformer to draw out the excess heat. Also the camera will have to be test run in a bell jar to characterize its temperature rise in a vacuum.

10.2.7.2 ADAC Hardware

The following calculation was done to consider attitude determination and control hardware as a source of heat loads. The maximum possible heat loads capable of being produced by all attitude control hardware is considered beyond the ability of heat transfer to accurately predict. Attitude control heat generation can therefore be safely ignored.

Spartnik ADAC Systems Heat Dissipation:

For this analysis it will be assumed that the spacecraft is operating in steady-state mode, where ADAC systems convert all disturbances and perturbations into heat. The total worst case torques will be used to determine the case heat dissipation of all ADAC systems.

Worst Case Torque Disturbances:

Worst case disturbances were taken from the ADAC report, assuming worst angle worst parameters for each graph

Gravity Gradient Torque (lowest)	$T_{\text{grav}} := 2.2 \cdot 10^{-8} \cdot \text{newton} \cdot \text{m}$
Solar Pressure Torque (worst incident)	$T_{\text{solar}} := 4.5 \cdot 10^{-8} \cdot \text{newton} \cdot \text{m}$
Magnetic Field Torque: (lowest)	$T_{\text{mag}} := 5.6 \cdot 10^{-5} \cdot \text{newton} \cdot \text{m}$
Aerodynamic Torques (lowest)	$T_{\text{aero}} := 0.1 \cdot 10^{-4} \cdot \text{newton} \cdot \text{m}$

Total Torques (worst case)

$$T_{\text{total}} := T_{\text{grav}} + T_{\text{solar}} + T_{\text{mag}} + T_{\text{aero}} \quad T_{\text{total}} = 6.60710^{-5} \cdot \text{joule}$$

Total Heat Loads from ADAC

To calculate the total heat load per orbit, an orbital period of 90 minutes is assumed:

$$W_{\text{total}} := T_{\text{total}} \cdot 90 \cdot 60 \quad W_{\text{total}} = 0.357 \cdot \text{joule}$$

This is the maximum heat load that the ADAC hardware can dissipate on orbit. Heat load will be distributed between the nutation damper and the hysteresis. This heat load is a fraction of the order of magnitude of all other internal heat. All internal heat loads are considered negligible compared to external heat. ADAC dissipated heat loads are therefore considered

Figure 10-16 Attitude Control Heat Generation

10.2.8 Temperature Sensor Design and Placement

Spartnik will be instrumented with temperature sensors on flight:

- To verify predictions of thermal design performance.
- To meet thermal data acquisition requirements
- To provide the computer with operational thermal information.

- To perform any thermal systems experiments.

The type of temperature sensor chosen to meet these needs was the Analog Devices (AD) brand thermocouple. The temperature sensors will be located within Spartnik’s standard location labeling scheme, repeated here in figure 10-17 for reference.

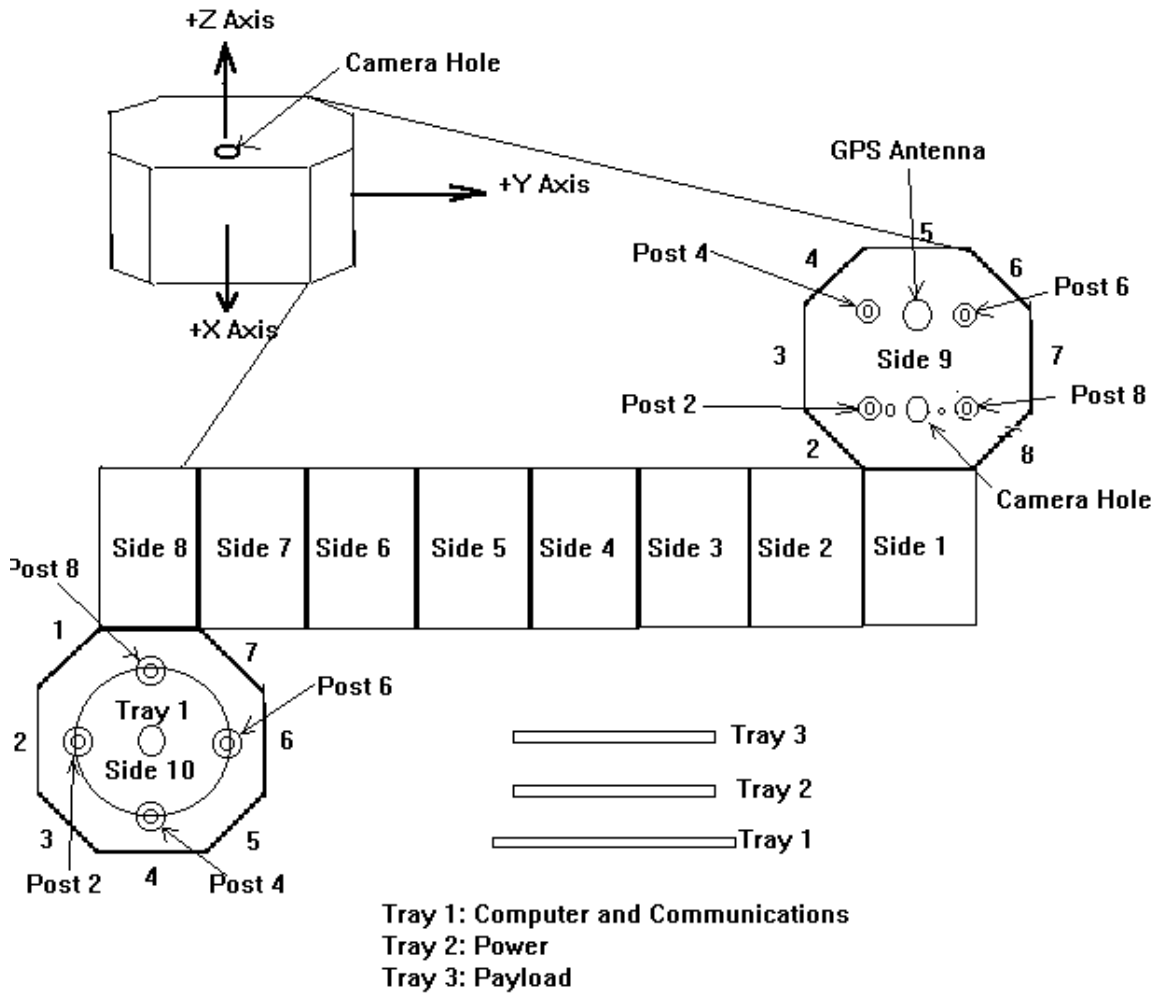


Figure 10-17 Spartnik Standard Location Labeling Scheme

Table 10-5 lists temperature sensor names, locations, and types that will be used to monitor the thermal condition of Spartnik. The table also lists the analog-to-digital converter that the computer will use to monitor the sensor. The sensors listed on the table are Analog Devices part number AD590K.

Table 10-5 Temperature Sensor Names, Locations

Sensor Name	Computer Interface	Sensor Description	Equipment Monitored
TEMPS1	ADC(D0)	Side 1, Center	Solar Panels
TEMPS3	ADC(D0)	Side 3, Center	Solar Panels
TEMPS5	ADC(D0)	Side 5, Center	Solar Panels
TEMPS7	ADC(D0)	Side 7, Center	Solar Panels
TEMPS9C	ADC(D0)	Side 9, Center	MMID
TEMPS10S1	ADC(D0)	Side 10, Near Side 1	Tray 1 Thermal Gradient
TEMPCPU	ADC(D0)	CPU Main Chip	CPU
TEMPCAM	ADC(D0)	Camera	Camera
TEMPP6B	ADC(D0)	Post 6, Bottom	Post 6 Conduction Path
TEMPP6T	ADC(D0)	Post 6, Top	Post 6 Conduction Path
TEMPT2S7	ADC(D0)	Tray 2, Near side 7	Tray 2 Thermal Gradient
TEMPPT2T	ADC(D0)	Tray 2, Center	Power Circuitry
TEMPBPA12	ADC(D0)	Battery A, Cells 1 & 2	Batteries
TEMPBPA34	ADC(D0)	Battery A, Cells 3 & 4	Batteries
TEMPBPA56	ADC(D0)	Battery A, Cells 5 & 6	Batteries
TEMPBPAP	ADC(D0)	Battery A, Equivalent to Post 2	Conduction Path
TEMPS2	ADC(D1)	Side 2, Center	Solar Panels
TEMPS4	ADC(D1)	Side 4, Center	Solar Panels
TEMPS6	ADC(D1)	Side 6, Center	Solar Panels
TEMPS8	ADC(D1)	Side 8, Center	Solar Panels
TEMPS9S5	ADC(D1)	Side 9, Near Side 5	Top Panel Thermal Gradient
TEMP10C	ADC(D1)	Side 10, Center	Top Panel Thermal Gradient
TEMPRF	ADC(D1)	Communications	Communications
TEMPP2B	ADC(D1)	Post 2, Bottom	Post 2 Conduction Path
TEMPP2T	ADC(D1)	Post 2, Top	Post 2 Conduction Path
TEMPT3C	ADC(D1)	Tray 3, Center	Payload Circuitry
TEMP3S3	ADC(D1)	Tray 3, Near Side 3	Tray 3 Thermal Gradient
TEMPBPB12	ADC(D1)	Battery B, Cells 1 & 2	Batteries
TEMPBPB34	ADC(D1)	Battery B, Cells 3 & 4	Batteries
TEMPBPB56	ADC(D1)	Battery B, Cells 5 & 6	Batteries
TEMPBPBP	ADC(D1)	Battery Pack B, Equivalent to Post 6	Batteries

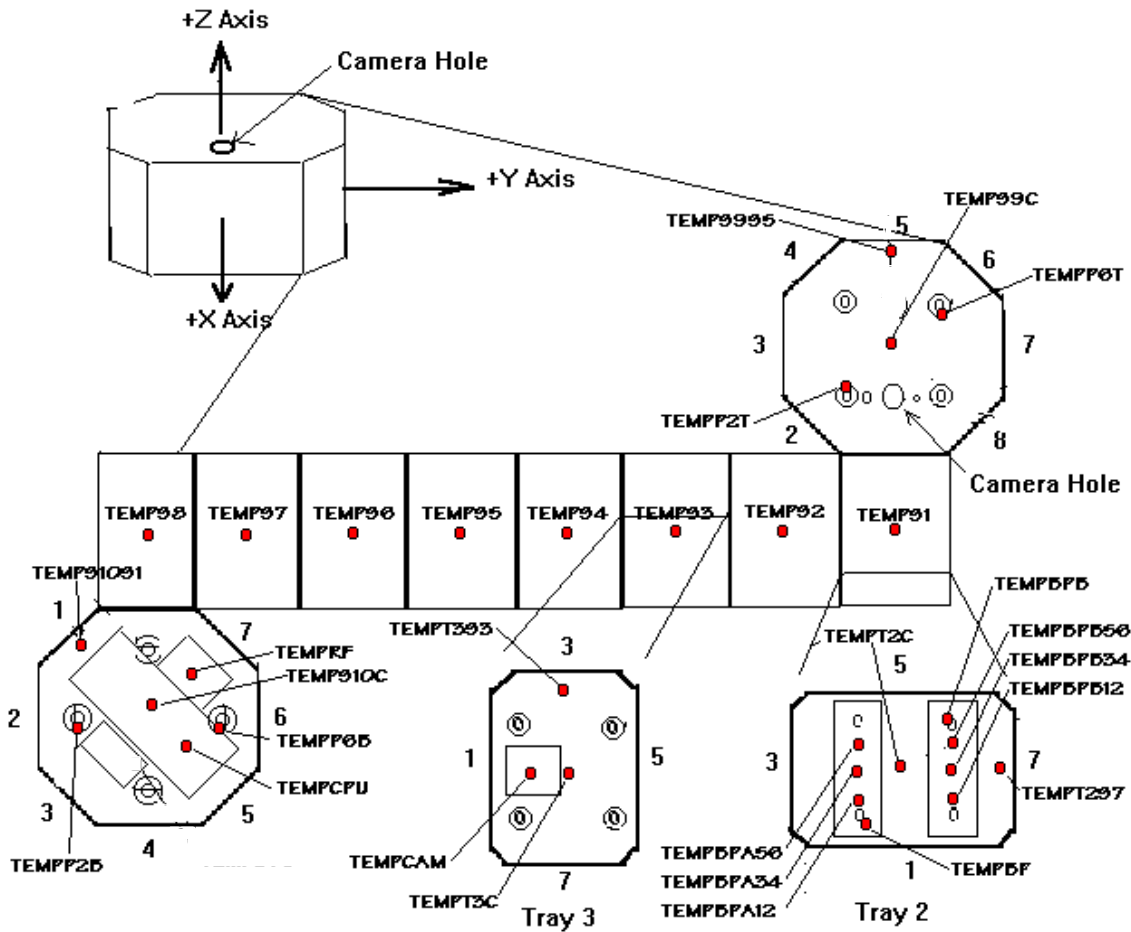


Figure 10-18 Temperature Sensor Locations

Figure 10-18 illustrates temperature sensor locations. It is believed that with 31 temperature sensors on a craft smaller than most commercial satellite equipment bays, the current design will adequately characterize temperature throughout the bus. This temperature sensor array design:

- Allots special sensor density to thermal data acquisition requirements of the batteries.
- Adequately gathers operational temperature information on all electronic components.
- Provides adequate characterization of critical thermal conduction path operation.
- Allows for measurement of radiation surface temperatures to characterize environment.
- Provides measurements that can be used to characterize lateral conduction in payload shelves.

These sensor locations will be used as nodes in subsequent calculations and in operational considerations.

10.2.9 SINDA Analysis

A SINDA software model was constructed of Spartnik in order to predict the amount of external thermal covering needed to keep the spacecraft within thermal limits. SINDA is an industry standard, network style, thermal analysis program. It numerically integrates the governing equations using the finite difference method. Thermal analysis methods are discussed in Appendix 10.9.2.

A 36-node SINDA model was constructed for a preliminary analysis. The model included nodes for the inner and outer surfaces of Spartnik and for all of the major interior components. This model was the basis for evaluation of all the heat rate files generated in order to obtain a general idea of how Spartnik will respond to its environment.

A 304-node SINDA model was constructed to serve as the final model for prediction of the realistic thermal behavior of Spartnik in orbit. It was based largely on the 36-node model of Spartnik with the difference being that the inner and outer surfaces were discretized into 9 nodes per side and 16 nodes for the plus and minus Z surfaces. Figure 10-19 shows the numbering of the inner and outer surface nodes for the 304-node model. Figure 10-20 shows the interior node scheme that applies to both the 304-node and 36-node models. The entire input file can be found in Appendix 10.9.4.1 with explanations of each feature.

The SINDA model has been constructed to serve a wide range of thermal analysis. The thermal-optical properties of the satellite can be varied to simulate different types and amounts of thermal coverings used on Spartnik for passive thermal control. Appendix 10.9.4 explains how this is done.

The Aluminum Stand Off (ASO) is the critical conduction path through the satellite. A 14-node model of an ASO was created to obtain the exact conductor value for implementation in the SINDA modeling. Code was written in the 36-node model of Spartnik to take advantage of these values and later adapted to the 304-node model of Spartnik after testing.

The SINDA model imports heat rates that are generated on Thermal Analysis Software (TAS) software for a particular orbit. The heat rate generation is described in Section 10.2.2. After the final orbit has been determined, a new heat rate file will have to be created. The SINDA input file has been written so that only a few lines of code will have to be changed to analyze the new heat rates. The first line is `INCLUDE XXX.HR`. Simply replace the `XXX.HR` with the new heat rate file name. The other lines that need to be changed are the entries in the `TIMEND` and `DA11MC` calls because they contain entries for the period of the orbit. This is explained in detail in Section 10.8.4. It is important that the heat rates be in the same form as those created initially in 1994 to characterize a range of thermal environments for Spartnik. As the SINDA input file currently exists the heat rate file must take into account the tumbling motion of Spartnik and its precession about the Z-axis. It is not necessary to include the spin rate in the heat rate file since FORTRAN logic has already been written into the SINDA input file to take this into account. Section 10.9.4 explains what the spin rate is and how it was programmed into the input file.

SINDA 3D is a graphical user interface that uses SINDA/G as a backbone for its analysis. Basically, it gives the engineer a 3D model that can be seen instead of the model that is imaginary. In making a model, one has to decide the main components that will affect the spacecraft in any way thermally related. Thermal modeling in SINDA 3D is comprised of multiple nodes, planes that connect a number of nodes together. Then using the circuit method to analyze the interaction of the nodes and planes as a whole. The steps are as follows:

- Decide on which components have an effect on the Spacecraft. Make sure you model everything around this component.
- Think of a simple geometry that best describes your spacecraft. Depending on the complexity and/or “what you want to get out of the model” will depend on the number of nodes that will be used.
- For each corner and surface of the geometry you place a node wherever there are corners. Each node has to be inputted into SINDA 3D using coordinates in the Cartesian system (X,Y,Z).
- Put thermal components, where needed.
- Apply temperatures and boundary conditions to thermal components.
- Run SINDA Analysis.

From the SINDA analysis there will be two types of results that one can retrieve information. The first are graphs that show temperature of different nodes. For example, the transient solution the graph will show Temperature with respect to Time for any given node. The second type of result deals with the model itself.

Interior Walls

100	101	102
103	104	105
106	107	108

200	201	202
203	204	205
206	207	208

300	301	302
303	304	305
306	307	308

400	401	402
403	404	405
406	407	408

500	501	502
503	504	505
506	507	508

600	601	602
603	604	605
606	607	608

700	701	702
703	704	705
706	707	708

800	801	802
803	804	805
806	807	808

Exterior Walls

10	11	12
13	14	15
16	17	18

20	21	22
23	24	25
26	27	28

30	31	32
33	34	35
36	37	38

40	41	42
43	44	45
46	47	48

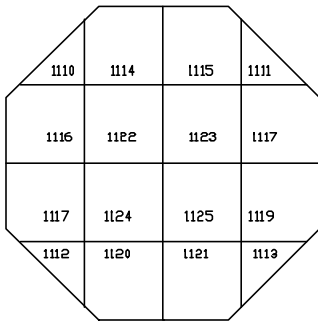
50	51	52
53	54	55
56	57	58

60	61	62
63	64	65
66	67	68

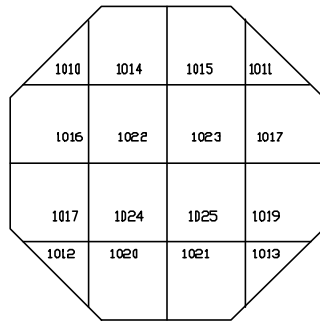
70	71	72
73	74	75
76	77	78

80	81	82
83	84	85
86	87	88

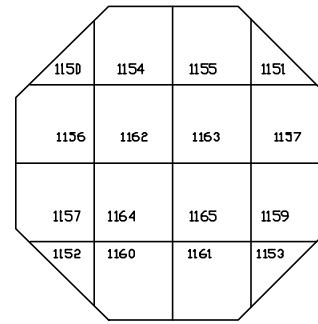
Interior +Z



Exterior +Z



Interior -Z



Exterior -Z

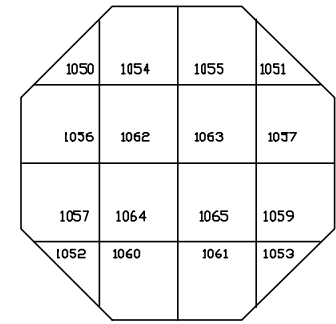


Figure 10-19 Spartnik Shell Node Diagram

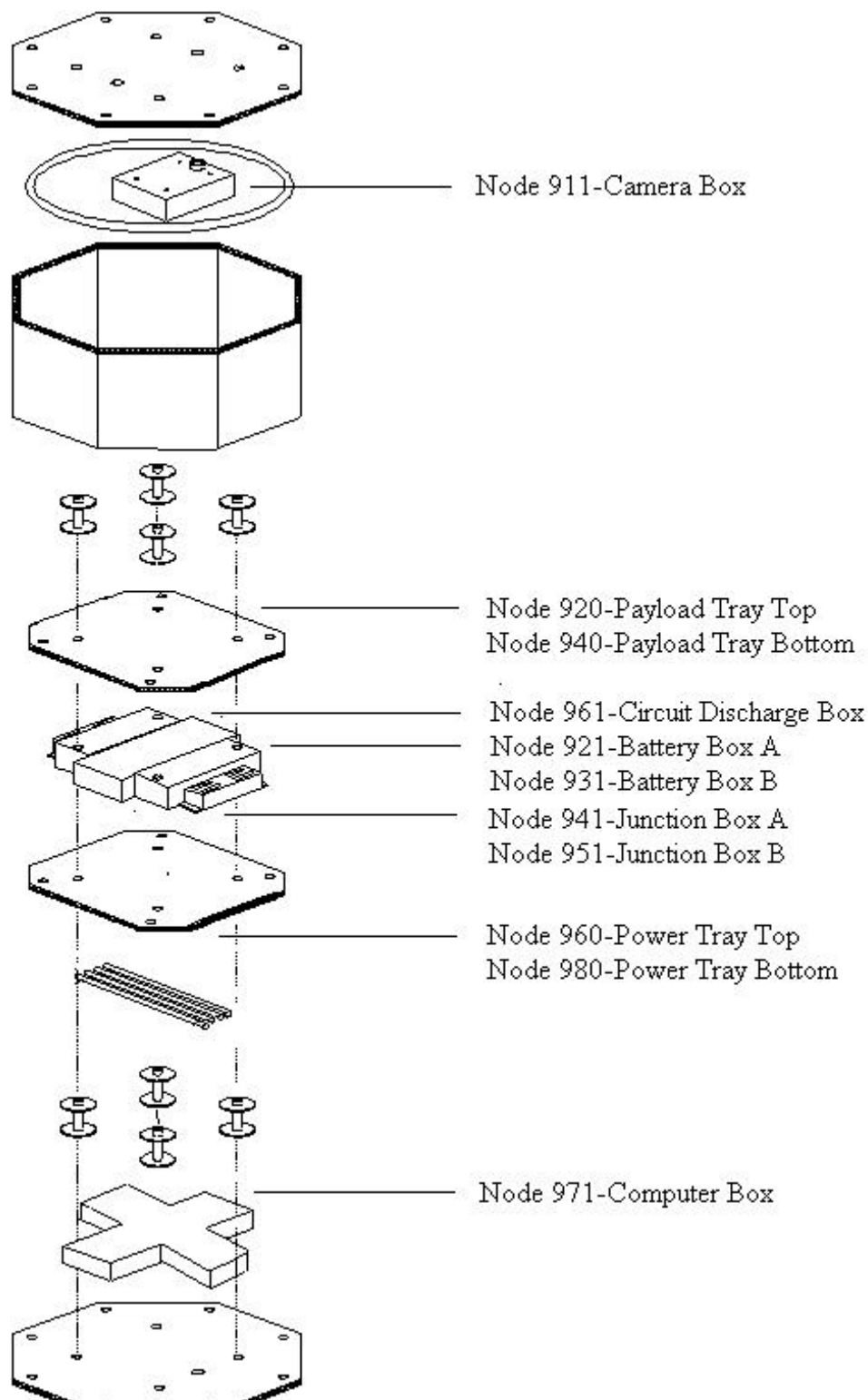


Figure 10-20 Spartnik Interior Node Diagram

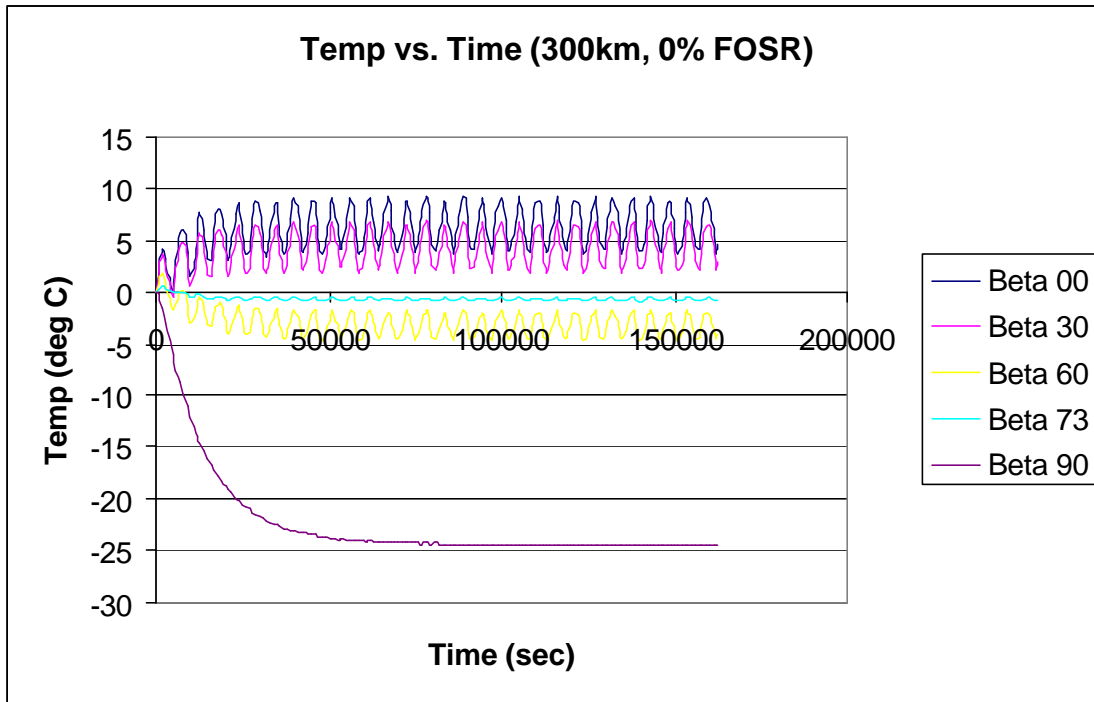


Figure 10-21 SINDA Results for Battery Temp Over 30 Orbits

The output of the SINDA program was organized into various plots. The entire set of plots can be found in Appendix 10.9.4.2. Figure 10-21 displays the results of battery temperature cycling over the course of 30 orbits for five different beta angles at 300-km altitude.

It can be seen that orbits with a beta angle of 90 degrees should be avoided. This drop in temperature, at what should theoretically be a spacecraft's hottest orbit, is due to the geometry of Spartnik. On an orbit with a beta angle of 90 degrees, the plus and minus Z faces of Spartnik never "see" the Sun (only the sides of the octagonal shell do). Although the larger area plus and minus Z faces see Earthshine, the dominant heat source of the Sun and albedo are limited to the smaller area of the sides of the spacecraft resulting in a low Spartnik temperature.

When the actual orbit of Spartnik is determined, new heat rates will need to be generated. These heat rates can be plugged into the 36-node model of Spartnik to adequately characterize its thermal response to its environment. After initial analysis the 304-node model can be used to obtain a thorough understanding of Spartnik's thermal response.

10.3 Construction And Assembly

TCS monitoring ensures that all components of the Spartnik satellite are constructed and handled within the temperature operating constraints set in Section 10.1.1.1.

After the Structures subsystem team assembled the spacecraft, the TCS team applied black paint to the inside walls of Spartnik using off-the-shelf paintbrushes and an airbrush. When the satellite is completely assembled, the TCS team will apply the external FOSR coverings to the top

and bottom of Spartnik, as well as apply the black paint to the exposed surfaces of Spartnik. Currently black paint had been applied to the inside wall of both top and bottom plates.

Thermally conductive silicone grease will be used on the contact area of the aluminum spacers to decrease the contact resistance for conduction and insure a good conduction path through the spacecraft. The spacers will be installed on the +Z and -Z faces prior to final construction. To make sure that a good seal is made the spacers will be torqued down to the +Z and -Z faces with 160 in-lbs of torque. A 1-inch o.d. washer will be used on the shell so that the shell will not be damaged.

The thermocouples will be anchored in place with a thermally conductive epoxy.

10.4 TCS Testing

Spartnik Thermal Control Systems (TCS) engineers must consider spacecraft, subsystem and component exposure to the thermal environments in all proposed tests. In addition, TCS must be responsible for all tests performed on the spacecraft and its components specifically for Thermal Control Systems purposes.

Each test proposed or performed by other Spartnik subsystems, on any part of Spartnik, will be discussed from a TCS perspective in sections to follow.

Spartnik Thermal Systems testing will be performed to meet the following design requirements in order of priority:

1. Verifying TCS design functionality and analysis predictions.
2. Verifying actual hardware will operate under expected conditions.
3. Certify Spartnik as rigorously as possible.

There are three levels of testing possible on the Spartnik project:

- Component testing.
- Hardware module testing.
- Spacecraft testing.

There are three types of thermal systems tests considered:

- Vacuum testing is performed to verify that electronic components will operate in an environment of low-pressure, high electrical conductivity atmosphere. These environments are encountered as component housings accumulate free-molecular gasses emitted by electronic components. Damage may be caused by circuit boards “arcing” through this atmosphere and unintentionally shorting out subsystems.
- Thermal cycling tests are performed to verify a components ability to start and operate at stated hot and cold temperature limits as well as in rapid temperature changes across temperature extremes. These tests are done at atmospheric pressures in a thermal chamber to verify component or system temperature ranges.

- Burn-in tests are performed to stress systems and components over long periods of time in an effort to screen out and replace defective hardware.

10.4.1 Thermal Control Systems Testing Industry Standards

Only two thermal testing specification documents are known to TCS to exist. MIL-STD-1540B, intended to specify quality of military space equipment, specifies testing standards considered too extreme for application to Spartnik. MIL-HDBK-343 specifies testing requirements for smaller projects.

10.4.1.1 MIL-STD 1540B as Pertaining to Thermal Control Systems Testing

For comparison, MIL-STD-1540B specifications are included in Figure 10-32 below. Qualification tests are performed to verify thermal and other systems design. Acceptance tests are performed to verify the quality and reliability of the actual hardware components used in the spacecraft. In Table 10-6, “R” denotes a required test “O” denotes an optional test and “-“ represents tests not required for Spartnik. Functional tests involve operating the components prior to and following any other environmental tests.

It should be noted here that components which will be tightly thermally controlled on orbit, Spartnik’s batteries for example, are exempted in MIL-STD-1540B from adding temperature margins to extreme temperatures during these tests.

Table 10-6 MIL-STD-1540B Testing Specifications³

MIL-STD 1540B Reference Paragraph	Qualification			Acceptance			
	Functional	Thermal Vacuum	Thermal Cycling	Functional	Thermal Vacuum	Thermal Cycling	Burn- In
	6.4.1	6.4.2	6.4.3	7.3.1	7.3.2	7.3.3	7.3.9
<i>Hardware</i>							
Electronic or Electrical Equipment	R	R	R	R	R	R	O
Antennas	R	R	O	R	O	O	-
Moving Mechanical Assembly	R	R	O	R	R	O	O
Solar Panel	R	R	O	R	O	O	-
Batteries	R	R	O	R	R	O	-
Valves	R	R	O	R	R	O	R
Fluid or Propulsion Equipment	R	R	O	R	R	O	-
Pressure Vessels	R	O	-	R	O	-	-
Thrusters	R	R	-	R	R		R
Thermal Equipment	R	R	-	R	R	-	-
Optical Equipment	R	R	-	R	R	-	-

10.4.1.2 *MIL-HDBK-343 as Pertaining to Thermal Control Systems Testing*

Spartnik is classified as a MIL-HDBK-343 Class D spacecraft. The following is an excerpt of the MIL-HDBK-343 specifications and classifications. Table 10-6 details certification requirements for the various classes. Class D requirements specify the minimum preflight testing for Spartnik. Resources permitting, testing schedules will be planned to upgrade Spartnik’s classification. Higher classifications will facilitate the acquisition of a donated launch.

“Military Handbook 343 (MIL-HDBK-343) was written to identify cost-saving measures that are reasonable for one-of-a-kind space equipment or for the first of a series of space vehicles. MIL-HDBK-343 defines the four classes of space programs, space vehicles, and space experiments as follows:

Class A High Priority, Minimum Risk. Class A is defined as a high-priority, minimum-risk effort. The characteristics for Class A usually also involve some combination of the following features: high national prestige, long life, high complexity, high use of redundancy, soft failure modes, independent qualification items, complete flight spares, highest cost, and a critical launch time. Vehicle and experiment retrievability or in-orbit maintenance is usually not possible.

Class B Risk with Cost Compromises. Class B is defined as a high-priority, medium-risk effort, with cost-saving compromises made primarily in areas other than design and

construction. The characteristics for Class B usually involve some combination of the following features: high national prestige, medium life, high complexity, soft failure modes, proto-flight qualification, limited flight spares, limited use of redundancy, high cost, short schedule, and a critical launch time. Vehicle and experiment retrievability or in-orbit maintenance is usually not possible.

Class C Economically Re-flyable or Repeatable. Class C is defined as a medium- or higher-risk effort that is economically re-flyable or repeatable. The characteristics for Class C usually involve some combination of the following features: medium to high national prestige, short life, low to medium complexity, small size, single-string designs, hard failure modes, very limited flight spares, medium cost, short schedule, and a non-critical launch time. Vehicle and experiment retrievability or in-orbit maintenance is usually possible, such as typified by Spacelab or Orbiter-attached payloads.

Class D Minimum Acquisition Cost. Class D is defined as a higher-risk, minimum-cost effort. The characteristics for Class D usually involve some combination of the following features: medium to low national prestige, short life, low complexity, small size, single-string designs, spares, lowest cost, short schedule, and non-critical launch schedule. Vehicle and experiment retrievability or in-orbit maintenance may not be possible.”⁴

Table 10-7 MIL-HDBK-343 Testing Specifications per Classification⁵

Comparison of Typical Test Requirements for Space Vehicles of Space Experiments of Each Class				
<i>Test Requirements</i>	<i>Class A</i>	<i>Class B</i>	<i>Class C</i>	<i>Class D</i>
Computer Thermal Model	Required (Software)	Required (Software)	Required (Software)	Not Required
Thermal Verification of Computer Model	Thermal Vacuum Test	Thermal Vacuum Test	Thermal Vacuum Test	Not Required
Maximum Operating Environments	MIL-STD-1540B definitions for each assembly level	MIL-STD-1540 definitions for each assembly level	MIL-STD-1540 definitions for each assembly level	MIL-STD-1540 definitions for each assembly level
Testing Tolerances	MIL-STD-1540	MIL-STD-1540	MIL-STD-1540	MIL-STD-1540
Development Tests	As Required	As Required	As Required	As Required
Component Acceptance	MIL-STD-1540 (component acceptance)	Not required on 1st item; protoflight test only	MIL-STD-1540 (component acceptance)	Not Required
Component Qualification	MIL-STD-1540 (qual.) to design levels	LIL-STD-1540 (protoflight) to design levels	Not required (acceptance test only)	Not Required
Qual. thermal margin	10 deg C	5 deg C	0 deg C	0 deg C
Experiment acceptance	MIL-STD-1540 (vehicle acceptance)	Not required on 1st item; protoflight test only	MIL-STD-1540 (vehicle acceptance)	MIL-STD-1540 (vehicle acceptance)
Experiment qualification	MIL-STD-1540 (vehicle qualification)	MIL-STD 1540 (protoflight) to design levels	Not Required (acceptance test only)	Not Required (acceptance test only)
Qual. margins (environ.)	10 deg C	10 deg C	0	0
Vehicle Acceptance	MIL-STD-1540 (vehicle acceptance)	Not required on 1st item; protoflight test only	MIL-STD-1540 (vehicle acceptance)	MIL-STD-1540 (vehicle acceptance)
Vehicle qualification	MIL-STD-1540 (vehicle qualification)	MIL-STD 1540 (protoflight) to design levels	Not Required (acceptance test only)	Not Required (acceptance test only)
Qual. margins (environ.)	10 deg C	10 deg C	0	0

10.4.2 TCS Testing Schedule

In scheduling TCS specific tests, consideration has first been given as to what tests are necessary and reasonable to perform. TCS testing schedules must consider:

- The availability of testing facilities, personnel, and Spartnik hardware.

- A project deadline of one academic semester has been set to perform all tests.
- The testing schedule for Spartnik must meet minimum industry standards to be allowed to use a launch vehicle (MIL-HDBK-343 described above in Table 10-7).
- Individual launch vehicles may impose additional thermal testing requirements.

10.4.3 TCS Test Plan

According to the MIL-HDBK-343, Spartnik is considered a Class D Spacecraft. The MIL-STD-1540 requires one thermal vacuum test of the completed spacecraft. This test has been delayed until a time closer to the launch date. No changes can be made to the spacecraft after this test has been performed other than repairs, or the test will have to be redone. Lockheed Martin has facilities to perform this test and has quoted an estimate price of \$3200. Eric C. Heilmann is the contact at LMMS for this test.

The following is a proposed vehicle thermal test plan for Spartnik. Its intent is to satisfy the MIL-HDBK-343 requirement for a Class D spacecraft as defined in 10.4.1.2. Two tests are required, a thermal vacuum test and a thermal-cycle test. Both tests are to be run as acceptance tests only.

10.4.3.1 *Vehicle Thermal Vacuum Test Parameters*

One component from each vehicle equipment area must be tested. There are three equipment areas on Spartnik and the components to be tested are:

- camera
- power box circuitry
- CPU

The temperature range of the test is from minimum predicted to maximum predicted temperatures. There must be a minimum of four cycles with an eight-hour soak at each temperature extreme of each cycle. Pressure of the test environment must be no greater than 10^{-4} Torr.

10.4.3.2 *Vehicle Thermal Cycle Test Parameters:*

This test requires a minimum of 40 thermal cycles from -10°C to 40°C of the completed spacecraft. No duration is specified. On the last cycle only, a functional test must be performed at each extreme.

10.4.3.3 *Thermal Balance Test*

The data gathered from the above tests must be compared with the predicted values from earlier analysis.

The above test plans were derived in accordance with the Thermal Testing Section in Satellite Thermal Handbook, David G. Gilmore, pages 9-3 through 9-35.

10.4.4 San Jose State Thermal Vacuum Chamber

A feasibility study concerning the implementation of a Thermal Vacuum chamber at San Jose State was carried out under the leadership of Dr. Desautel during Spring Semester 1998. This included researching literature that was donated by Space Systems Loral, as well as visiting the construction site of a new Thermal Vacuum chamber being implemented at Loral. It was decided that a vacuum chamber donated by Loral could be modified to be used as a thermal vacuum chamber. This is now a mechanical engineering senior project under the supervision of Dr. Lambert

The modifications consist mainly of building an aluminum shroud with copper D-tubing clamped on to the exterior of the shroud, for placement inside the existing vacuum chamber. It was determined that cal rods would be used as a heat source instead of lamps because of the need to simulate both the tumble and spin of Spartnik and because lamps are prohibitively expensive.

The TCS team is currently researching the addition of a cold plate to the chamber. The plate would be cooled by liquid helium. This addition would allow dirt particles to be baked off the satellite. They would then condense on the plate rather than back onto the satellite. This is important because any particles on the satellite could potentially be outgassed during launch and redistribute onto the optics of the primary payload. By adding the cold plate, spartnik increases its chances of getting a launch.

The other projects under development include a connector panel in the thermal chamber, and a satellite mounting system. It was determined that the current Spartnik requires at minimum an eight pin connector, however considering future satellites, additional connectors will be mounted. The means by which Spartnik will be mounted into the vacuum chamber is still in development.

10.4.5 Thermal Transducer Testing

The thermal transducers to be used during Spartnik's flight have been tested to ensure proper response and to provide for correction factors for sensor input to the data acquisition system. Test results are included as Appendix 10.9.5.

10.5 Operations

The 31 onboard temperature sensors will monitor Spartnik TCS in flight operations. These temperatures will be gathered throughout the spacecraft's lifetime to provide an accurate picture of how the spacecraft responds thermally. The data corresponding to the Kodak digital camera and the rechargeable Ni-Cad batteries from Eagle Pitcher will be given to those respective companies for their use in further studies.

10.6 Safety

There are two primary areas of interest concerning safety and TCS.

First and foremost is one of personnel safety during assembly of the satellite. TCS will use a number of chemical compounds to facilitate heat transfer, some of which are hazardous. Safety precautions are detailed in the Material Safety Data Sheets (MSDS), which are kept with the materials. Additionally, the Safety Team maintains copies of each applicable MSDS.

The second area of concern is safety in relation to the launch vehicle. The launch provider must be assured that Spartnik will not pose a significant safety hazard to their launch vehicle. As TCS is a passive system, there are few potential problem areas. There are no moving parts, and no pressure vessels in TCS. Of particular concern to the launch provider is material outgassing. All of the compounds used in TCS are certified to be low outgassing, and have been tested in accordance with ASTM-E-595 by their respective manufacturers.

10.7 Conclusions

Spartnik's temperature sensors will return adequate data for determining the characteristics of the individual components and the satellite as a whole for future microsatellite projects. ADAC hardware dissipates negligible heat during orbital operation. The battery box time constant is sufficiently large enough to "coast" through most orbital thermal perturbations, including umbra traverses. Battery box performance is not greatly affected by potting materials used. SINDA analysis has shown that orbits with a beta angle of 90 degrees should be avoided.

10.8 Reference List

The following is a list of references used in this report and resources used in the completion of the Spartnik Thermal Systems project. Referenced material in this report is endnoted by author and page number.

Gilmore, David G., Bello, Mel, Executive Editors, Satellite Thermal Control Handbook, Spacecraft Thermal Department, Aerospace Corporation, 1994.

Incropera, Frank P., DeWitt, David P., Fundamentals of Heat And Mass Transfer, 3rd Edition, John Wiley & Sons, 1990.

Medina, Sean, Thermal Mentor, Inter-Project Communication: Thermo-Optical Properties for Spartnik, Lockheed Martin, 12 Jan 1994.

10.9 Appendices

10.9.1 Discussion of Thermodynamic and Heat Transfer Theory Used in Analysis.

A functional theory is required for the analysis and verification of spacecraft thermal designs. Principles from both the science of thermodynamics and the science of heat transfer. Thermodynamics provides the basic concepts of heat, temperature and energy balances used extensively in subsequent analysis. Thermodynamics can not provide information about the rates that processes occur.

The science of heat transfer is an extension of thermodynamics attempting to address rates of heat flow. Solutions for the temperature of an object as a function of time and mid-object location are possible with knowledge of heat flow rates.

Heat transfer is defined as energy in transit due to a temperature difference. The science of heat transfer classifies this energy transfer into three phenomena: conduction, convection and radiation. One key equation in heat transfer analysis is the heat rate equation. This equation involves a heat rate, constants depending on the type of heat transfer present in the problem, and a temperature gradient.

Heat transfer analysis begins with the heat rate equation relating heat flow to temperature gradient. If the temperature gradient has not been specified, the three modes of heat transfer provide a means of quantifying the temperature gradient. The scaling factors involved are dependent on the problem. Heat transfer solutions usually involve solving for the unspecified item in the heat rate equation of the problem. Figure 10.9.1 includes several basic forms derived for the heat rate equation for the three modes of heat transfer. The table also describes the mechanism involved in each equation and the units of the transport property of coefficient involved with each heat transfer mode.⁶

<i>Mode</i>	<i>Mechanism</i>	<i>Rate Equation</i>	<i>Transport Property or Coefficient</i>
Conduction	Diffusion of energy due to random molecular motion	$\overline{q}_x \cdot \frac{W}{m^2} := -k \cdot \frac{dT}{dx}$	$k \cdot \left(\frac{W}{m \cdot K} \right)$
Convection	Diffusion of energy due to random molecular motion plus energy transfer due to bulk motion (advection)	$\overline{q}_x \cdot \frac{W}{m^2} := h(T_s - T_{inf})$	$h \cdot \left(\frac{W}{m^2 \cdot K} \right)$
Radiation	Energy transfer by electromagnetic waves	$\overline{q}_x \cdot \frac{W}{m^2} := \varepsilon \cdot \sigma \cdot (T_s^4 - T_{sur}^4)$ or $\overline{q}_x \cdot \frac{W}{m^2} := h_r \cdot A \cdot (T_s - T_{sur})$	ε
	where	$h_r := \varepsilon \cdot \sigma \cdot (T_s + T_{sur}) \cdot (T_s^2 + T_{sur}^2)$	$h \cdot \left(\frac{W}{m^2 \cdot K} \right)$

Figure 10.9.1 Basic Heat Rate Equations

Each type of heat transfer and its importance to Thermal Systems will be briefly discussed below.

Several methods of manipulating heat transfer problems have been developed. These methods include the lumped capacitance method, the electric circuit analogy and nodal analysis. Each of these methods will be briefly discussed in sections below.

10.9.1.1 Conduction

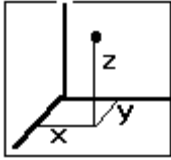
Conduction is the motion of thermal energy across a solid due to a temperature gradient within the solid. Conduction enables thermal energy to be transferred through the spacecraft hardware itself. Thermal Systems must consider all spacecraft hardware and structure as paths to convey thermal energy by conduction.

Two items of interest to Thermal Systems engineers are the conduction heat equation and contact resistance.

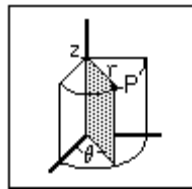
10.9.1.2 The Heat Equation

The heat equation is derived from a thermodynamics energy balance around a differential volume of the solid under study. Figure 10.9.2 lists the heat equation in three coordinate systems.

Cartesian
$$\frac{d}{dx} \left(k \frac{dT}{dx} \right) + \frac{d}{dy} \left(k \frac{dT}{dy} \right) + \frac{d}{dz} \left(k \frac{dT}{dz} \right) + \frac{d}{dt} q := \rho \cdot c_p \frac{dT}{dt}$$



Cylindrical
$$\frac{1}{r} \frac{d}{dr} \left(k \cdot r \frac{dT}{dr} \right) + \frac{1}{r^2} \frac{d}{d\theta} \left(k \frac{dT}{d\theta} \right) + \frac{d}{dz} \left(k \frac{dT}{dz} \right) + \frac{d}{dt} q := \rho \cdot c_p \frac{dT}{dt}$$



Spherical
$$\frac{1}{r^2} \frac{d}{dr} \left(k \cdot r^2 \frac{dT}{dr} \right) + \frac{1}{r^2 \cdot \sin^2 \theta} \frac{d}{d\phi} \left(k \frac{dT}{d\phi} \right) + \frac{1}{r^2 \cdot \sin \theta} \frac{d}{d\theta} \left(k \cdot \sin \theta \frac{dT}{d\theta} \right) + \frac{d}{dt} q := \rho \cdot c_p \frac{dT}{dt}$$

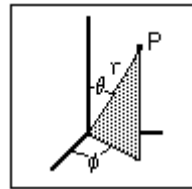


Figure 10.9.2 The Heat Equation

Important features of the heat equation include:

- Temperature gradients along coordinates. Many systems can be reduced to two or one dimensional heat flow problems to simplify analysis.
- Dependence on k, the thermal conductivity of the material. This term can be brought out of the directional derivatives in isotropic materials. Material properties measured at appropriate temperatures must be used whenever possible in a heat transfer analysis.
- Time variable internal heat generation terms q. These terms may be considered constant in steady-state analysis.

- Transient heat storage term on right hand side of equation that accounts for changes in temperature with time. This term can be dropped in steady-state analysis.

The heat equation can not be solved analytically for most problems. Simplified forms of the heat equation may approximate many solutions. Figure 10.9.3 lists three forms of the heat equation and solutions for temperature gradients assuming:

- One dimensional heat flow
- Steady-state solutions
- no generation terms

	<i>Plane Wall</i>	<i>Cylindrical Wall</i>	<i>Spherical Wall</i>
Heat Equation	$\frac{d^2 \cdot T}{d \cdot x^2} := 0$	$\frac{1}{r} \cdot \frac{d}{dr} \cdot \left(r \cdot \frac{dT}{dr} \right) := 0$	$\frac{1}{r^2} \cdot \frac{d}{dr} \cdot \left(r^2 \cdot \frac{dT}{dr} \right) := 0$
Temperature distribution	$T_{s,1} - \Delta T \cdot \frac{x}{L}$	$T_{s,2} + \Delta T \cdot \frac{\ln\left(\frac{r}{r_2}\right)}{\ln\left(\frac{r_1}{r_2}\right)}$	$T_{s,1} - \Delta T \cdot \frac{\left[1 - \left(\frac{r_1}{r}\right) \right]}{\left[1 - \left(\frac{r_1}{r_2}\right) \right]}$
Heat Flux (q")	$k \cdot \frac{\Delta T}{L}$	$\frac{k \cdot \Delta T}{r \cdot \ln\left(\frac{r_2}{r_1}\right)}$	$\frac{k \cdot \Delta T}{r^2 \cdot \left[\left(\frac{1}{r_1}\right) - \left(\frac{1}{r_2}\right) \right]}$
Heat Rate (q)	$k \cdot A \cdot \frac{\Delta T}{L}$	$\frac{2 \cdot \pi \cdot L \cdot k \cdot \Delta T}{\ln\left(\frac{r_2}{r_1}\right)}$	$\frac{4 \cdot \pi \cdot k \cdot \Delta T}{\left(\frac{1}{r_1}\right) - \left(\frac{1}{r_2}\right)}$
Thermal Resistance	$\frac{L}{k \cdot A}$	$\frac{\ln\left(\frac{r_2}{r_1}\right)}{2 \cdot \pi \cdot L \cdot k}$	$\frac{\frac{1}{r_1} - \frac{1}{r_2}}{4 \cdot \pi \cdot k}$

Figure 10.9.3 Simplified Heat Equation⁷

Boundary conditions used when integrating the heat equation usually are derived from the heat transfer modes occurring at each respective boundary of the object under study. Figure 10.9.4 lists common boundary conditions for the heat equation.

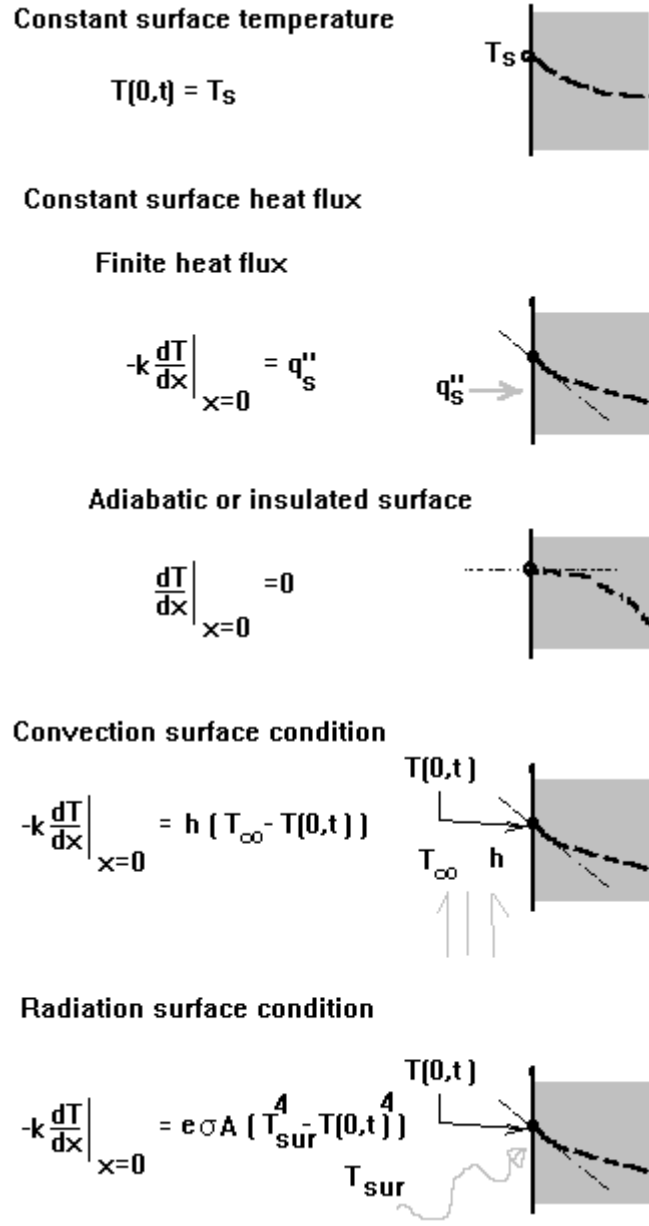


Figure 10.9.4 Heat Equation Boundary Conditions

10.9.1.3 Contact Resistance

In the design of a spacecraft thermal system, “it is important to recognize that, in composite systems, the temperature drop across the interface between materials may be appreciable. This temperature change is attributed to what is known as the thermal contact resistance, $R_{t,c}$. The effect is shown in Figure⁸ 10.8.5.

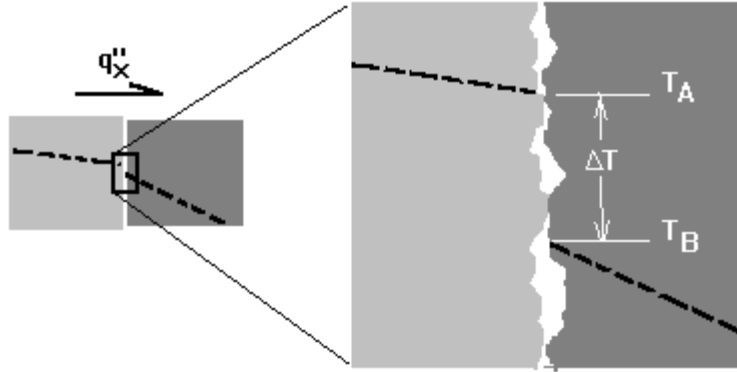


Figure 10.9.5 Contact Resistance Effect

For a unit area of the interface, the resistance is defined as

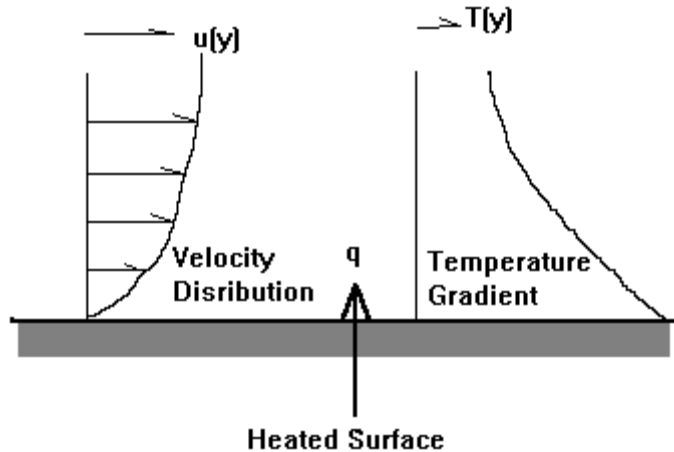
$$R''_{t,c} = (T_A - T_B) / q''_x$$

and is measured in $\text{m}^2 \text{K} / \text{W}$.

Thermal contact resistance may be decreased with increased joint pressure, or through the use of thermal sealant, such as RTV 566.

10.9.1.4 Convection

“The convection heat transfer *mode* is comprised of *two mechanisms*. In addition to energy transfer due to *random molecular motion* (diffusion), there is also energy being transferred by the *bulk, or macroscopic, motion* of the fluid. This fluid motion is associated with the fact that, at any instant, large numbers of molecules are moving collectively or as aggregates. Such motion, in the presence of a temperature gradient, will give rise to heat transfer. Because the molecules in the aggregate retain their random motion, the total heat transfer is then due to a superposition of energy transport by the random motion of the molecules and by the bulk motion of the fluid. It is customary to use the term *convection* when referring to this cumulative transport and the term *advection* when referring to the transport due to bulk fluid motion.”⁹



“A consequence of the fluid-surface interaction is the development of a region in the fluid through which the velocity varies from zero at the surface to a finite value u_∞ associated with the flow. This region of the fluid is known as the *hydrodynamic*, or *velocity*, *boundary layer*. Moreover, if the surface and flow temperatures differ, there will be a region of the fluid through which the temperature varies from T_s at $y = 0$ to T_∞ in the outer flow. This region, called the *thermal boundary layer*, may be smaller, larger, or the same size as that through which the velocity varies. In any case, if $T_s > T_\infty$, convection heat transfer will occur between the surface and the outer flow.

“Convection heat transfer may be classified according to the nature of the flow. We speak of *forced convection* when the flow is caused by external means, such as by a fan, a pump, or atmospheric winds. ... In contrast, for *free* (or *natural*) *convection* the flow is induced by buoyancy forces which arise from density differences caused by temperature variations in the fluid.”¹⁰

For TCS, convection is currently not a topic of analysis. The spacecraft will encounter convection heat transfer under three circumstances:

1. Inside the launch fairing under air conditioning on the launch pad.
2. Inside the launch fairing during the first 60 seconds of ascent, during which ambient pressure drops to zero, invalidating all known experimental correlations.
3. Component testing discussed in the procedures for each test.

10.9.1.5 Radiation

“Thermal radiation is energy *emitted* by matter that is at a finite temperature. Although we focus primarily on radiation from solid surfaces, emission may also occur from liquids (such as the Earth’s ocean) and gases (the primary source of Earthshine is the Earth’s atmosphere). Regardless of the form of matter, the emission may be attributed to changes in the electron configurations of the constituent atoms or molecules. Electromagnetic waves (or alternatively, photons) transport the energy of the radiation field. While the transfer of energy by conduction or convection requires the presence of a material medium, radiation does not. In fact, radiation transfer occurs most efficiently in a vacuum.”¹¹

Figure 10.9.6 illustrates one possible path of thermal energy passing through an emissive surface.

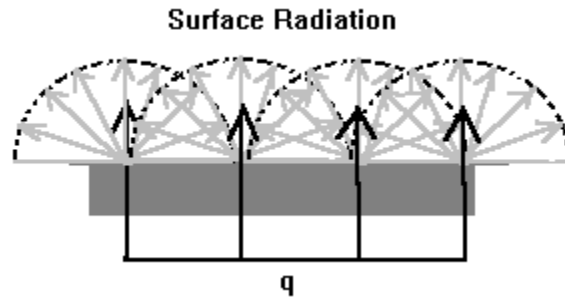


Figure 10.9.6 Illustration of Emissive Surface Radiation

The modifier “thermal” is usually used to distinguish thermal radiation which is directly coupled to the temperature of the radiating body; with hard radiation caused by radioactive emission, and other high and low frequency electromagnetic radiation. Figure 10.9.7 specifies the wavelengths thermal engineers are concerned with.

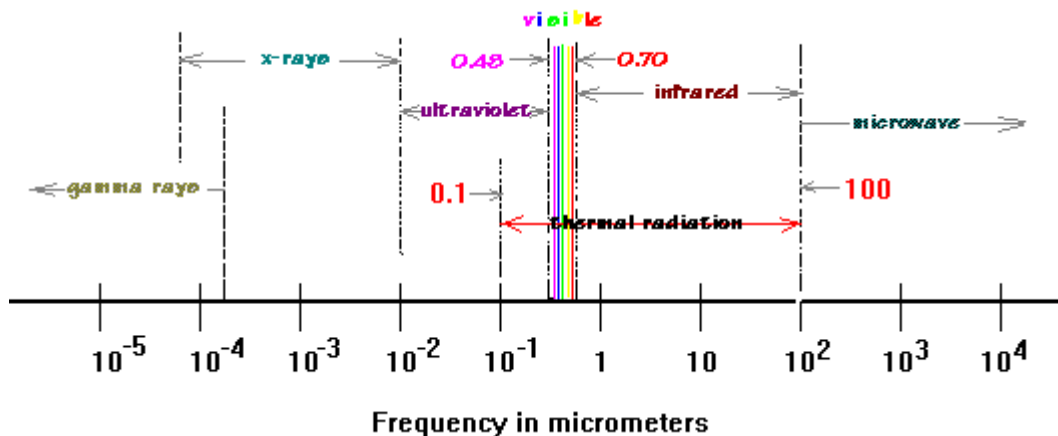
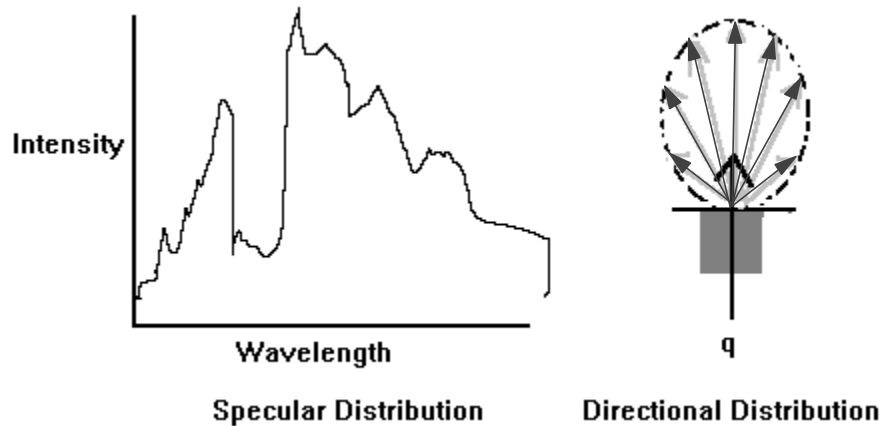


Figure 10.9.7 Spectrum of Electromagnetic Radiation

Radiation is a marginally understood phenomenon. Current basic analysis methods involve the Stefan-Boltzman law, spectral and directional considerations, black body ideal models, gray body approximations, and view factors. Each of these topics is discussed in sections to follow.

10.9.1.6 Radiation Intensity

Radiation intensity varies with both the wavelength of the electromagnetic carrier and the direction of emission. Figure 10.9.9 illustrates these effects on radiation intensity.



10.8.9 Wavelength and Directional Effects

To quantify the total radiation from a unit surface area, both spectral distributions and directional distributions must be considered. Both total emissive power per unit surface area E and total incident irradiation are the result of integrating over all radiation wavelengths and solid angle directions.

10.9.1.7 Blackbody Radiation

Blackbody radiation is introduced to simplify radiation analysis. The following idealizations define a black body:

- Absorbs all incident radiation regardless of direction or wavelength.
- Emits the maximum possible radiation for a prescribed surface temperature.
- Emits equally in all directions, or diffusely.

No real surface has all of these characteristics. Blackbody behavior is best approximated by a cavity with a small opening. Figure 10.9.10 depicts this behavior.

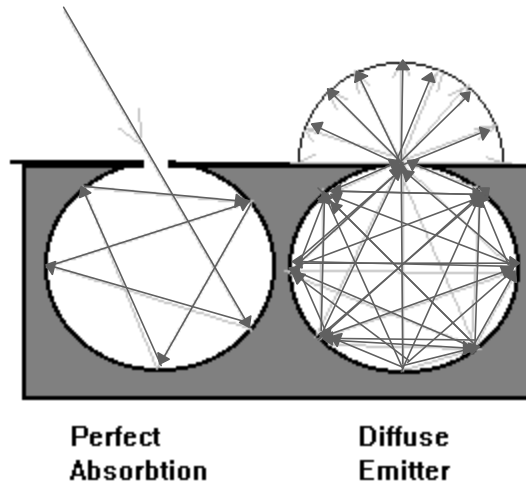


Figure 10.9.10 Cavity Blackbody Approximation

In radiating the maximum energy possible at a given temperature, blackbody radiation spectrally follows the Planck Distribution. An analysis of solar radiation as a black body is given as an example in figure 10.9.11.

Analysis of Solar Radiation Blackbody Spectral Distribution

$$j := 40..10 \quad \lambda(j) := \left(10^{\frac{j}{10}}\right) \cdot 10^{-3} \cdot \text{m} \quad \text{Wavelength Range}$$

$$T_b := 5800\text{K} \quad \text{Solar surface temperature}$$

$$h := 6.6256 \cdot 10^{-34} \cdot \text{joule} \cdot \text{sec} \quad \text{Universal Plank Constant}$$

$$k := 1.3808 \cdot 10^{-23} \cdot \frac{\text{joule}}{\text{K}} \quad \text{Universal Boltzmann Constant}$$

$$c_o := 2.998 \cdot 10^8 \cdot \frac{\text{m}}{\text{sec}} \quad \text{Speed of light in a vacuum}$$

$$E_{b_j} := \frac{2 \cdot \pi \cdot h \cdot c_o^2}{\lambda(j)^5 \cdot \left(e^{\frac{h \cdot c_o}{\lambda(j) \cdot k \cdot T_b}} - 1 \right)} \cdot 10^6 \quad \text{Plank blackbody distribution equation}$$

Given in W/m²μm

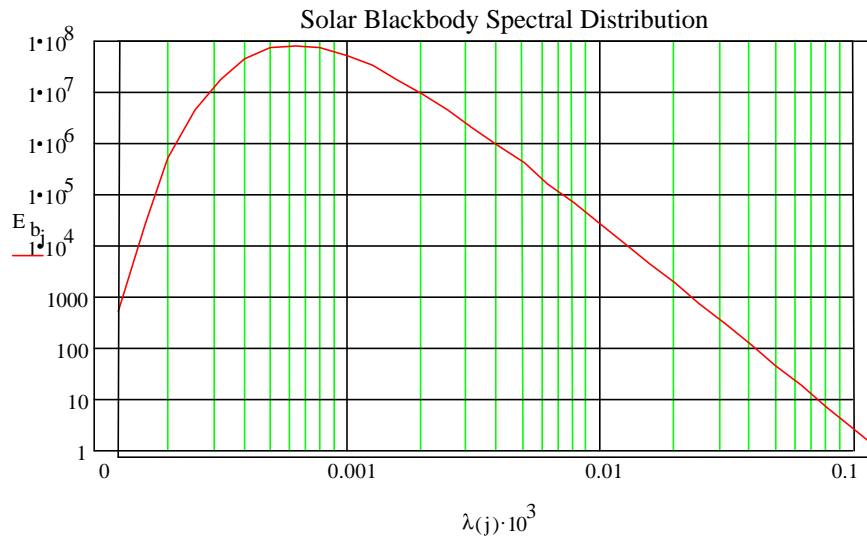


Figure 10.9.11 Solar Spectral Emissive Power Distribution

The following notes pertain to blackbody radiation:

- “The emitted radiation varies *continuously* with wavelength.
- At any wavelength the magnitude of the emitted radiation increases with increasing temperature.

- The spectral region in which the radiation is concentrated depends on the temperature, with *comparatively* more radiation appearing at shorter wavelengths as the temperature increases.
- A significant fraction of the radiation emitted by the sun, which may be approximated as a blackbody at 5800 K, is in the visible region of the spectrum. In contrast for $T < 800$ K, emission is predominantly in the infrared region of the spectrum and is not visible to the eye.”¹²
- The wavelength of maximum emissive power from a blackbody of temperature T is given by Wein’s Law:

$$\lambda_{\max}T = 2897.8\mu\text{m K}$$

- The total emissive power from a black body of temperature T is given by the Stefan-Boltzmann Law:

$$E_b = \sigma T^4$$

where $\sigma = 5.670 \times 10^{-8} \text{ W/ m}^2 \text{ K}$ is the Stefan-Boltzman constant.

- Because this emission is diffuse, it follows that

$$I_b = E_b/\pi$$

- For first order calculations, real surfaces can be approximated as blackbodies. Gray body approximations account for imperfections in surface/radiation interaction. View factors are used to account for the directionality of radiation. Both topics will be discussed in sections to follow.

10.9.1.8 *Gray Body Radiation*

Several factors are used to accommodate imperfect surface/radiation interaction. Because blackbody radiation is the ideal interaction, all of these factors have values ranging from 0 to 1. When these factors are in use in a calculation, the surfaces in question are modeled as “gray bodies”. These factors each account for one type of interaction and are:

- Absorbivity, α
- Reflectivity, ρ
- Transmissivity, τ

Figure 10.9.12 illustrates the phenomenon that these factors govern.

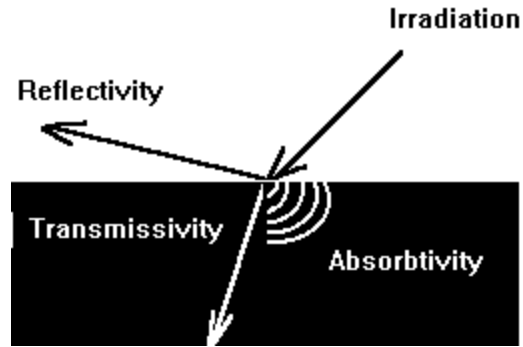


Figure 10.9.12 Incident Light Phenomenon

Gray surface analysis assumes:

- Both irradiation and surface are diffuse.
- Surface properties remain roughly constant over the temperature range of the problem.

Gray body factors are dependent on wavelength. Some gray body factors are tabulated for a variety of real surfaces at a variety of temperature ranges.

10.9.1.9 View Factor Calculations

View factors account for directionality between two objects in radiation analysis. View factors, like gray body factors, have a range of 0 to 1. View factors are defined as the solid angle taken up by one object when viewed from another, divided by the total solid angle visible to the surface. Figure 10.9.13 illustrates this definition.

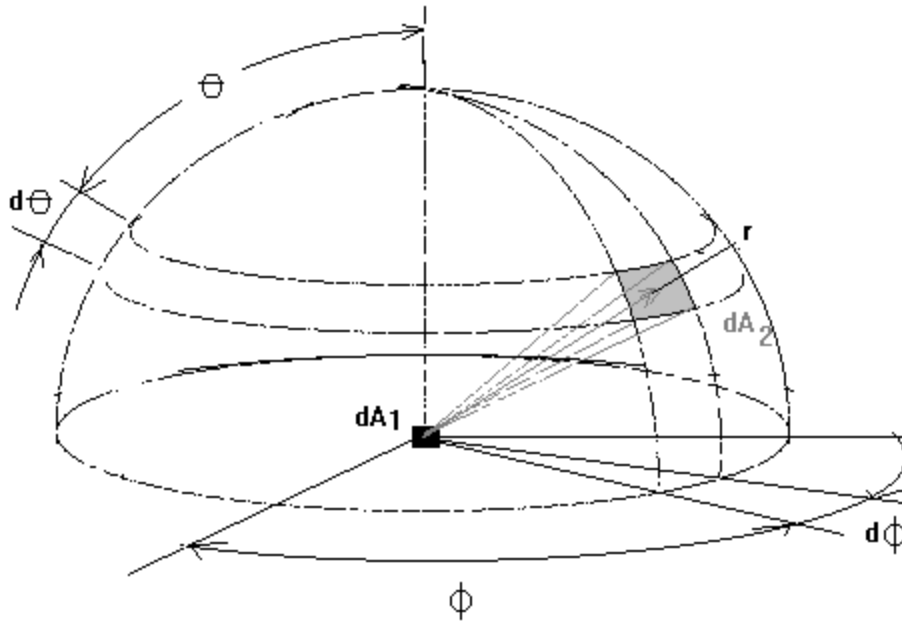
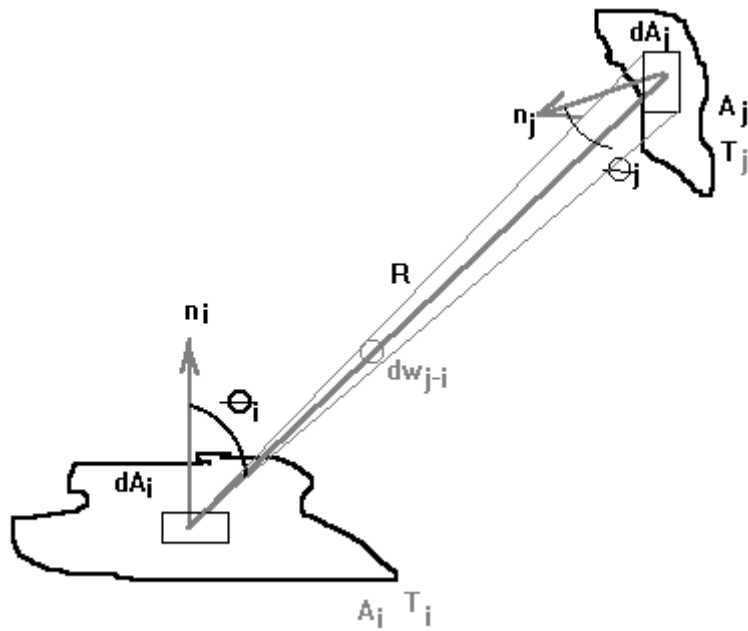


Figure 10.9.13 View Factor Calculation

Usual view factor calculation involves integrating this geometrical model over both surfaces.



$$F_{ij} := \frac{1}{A_i} \iint \frac{\cos(\theta_i) \cdot \cos(\theta_j)}{\pi \cdot R^2} dA_i dA_j$$

Formulas and charts are available in Reference 2 for many common geometries. One important formula in view factor calculation is reciprocity:

$$A_i F_{ij} = A_j F_{ji}$$

10.9.2 Heat Transfer Analysis Methods

Several methods are available in the analysis of complex heat transfer problems. A cautionary discussion of the expected accuracy precedes a discussion of methodology. The circuit analogy method allows for the analysis of complex thermal systems as electric networks. The lumped capacitance method allows for simplification of analysis under certain conditions. Nodal analysis methods rely on the circuit analysis methodology and matrix algebra to solve extremely complex thermal system problems.

10.9.2.1 *Expected Accuracy*

Caution is advised in relying on heat transfer analysis results. The many assumptions made in modeling thermal systems for heat transfer analyses have varying degrees of validity. Errors of 20-25% are common and unavoidable.

Material and surface properties are the primary source of error. Material imperfections can disrupt homogeneous material assumptions. Surface properties vary drastically within a surface sample depending on surface condition, disrupting gray body factor assumptions. Perhaps the most problematic analysis involves convection, for obvious reasons. Overall, heat transfer analysis results should be expected to vary 20-25% from the real system solution. Safety factors and operational testing become important in thermal systems.

10.9.3 Panel-Wise Heat Rate Calculations

Figures 10.8.14 through 10.8.22 display the results of the entire panel-wise orbit heat rate calculations done as a preliminary study in 1994. Lockheed Martin using TSS code provided the raw data used for the calculations.

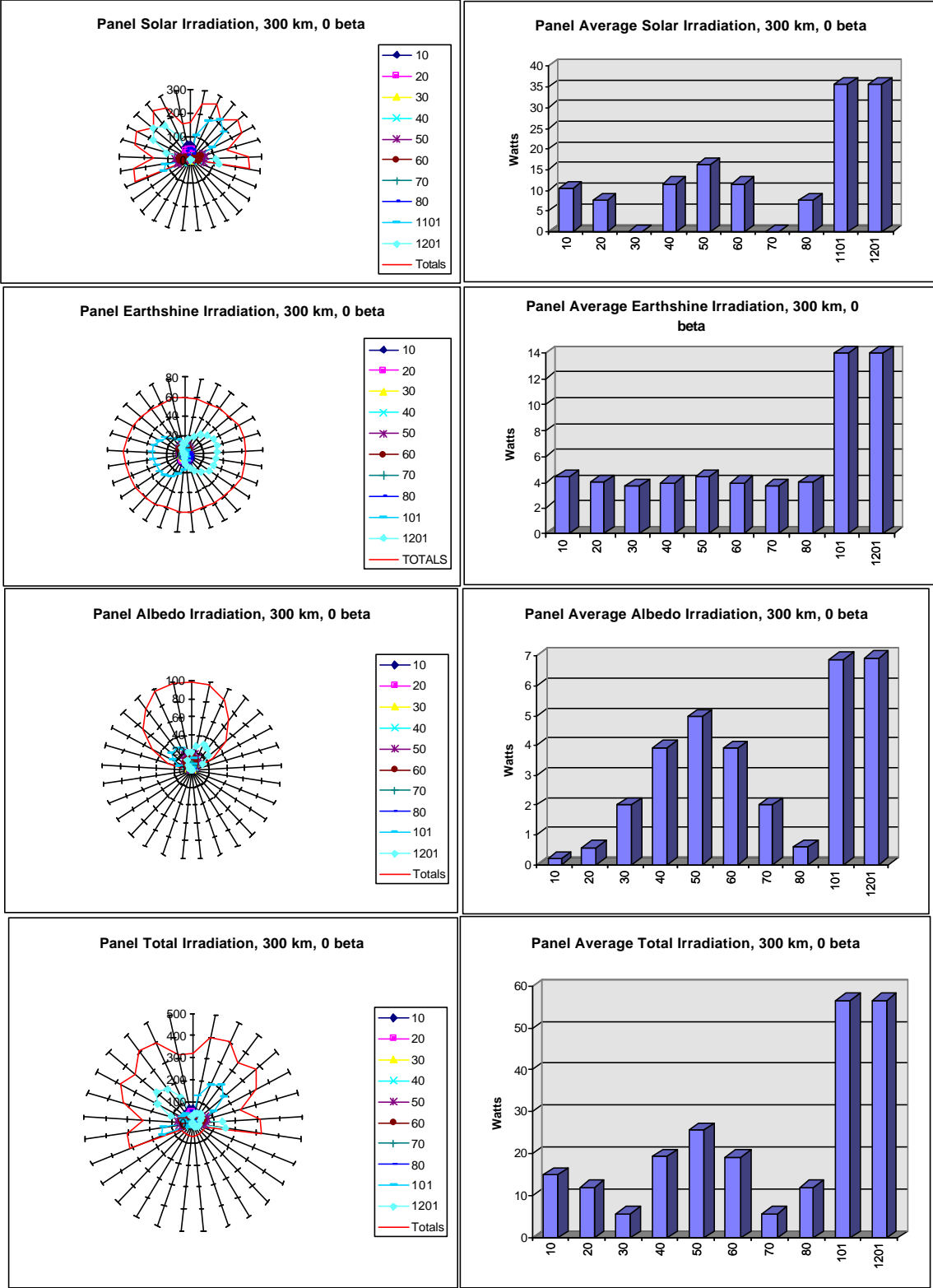


Figure 10.9.14 Panel-Wise Orbit Heat Rates, 300 km, 0 deg beta

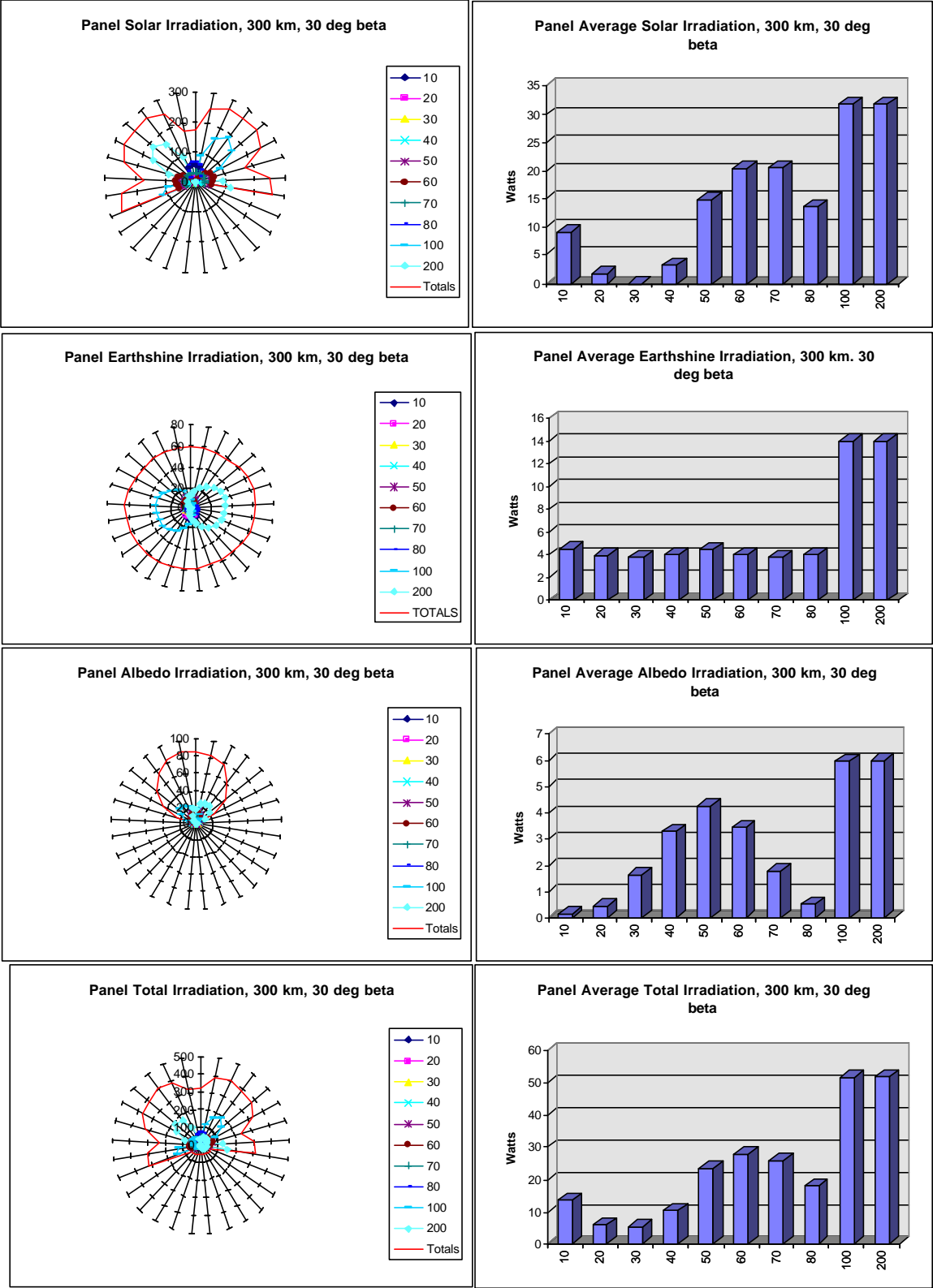


Figure 10.9.15 Panel-Wise Orbit Heat Rates, 300 km, 30 deg beta

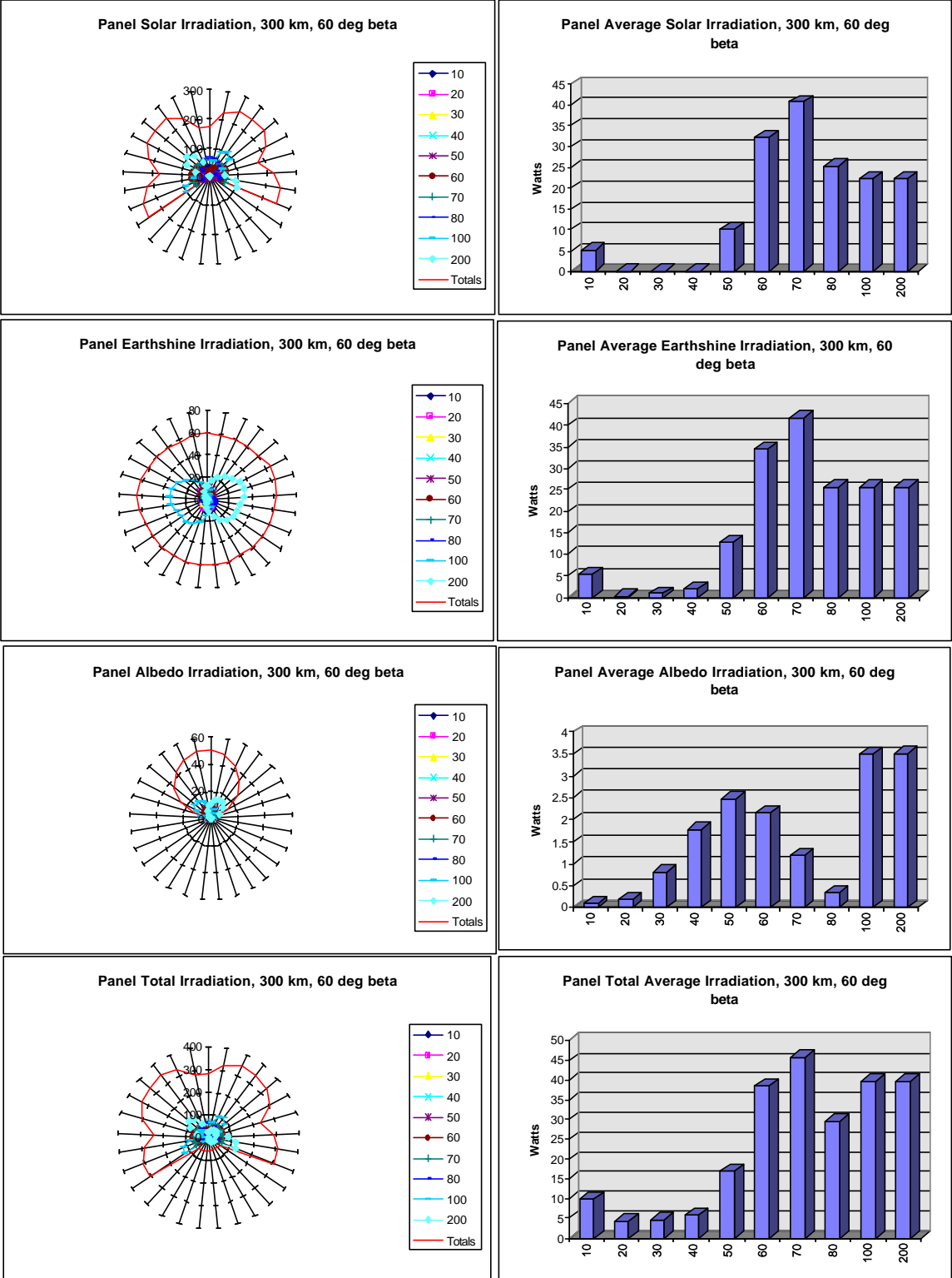


Figure 10.9.16 Panel-Wise Orbit Heat Rates, 300 km, 60 deg beta

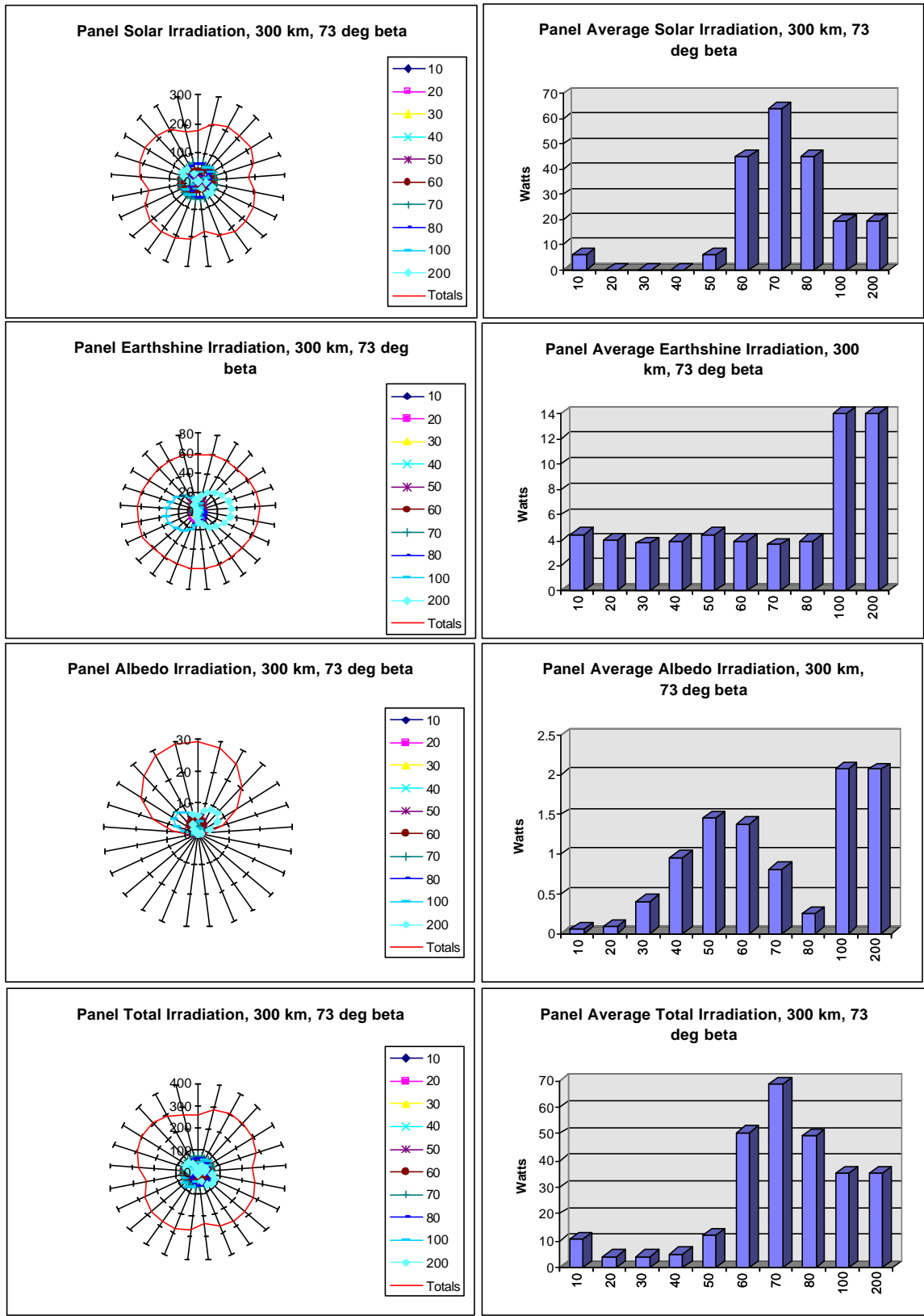


Figure 10.9.17 Panel-Wise Orbit Heat Rates, 300 km, 73 deg beta

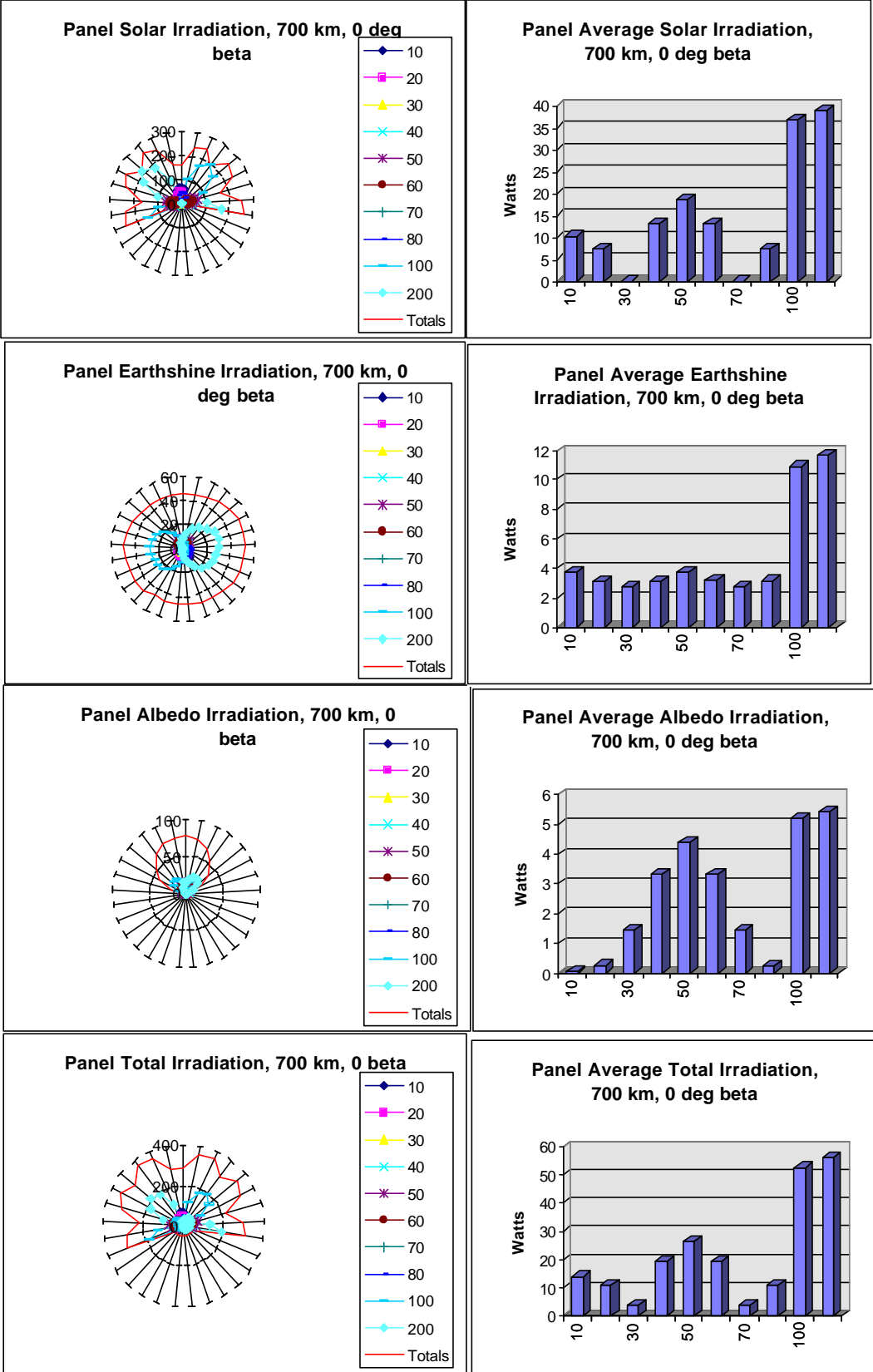


Figure 10.9.18 Panel-Wise Orbit Heat Rates, 700 km, 0 deg beta

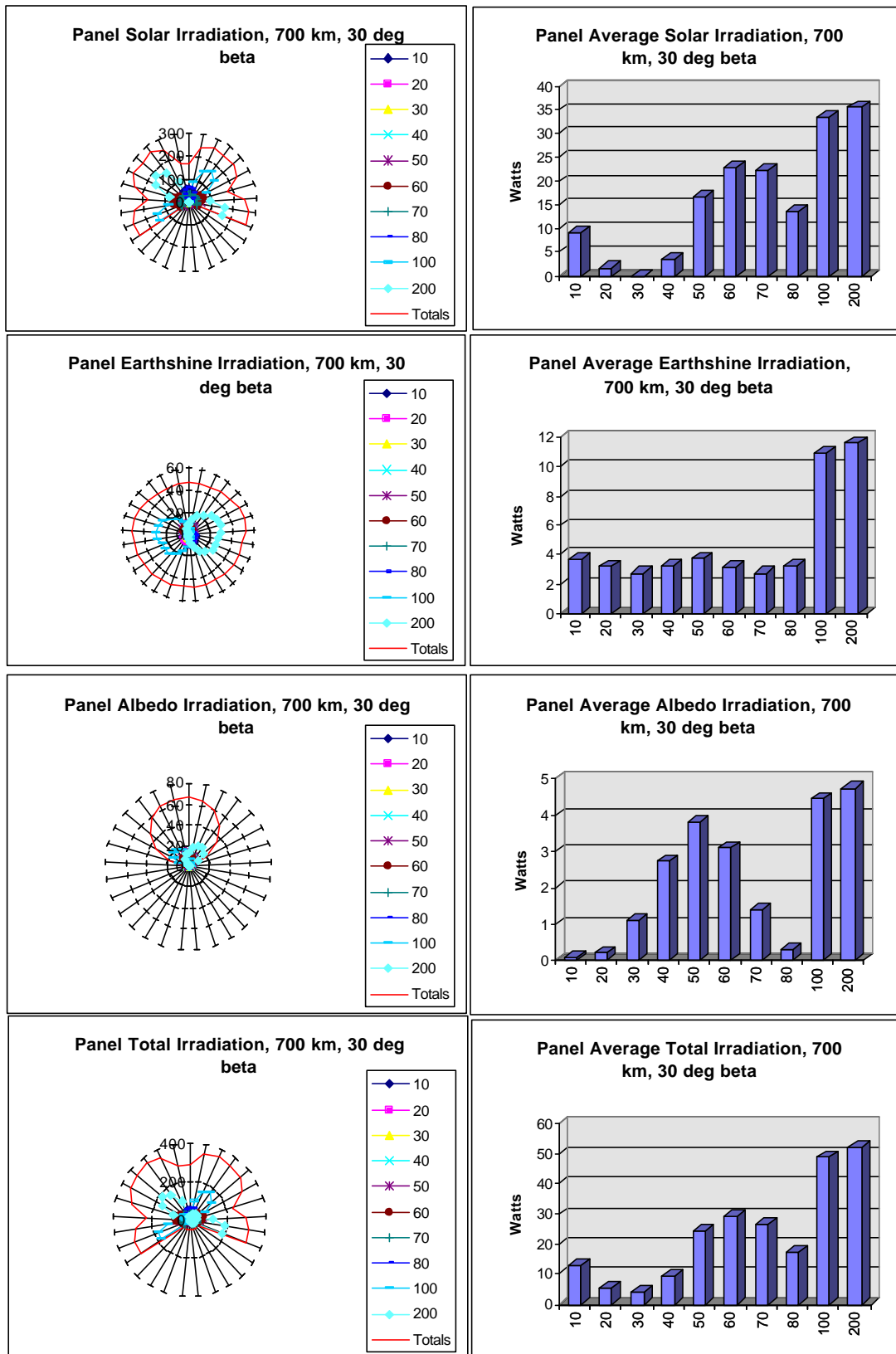


Figure 10.9.19 Panel-Wise Orbit Heat Rates, 700 km, 30 deg beta

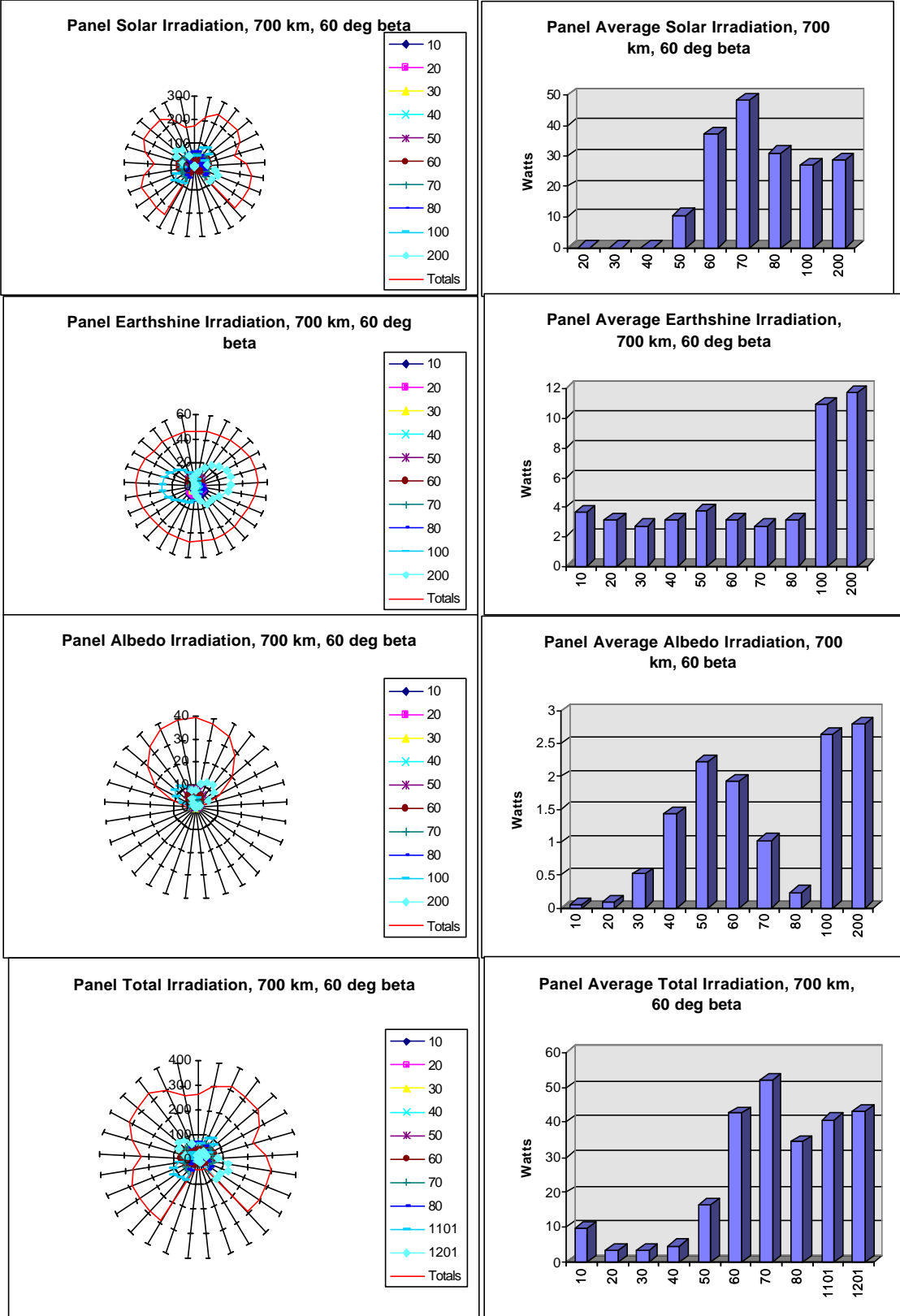


Figure 10.9.20 Panel-Wise Orbit Heat Rates, 700 km, 60 deg beta

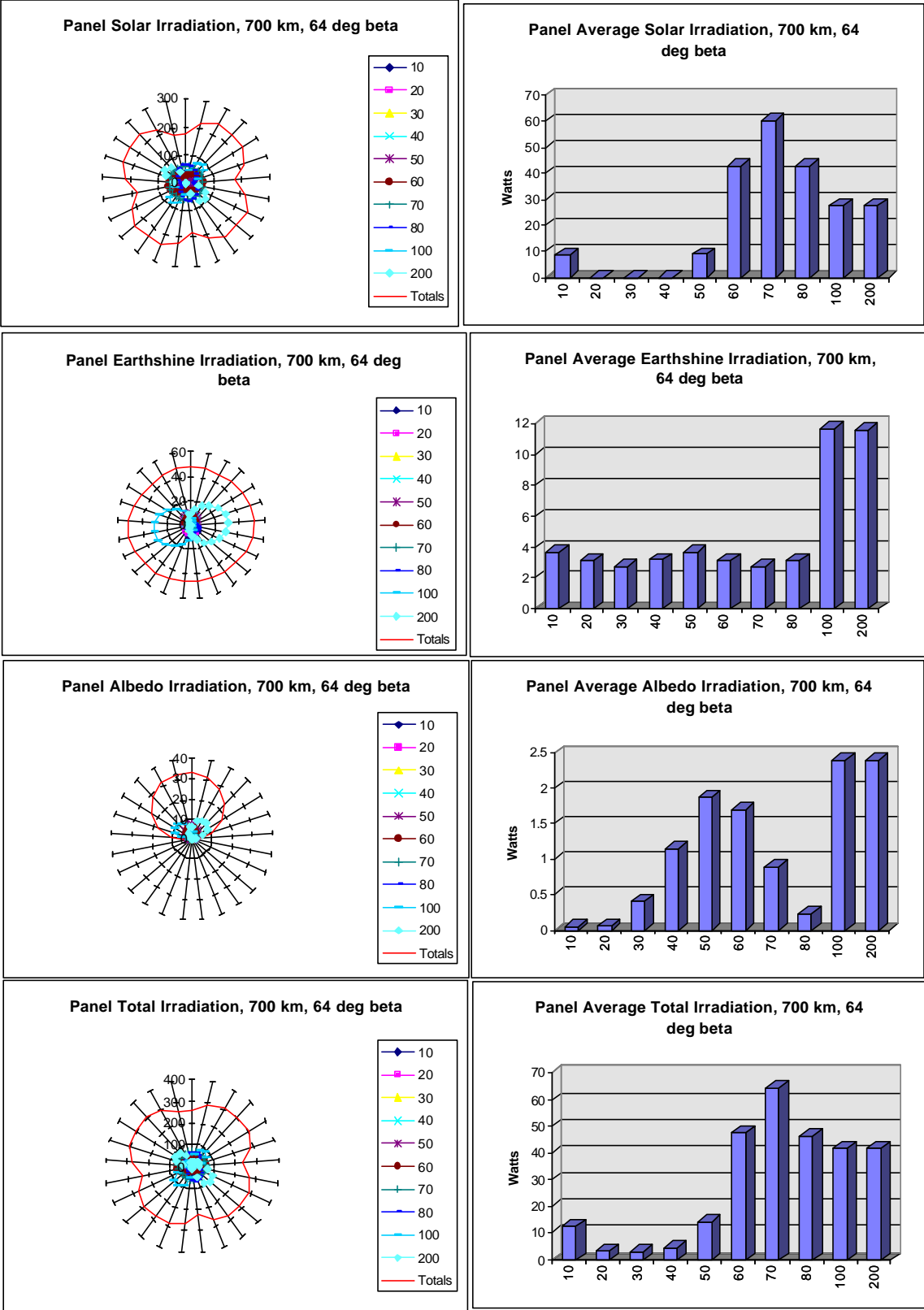


Figure 10.9.21 Panel-Wise Orbit Heat Rates, 700 km, 64 deg beta

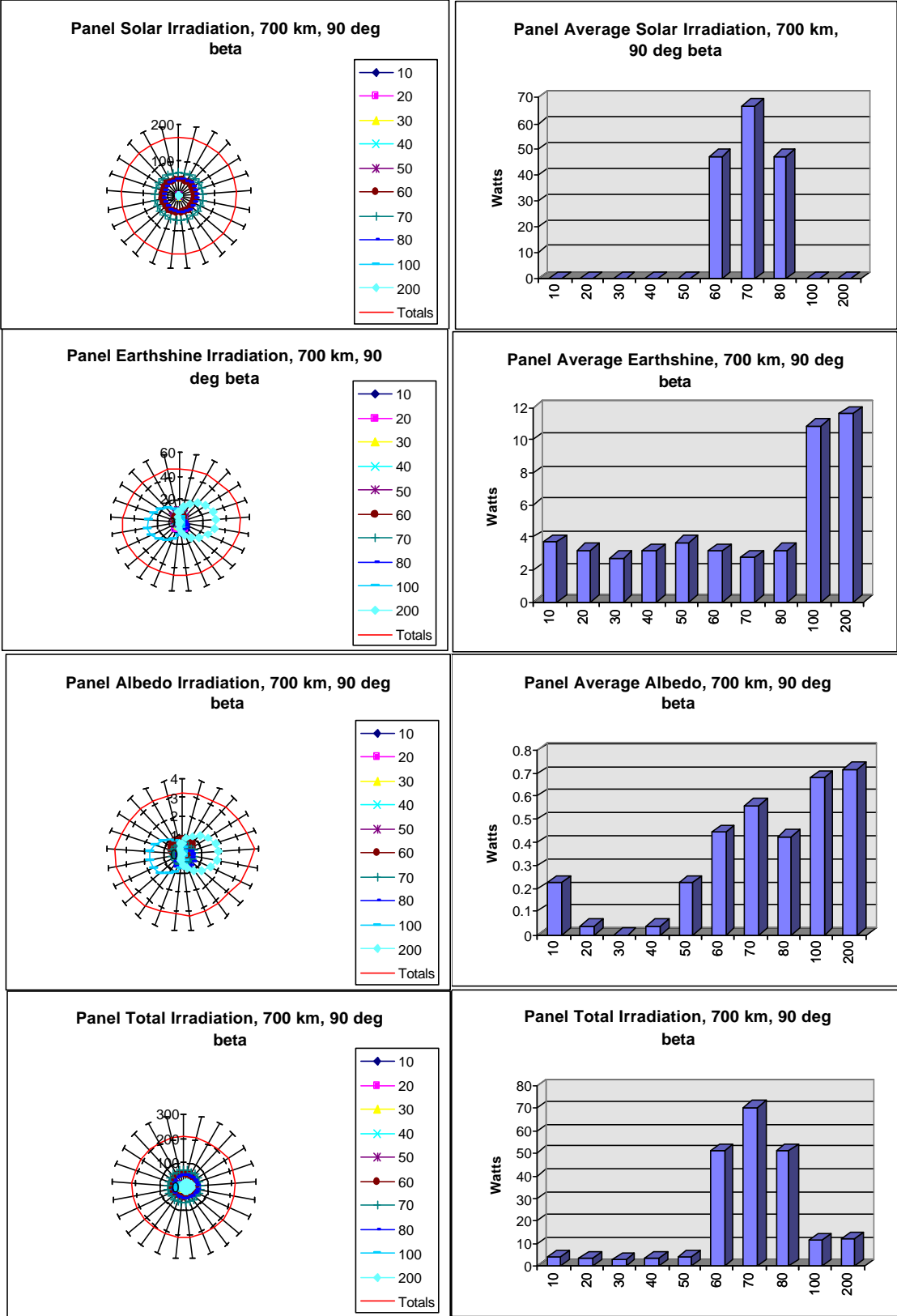


Figure 10.9.22 Panel-Wise Orbit Heat Rates, 700 km, 90 deg beta

10.9.4 SINDA Analysis

10.9.4.1 *SINDA Files*

The following file is spart304.inp, which is the input file for the 304-node model of Spartnik. The code has been broken up with explanations in places where the comments within the code are inadequate.

```
TITLE SPARTNIK 302_node MODEL
MODEL=MODEL
USER1= tmp.out
OUTPUT = scsub.out
```

HEADER USER DATA, GLOBAL

```
QS1=0.
QS2=0.
QS3=0.
QS4=0.
QS5=0.
QS6=0.
QS7=0.
QS8=0.
QS9=0.
QS10=0.
QE1=0.
QE2=0.
QE3=0.
QE4=0.
QE5=0.
QE6=0.
QE7=0.
QE8=0.
QE9=0.
QE10=0.
QSOL=0.
QES=0.
QSOLTB=0.
QESTB=0.
```

HEADER CONTROL DATA, GLOBAL

```
ABSZRO = -273.15
SIGMA = 5.67E-8
NLOOPS = 1000
```

OUTPUT = 1000.
DTIMEH = 60.
DTIMES = 0.0

TIMEND is the time to complete one orbit multiplied by the amount of orbits desired for analysis. The time to complete one orbit will need to change depending on what orbit is used to generate the heat rate file listed in the INCLUDE statement.

TIMEND = 5422.1*2 \$2 ORBITS
TIMEO = 0.0

The following are the node definitions for the 304 nodes in this model. The last entry of each line of code is the mass multiplied by c_p . The value of c_p used is 875 J/kg*K. The values for the mass can be found in the Structures FDR.

HEADER NODE DATA, MAIN

GEN 10,9,1, 0., 32.36285	\$ OUTER FACES W/ SP
GEN 20,9,1, 0., 32.36285	\$ 875 =Cp OF 2024 T-3
GEN 30,9,1, 0., 32.36285	\$ IN J/kg*K
GEN 40,9,1, 0., 32.36285	\$ MASS OF SIDE IN kg
GEN 50,9,1, 0., 32.36285	
GEN 60,9,1, 0., 32.36285	
GEN 70,9,1, 0., 32.36285	
GEN 80,9,1, 0., 32.36285	
GEN 1010,4,1, 0., 7.66346	+\$Z,OUTSIDE
GEN 1014,8,1, 0., 48.16324	\$W/ SP
GEN 1022,4,1, 0., 22.241625	
GEN 1050,4,1, 0., 7.22691375	-\$Z,OUTSIDE
GEN 1054,8,1, 0., 46.914875	\$W/ SP
GEN 1062,4,1, 0., 304.518375	\$W/ LVA
GEN 100,4,1, 0., 9.02951389	\$ INSIDE FACES
104, 0., 360.63247	\$ MASS ENHANCER
GEN 105,4,1, 0., 9.029514	
GEN 200,9,1, 0., 9.029514	
GEN 300,9,1, 0., 9.029514	
GEN 400,9,1, 0., 9.029514	
GEN 500,4,1, 0., 9.029514	
504, 0., 360.63247	\$ MASS ENHANCER
GEN 505,4,1, 0., 9.029514	
GEN 600,9,1, 0., 9.029514	
GEN 700,9,1, 0., 9.029514	
GEN 800,9,1, 0., 9.029514	
GEN 1110,4,1, 0., 875 * .00875824	+\$Z,inside
GEN 1114,8,1, 0., 875 * .0250437	
GEN 1122,4,1, 0., 875 * .025419	

```

GEN 1150,4,1, 0., 875 * .00825933    $-Z,inside
GEN 1154,8,1, 0., 875 * .023617
GEN 1162,4,1, 0., 875 * .023971
911,0., 875 * 2.748                    $camera w/ camera box
921,0., 875 * 2.9392                    $ bat box A
925,0., 836.7                            $ bat A
931,0., 875 * 2.9392                    $ bat box B
935,0., 836.7                            $ bat B
941,0., 875 * .1227                      $ junction box A
951,0., 875 * .1227                      $ junction box B
961,0., 875 * .96                        $ circuit discharge box/POWBX
971,0., 875 * 2.8654                      $ computer box
920,0., 875 * .20585                      $ payload tray,top
940,0., 875 * .20585                      $ payload tray,bottom
960,0., 875 * .32785                      $ power tray,top
980,0., 875 * .32785                      $ power tray,bottom!!21.391325 kg
GEN 981,16,1, 0., 875 * .02099           $ VERTEX BRACKETS
-2001, -273.15, 1.                        $Space

```

The nodes below are arithmetic nodes. Arithmetic nodes have zero capacitance. They have been used here to model interior radiation. The use here is for estimation since no software was available at this time for view factor calculation.

```

C    ARITHMETIC NODES FOR INTERIOR RADIATION
9000,0., -1.                            $ TOP THIRD
9500,0., -1.                            $ BOTTOM THIRD

```

These are the heat inputs generated by Spartnik. These are orbit average values. A function can be written instead to better characterize the spikes in temperature but this was deemed unnecessary.

```

HEADER SOURCE DATA, MAIN
925, 3.354                                $BAT A
C    935, 3.354                            $BAT B
911, 0.0725                               $CAMERA BOX
971, 7.0                                  $COMPUTER BOX

```

The following are conductors and radiation conductors (RADK). RADKs are preceded by negative signs.

The conductors immediately below represent the conduction through the honeycomb shell and the radiation between the two facing aluminum sheets of the honeycomb shell. The values used for these are from a proprietary Lockheed document. These values also apply to the payload and power trays.

```

HEADER CONDUCTOR DATA, MAIN
C    CONDUCTION THROUGH THE HONEYCOMB SHELL

```

GEN 2010,9,1, 10,1, 100,1, .14274	\$SIDE 1
GEN 2020,9,1, 20,1, 200,1, .14274	
GEN 2030,9,1, 30,1, 300,1, .14274	
GEN 2040,9,1, 40,1, 400,1, .14274	
GEN 2050,9,1, 50,1, 500,1, .14274	
GEN 2060,9,1, 60,1, 600,1, .14274	
GEN 2070,9,1, 70,1, 700,1, .14274	
GEN 2080,9,1, 80,1, 800,1, .14274	
GEN 2090,4,1, 1010,1, 1110,1, 25.9*.0040658	\$+-Z FACE
GEN 2100,8,1, 1014,1, 1114,1, 25.9*.01162608	
GEN 2110,4,1, 1022,1, 1122,1, 25.9*.0118	
GEN 2120,4,1, 1050,1, 1150,1, 25.9*.0040658	
GEN 2130,8,1, 1054,1, 1154,1, 25.9*.01162608	
GEN 2140,4,1, 1062,1, 1162,1, 25.9*.0118	

C RADK BETWEEN SIDES WITHIN THE HONEY COMB

GEN -9010,9,1, 10,1, 100,1, 1038.5*.0496/9	\$SIDE 1
GEN -9020,9,1, 20,1, 200,1, 1038.5*.0496/9	
GEN -9030,9,1, 30,1, 300,1, 1038.5 *.0496/9	
GEN -9040,9,1, 40,1, 400,1, 1038.5 *.0496/9	
GEN -9050,9,1, 50,1, 500,1, 1038.5 *.0496/9	
GEN -9060,9,1, 60,1, 600,1, 1038.5*.0496/9	
GEN -9070,9,1, 70,1, 700,1, 1038.5*.0496/9	
GEN -9080,9,1, 80,1, 800,1, 1038.5*.0496 /9	
GEN -9090,4,1, 1010,1, 1110,1, 1038.5*.0040658	\$+-Z FACE
GEN -9100,8,1, 1014,1, 1114,1, 1038.5*.01162608	
GEN -9110,4,1, 1022,1, 1122,1, 1038.5*.0118	
GEN -9120,4,1, 1050,1, 1150,1, 1038.5*.0040658	
GEN -9130,8,1, 1054,1, 1154,1, 1038.5*.01162608	
GEN -9140,4,1, 1062,1, 1162,1, 1038.5*.0118	

The following are the conductors for the interior components of Spartnik.

C INTERIOR CONDUCTION	k=168 W/m*K for 6061 T-6 AL
2200,961,960, 168 * .024194/.03175	\$circuit discharge to power tray bottom
2201,961,921, 168 * .01613/.07949	\$circuit discharge to bat A
2202,961,931, 168 * .01613/.07949	\$circuit discharge to bat B
2203,920,940, .098759 *25.9	\$cond through payload tray
2204,960,980, .098759 *25.9	\$cond through power tray

In order to better characterize the temperature of the batteries rather than the temperature of the battery box, separate nodes were added to represent the batteries. Also, the G value for the conductors that connect the payload and power trays were calculated by adding separate conductors for the connections between the battery box cover and the payload tray and the battery box cover to the battery box in series. This gives a better representation of what the battery temperature really is as compared to having only a single node for each battery box assembly.

2205,921,940, 36.6	\$bat A to payload tray bottom
2206,921,960, 36.6	\$bat A to power tray top
2207,931,940, 36.6	\$bat B to payload tray bottom
2208,931,960, 36.6	\$bat B to power tray top
2209,941,960, 168 * .0062097/.01905	\$junction A to power tray top
2210,951,960, 168 * .0062097/.01905	\$junction B to power tray top
2211,941,921, 168 * .0053226/ .05687	\$junct. A to bat A
2212,951,931, 168 * .0053226 / .05687	\$junct. B to bat B
GEN 2220,4,1, 1162,1, 971,0, 1.281	\$comp. to -Z OK?
GEN 2240,4,1, 1122,1, 911,0, 2.0	\$camera to +Z

The G values calculated by adding the G values battery core to the battery and the battery to the battery box in series.

2255,921,925,246.8	\$batA to batboxA
2256,931,935,246.8	\$batB to batboxB

The aluminum stand-offs were not modeled with nodes. Instead they were modeled using the G value from the program post.inp which was a SINDA program with TSS RADK values of one aluminum standoff in a cavity.

C CONDUCTION THROUGH ALUMINUM POSTS

C correct G value for conduction post based on
C tray and Z face Temps. G value comes from the post.inp
C model
GEN 2260,4,1, 1122,1, 920,0, .248
GEN 2264,4,1, 1162,1, 980,0, .248

C LATERAL CONDUCTION THROUGH THE SHELL INSIDE FACE

GEN 2275,2,1, 100,1, 101,1, 177 * .000635*.083/.06 \$OUTSIDE
GEN 2278,2,1, 200,1, 201,1, 177 * .000635*.083/.06 \$CONNECTED
GEN 2280,2,1, 300,1, 301,1, 177 * .000635*.083/.06 \$ROW 1
GEN 2283,2,1, 400,1, 401,1, 177 * .000635*.083/.06 \$HORIZ.
GEN 2285,2,1, 500,1, 501,1, 177 * .000635*.083/.06 \$k=177W/m*K
GEN 2388,2,1, 600,1, 601,1, 177 * .000635*.083/.06 \$2024 T-3AL
GEN 2290,2,1, 700,1, 701,1, 177 * .000635*.083/.06
GEN 2293,2,1, 800,1, 801,1, 177 * .000635*.083/.06
GEN 2295,2,1, 103,1, 104,1, 177 * .000635*.083/.06 \$OUTSIDE
GEN 2298,2,1, 203,1, 204,1, 177 * .000635*.083/.06 \$CONNECTED
GEN 2300,2,1, 303,1, 304,1, 177 * .000635*.083/.06 \$ ROW 2
GEN 2303,2,1, 403,1, 404,1, 177 * .000635*.083/.06 \$ HORIZ.
GEN 2305,2,1, 503,1, 504,1, 177 * .000635*.083/.06
GEN 2308,2,1, 603,1, 604,1, 177 * .000635*.083/.06
GEN 2310,2,1, 703,1, 704,1, 177 * .000635*.083/.06
GEN 2313,2,1, 803,1, 804,1, 177 * .000635*.083/.06

GEN 2315,2,1, 106,1, 107,1, 177 * .000635*.083/.06 \$OUTSIDE
 GEN 2318,2,1, 206,1, 207,1, 177 * .000635*.083/.06 \$ROW 3
 GEN 2320,2,1, 306,1, 307,1, 177 * .000635*.083/.06 \$ HORIZ.
 GEN 2323,2,1, 406,1, 407,1, 177 * .000635*.083/.06
 GEN 2325,2,1, 506,1, 507,1, 177 * .000635*.083/.06
 GEN 2328,2,1, 606,1, 607,1, 177 * .000635*.083/.06
 GEN 2330,2,1, 706,1, 707,1, 177 * .000635*.083/.06
 GEN 2333,2,1, 806,1, 807,1, 177 * .000635*.083/.06
 GEN 2335,2,1, 100,3, 103,3, 177 * .000635*.06/.083 \$VERT.
 GEN 2338,2,1, 101,3, 104,3, 177 * .000635*.06/.083 \$SIDE 1
 GEN 2340,2,1, 102,3, 105,3, 177 * .000635*.06/.083
 GEN 2345,2,1, 200,3, 203,3, 177 * .000635*.06/.083 \$SIDE 2
 GEN 2350,2,1, 201,3, 204,3, 177 * .000635*.06/.083
 GEN 2355,2,1, 202,3, 205,3, 177 * .000635*.06/.083
 GEN 2360,2,1, 300,3, 303,3, 177 * .000635*.06/.083 \$SIDE 3
 GEN 2365,2,1, 301,3, 304,3, 177 * .000635*.06/.083
 GEN 2370,2,1, 302,3, 305,3, 177 * .000635*.06/.083
 GEN 2375,2,1, 400,3, 403,3, 177 * .000635*.06/.083 \$SIDE 4
 GEN 2380,2,1, 401,3, 404,3, 177 * .000635*.06/.083
 GEN 2385,2,1, 402,3, 405,3, 177 * .000635*.06/.083
 GEN 2390,2,1, 500,3, 503,3, 177 * .000635*.06/.083 \$SIDE 5
 GEN 2395,2,1, 501,3, 504,3, 177 * .000635*.06/.083
 GEN 2405,2,1, 502,3, 505,3, 177 * .000635*.06/.083
 GEN 2410,2,1, 600,3, 603,3, 177 * .000635*.06/.083 \$SIDE 6
 GEN 2415,2,1, 601,3, 604,3, 177 * .000635*.06/.083
 GEN 2420,2,1, 602,3, 605,3, 177 * .000635*.06/.083
 GEN 2425,2,1, 700,3, 703,3, 177 * .000635*.06/.083 \$SIDE 7
 GEN 2430,2,1, 701,3, 704,3, 177 * .000635*.06/.083
 GEN 2435,2,1, 702,3, 705,3, 177 * .000635*.06/.083
 GEN 2440,2,1, 800,3, 803,3, 177 * .000635*.06/.083 \$SIDE 8
 GEN 2445,2,1, 801,3, 804,3, 177 * .000635*.06/.083
 GEN 2450,2,1, 802,3, 805,3, 177 * .000635*.06/.083

C LATERAL CONDUCTION THROUGH THE SHELL OUTSIDE FACE

GEN 2500,2,1, 10,1, 11,1, 177 * .000635*.083/.06 \$OUTSIDE
 2509,12,20,177 * .000635*.083/.06 \$ROW 1 HORIZ.
 GEN 2510,2,1, 20,1, 21,1, 177 * .000635*.083/.06
 2519,22,30,177 * .000635*.083/.06
 GEN 2520,2,1, 30,1, 31,1, 177 * .000635*.083/.06
 2529,32,40,177 * .000635*.083/.06
 GEN 2530,2,1, 40,1, 41,1, 177 * .000635*.083/.06
 2539,42,50,177 * .000635 *.083/.06
 GEN 2540,2,1, 50,1, 51,1, 177 * .000635*.083/.06
 2549,52,60,177 * .000635*.083/.06
 GEN 2550,2,1, 60,1, 61,1, 177 * .000635*.083/.06
 2559,62,70,177 * .000635*.083/.06

C

GEN 2560,2,1, 70,1, 71,1, 177 * .000635*.083/.06
2569,72,80,177 * .000635*.083/.06
GEN 2570,2,1, 80,1, 81,1, 177 * .000635 *.083/.06
GEN 2580,2,1, 13,1, 14,1, 177 * .000635 *.083/.06 \$OUTSIDE
\$CONNECTED
\$ROW 2 HORIZ.
2589,15,23,177 * .000635*.083/.06
GEN 2590,2,1, 23,1, 24,1, 177 * .000635*.083/.06
2599,25,33,177 * .000635*.083/.06
GEN 2600,2,1, 33,1, 34,1, 177 * .000635*.083/.06
2609,35,43,177 * .000635*.083/.06
GEN 2610,2,1, 43,1, 44,1, 177 * .000635*.083/.06
2619,45,53,177 * .000635*.083/.06
GEN 2620,2,1, 53,1, 54,1, 177 * .000635*.083/.06
2629,55,63,177 * .000635*.083/.06
GEN 2630,2,1, 63,1, 64,1, 177 * .000635*.083/.06
2639,65,73,177 * .000635 *.083/.06
GEN 2640,2,1, 73,1, 74,1, 177 * .000635*.083/.06
2649,75,83,177 * .000635*.083/.06
GEN 2650,2,1, 83,1, 84,1, 177 * .000635*.083/.06

GEN 2660,2,1, 16,1, 17,1, 177 * .000635*.083/.06 \$OUTSIDE
2669,18,26,177 * .000635 *.083/.06 \$CONNECTED
GEN 2670,2,1, 26,1, 27,1, 177 * .000635*.083/.06 \$ROW 3 HORIZ.
2679,28,36,177 * .000635 *.083/.06
GEN 2680,2,1, 36,1, 37,1, 177 * .000635*.083/.06
2689,38,46,177 * .000635 *.083/.06
GEN 2690,2,1, 46,1, 47,1, 177 * .000635*.083/.06
2699,48,56,177 * .000635 *.083/.06
GEN 2700,2,1, 56,1, 57,1, 177 * .000635*.083/.06
2709,58,66,177 * .000635 *.083/.06
GEN 2710,2,1, 66,1, 67,1, 177 * .000635*.083/.06
2719,68,76,177 * .000635 *.083/.06
GEN 2720,2,1, 76,1, 77,1, 177 * .000635*.083/.06
2729,78,86,177 * .000635 *.083/.06
GEN 2730,2,1, 86,1, 87,1, 177 * .000635*.083/.06
GEN 2735,2,1, 10,3, 13,3, 177 * .000635*.06/.083 \$VERT.CONNECT.
GEN 2740,2,1, 11,3, 14,3, 177 * .000635*.06/.083 \$SIDE 1
GEN 2745,2,1, 12,3, 15,3, 177 * .000635*.06/.083
GEN 2750,2,1, 20,3, 23,3, 177 * .000635*.06/.083 \$SIDE 2
GEN 2755,2,1, 21,3, 24,3, 177 * .000635*.06/.083
GEN 2760,2,1, 22,3, 25,3, 177 * .000635*.06/.083
GEN 2765,2,1, 30,3, 33,3, 177 * .000635*.06/.083 \$SIDE 3
GEN 2770,2,1, 31,3, 34,3, 177 * .000635*.06/.083
GEN 2775,2,1, 32,3, 35,3, 177 * .000635*.06/.083
GEN 2780,2,1, 40,3, 43,3, 177 * .000635*.06/.083 \$SIDE 4
GEN 2785,2,1, 41,3, 44,3, 177 * .000635*.06/.083

GEN 2790,2,1, 42,3, 45,3, 177 * .000635*.06/.083
 GEN 2795,2,1, 50,3, 53,3, 177 * .000635*.06/.083 \$SIDE 5
 GEN 2800,2,1, 51,3, 54,3, 177 * .000635*.06/.083
 GEN 2805,2,1, 52,3, 55,3, 177 * .000635*.06/.083
 GEN 2810,2,1, 60,3, 63,3, 177 * .000635*.06/.083 \$SIDE 6
 GEN 2815,2,1, 61,3, 64,3, 177 * .000635*.06/.083
 GEN 2820,2,1, 62,3, 65,3, 177 * .000635*.06/.083
 GEN 2825,2,1, 70,3, 73,3, 177 * .000635*.06/.083 \$SIDE 7
 GEN 2830,2,1, 71,3, 74,3, 177 * .000635*.06/.083
 GEN 2835,2,1, 72,3, 75,3, 177 * .000635*.06/.083
 GEN 2840,2,1, 80,3, 83,3, 177 * .000635*.06/.083 \$SIDE 8
 GEN 2845,2,1, 81,3, 84,3, 177 * .000635*.06/.083
 GEN 2850,2,1, 82,3, 85,3, 177 * .000635*.06/.083

C LATERAL CONDUCTION THROUGH +Z INNER FACE

2855, 1110,1114,177 * .000635 * .09 / .0998
 2856, 1111,1115,177 * .000635 * .09 / .0998
 2857, 1112,1120,177 * .000635 * .09 / .0998
 2858, 1113,1121,177 * .000635 * .09 / .0998
 2859, 1110,1116,177 * .000635 * .09 / .0998
 2860, 1111,1117,177 * .000635 * .09 / .0998
 2861, 1112,1118,177 * .000635 * .09 / .0998
 2862, 1113,1119,177 * .000635 * .09 / .0998
 2863, 1114,1122,177 * .000635
 2864, 1115,1123,177 * .000635
 2865, 1116,1122,177 * .000635
 2866, 1117,1123,177 * .000635
 2867, 1118,1124,177 * .000635
 2868, 1119,1125,177 * .000635
 2869, 1120,1124,177 * .000635
 2870, 1121,1125,177 * .000635
 2871, 1122,1123,177 * .000635
 2872, 1122,1124,177 * .000635
 2873, 1123,1125,177 * .000635
 2874, 1124,1125,177 * .000635

C LATERAL CONDUCTION THROUGH +Z OUTER FACE

2875, 1010,1014,177 * .000635 * .09 / .0998
 2876, 1011,1015,177 * .000635 * .09 / .0998
 2877, 1012,1020,177 * .000635 * .09 / .0998
 2878, 1013,1021,177 * .000635 * .09 / .0998
 2879, 1010,1016,177 * .000635 * .09 / .0998
 2880, 1011,1017,177 * .000635 * .09 / .0998
 2881, 1012,1018,177 * .000635 * .09 / .0998
 2882, 1013,1019,177 * .000635 * .09 / .0998
 2883, 1014,1022,177 * .000635

2884, 1015,1023,177 * .000635
2885, 1016,1022,177 * .000635
2886, 1017,1023,177 * .000635
2887, 1018,1024,177 * .000635
2888, 1019,1025,177 * .000635
2889, 1020,1024,177 * .000635
2890, 1021,1025,177 * .000635
2891, 1022,1023,177 * .000635
2892, 1122,1124,177 * .000635
2893, 1123,1125,177 * .000635
2894, 1124,1125,177 * .000635

C LATERAL CONDUCTION THROUGH -Z INNER FACE

2895, 1150,1154,177 * .000635 * .09 / .0998
2896, 1151,1155,177 * .000635 * .09 / .0998
2897, 1152,1160,177 * .000635 * .09 / .0998
2898, 1153,1161,177 * .000635 * .09 / .0998
2899, 1150,1156,177 * .000635 * .09 / .0998
2900, 1151,1157,177 * .000635 * .09 / .0998
2901, 1152,1158,177 * .000635 * .09 / .0998
2902, 1153,1159,177 * .000635 * .09 / .0998
2903, 1154,1162,177 * .000635
2904, 1155,1163,177 * .000635
2905, 1156,1162,177 * .000635
2906, 1157,1163,177 * .000635
2907, 1158,1164,177 * .000635
2908, 1159,1165,177 * .000635
2909, 1160,1164,177 * .000635
2910, 1161,1165,177 * .000635
2911, 1162,1163,177 * .000635
2912, 1162,1164,177 * .000635
2913, 1163,1165,177 * .000635
2914, 1164,1165,177 * .000635

C LATERAL CONDUCTION THROUGH -Z OUTER FACE

2915, 1150,1154,177 * .000635 * .09 / .0998
2916, 1151,1155,177 * .000635 * .09 / .0998
2917, 1152,1160,177 * .000635 * .09 / .0998
2918, 1153,1161,177 * .000635 * .09 / .0998
2919, 1150,1156,177 * .000635 * .09 / .0998
2920, 1151,1157,177 * .000635 * .09 / .0998
2921, 1152,1158,177 * .000635 * .09 / .0998
2922, 1153,1159,177 * .000635 * .09 / .0998
2923, 1154,1162,177 * .000635
2924, 1155,1163,177 * .000635
2925, 1156,1162,177 * .000635

2926, 1157,1163,177 * .000635
 2927, 1158,1164,177 * .000635
 2928, 1159,1165,177 * .000635
 2929, 1160,1164,177 * .000635
 2930, 1161,1165,177 * .000635
 2931, 1162,1163,177 * .000635
 2932, 1162,1164,177 * .000635
 2933, 1163,1165,177 * .000635
 2934, 1164,1165,177 * .000635

The following is the conduction through the aluminum vertex brackets inside the shell of Spartnik.

C LATERAL CONDUCTION THROUGH THE SHELL BRACKETS

GEN 2935,8,1, 102,100, 981,1, 168 * .0004937/.00191
 GEN 2943,8,1, 108,100, 989,1, 168 * .0004937/.00191
 GEN 2951,7,1, 981,1, 200,100, 168 * .0004937/.00191
 2958, 989, 100, 168 * .0004937/.00191
 GEN 2959,7,1, 989,1, 206,100, 168 * .0004937/.00191
 2967, 996, 106, 168 * .0004937/ .00191

C CONDUCTION THROUGH TOP OF SHELL THROUGH BRACKETS

GEN 2968,7,1, 1115,1, 981,1, 168 * .00115/.00191
 2975, 1114, 989, 168 * .00115/.00191
 GEN 2976,7,1, 1155,1, 989,1, 168 * .00115/.00191
 2983, 1154, 996, 168 * .00115/.00191

C RAK'S TO ENVIROMENT

GEN -3010,9,1, 10,1, 2001,0, .03968/9 \$ sides eBar = .80,
 GEN -3020,9,1, 20,1, 2001,0, .03968/9 \$A=.0496
 GEN -3030,9,1, 30,1, 2001,0, .03968/9
 GEN -3040,9,1, 40,1, 2001,0, .03968/9
 GEN -3050,9,1, 50,1, 2001,0, .03968/9
 GEN -3060,9,1, 60,1, 2001,0, .03968/9
 GEN -3070,9,1, 70,1, 2001,0, .03968/9
 GEN -3080,9,1, 80,1, 2001,0, .03968/9
 GEN -3100,4,1, 1010,1, 2001,0, .0040658*.85897 \$+z eBar=.859,
 GEN -3110,8,1, 1014,1, 2001,0, .01162608*.85897\$A=.156
 GEN -3120,4,1, 1022,1, 2001,0, .0118*.85897 \$CORRECT AREA Z
 GEN -3200,4,1, 1050,1, 2001,0, .0040658*.60897 \$-z eBar=.609,
 GEN -3210,8,1, 1054,1, 2001,0, .01162608*.60897\$ A=.156
 GEN -3220,4,1, 1062,1, 2001,0, .0118*.60897

The RADKs below are attached to arithmetic nodes. These RADKs represent the top and bottom thirds of the interior radiation model.

C RADK inside e * A

GEN -4001,3,1,100,1,9000,0, .8 * .01653/3	\$side1 to top a. n
GEN -4005,3,1,106,1,9500,0, .8 * .01653/3	\$side1 to bottom a. n
GEN -4010,3,1,200,1,9000,0, .8 * .01653/3	\$side2 to top a. n
GEN -4015,3,1,206,1,9500,0, .8 * .01653/3	\$side2 to bottom a. n
GEN -4020,3,1,300,1,9000,0, .8 * .01653/3	\$side3 to top a. n
GEN -4025,3,1,306,1,9500,0, .8 * .01653/3	\$side3 to bottom a.n
GEN -4030,3,1,400,1,9000,0, .8 * .01653/3	\$side4 to top a.n
GEN -4035,3,1,406,1,9500,0, .8 * .01653/3	\$side4 to bottom a.n
GEN -4040,3,1,500,1,9000,0, .8 * .01653/3	\$side5 to top a. n
GEN -4045,3,1,506,1,9500,0, .8 * .01653/3	\$side5 to bottom a. n
GEN -4050,3,1,600,1,9000,0, .8 * .01653/3	\$side6 to top a. n
GEN -4055,3,1,606,1,9500,0, .8 * .01653/3	\$side6 to bottom a. n
GEN -4060,3,1,700,1,9000,0, .8 * .01653/3	\$side7 to top a. n
GEN -4065,3,1,706,1,9500,0, .8 * .01653/3	\$side7 to bottom a. n
GEN -4070,3,1,800,1,9000,0, .8 * .01653/3	\$side8 to top a. n
GEN -4075,3,1,806,1,9500,0, .8 * .01653/3	\$side8 to bottom a. n
GEN -4080,16,1,1110,1,9000,0, .8 * .15647/16	\$+Z
-4100,911,9000, .8 * .0147032	\$camera side 1
-4105,911,9000, .8 * .0147032	\$camera side 3
-4110,911,9000, .8 * .0147032	\$camera side 5
-4115,911,9000, .8 * .0147032	\$camera side 7
-4120,911,9000, .8 * .047716	\$camera bottom
-4125,920,9000, .8 * .098759	\$payload tray
-4130,971,9500, .8 * .005	\$computer side 1
-4135,971,9500, .8 * .0305	\$computer side 3
-4140,971,9500, .8 * .005	\$computer side 5
-4145,971,9500, .8 * .0305	\$computer side 7
-4150,971,9500, .8 * .098759	\$power tray
GEN -4155,16,1,1150,1,9500,0, .8 * .15647/16	\$-Z

The following represents the middle third of the interior radiation model.

C RADK'S FOR BATTERY TO SHELL e*A*VF

GEN -4170,3,1, 921,0, 103,1, .8 * (.00287/3) * .2
GEN -4175,3,1, 921,0, 203,1, .8 * (.00415/3) * .8
GEN -4180,3,1, 921,0, 203,1, .8 * (.00147/3) * .1
GEN -4185,3,1, 921,0, 303,1, .8 * (.01292/3) * .9
GEN -4190,3,1, 921,0, 403,1, .8 * (.00147/3) * .1
GEN -4195,3,1, 921,0, 403,1, .8 * (.00415/3) * .8
GEN -4200,3,1, 921,0, 503,1, .8 * (.00287/3) * .2
GEN -4205,3,1, 931,0, 503,1, .8 * (.00287/3) * .2
GEN -4210,3,1, 931,0, 603,1, .8 * (.00415/3) * .8

```

GEN -4215,3,1, 931,0, 603,1, .8 * (.00147/3) * .1
GEN -4220,3,1, 931,0, 703,1, .8 * (.01292/3) * .9
GEN -4225,3,1, 931,0, 803,1, .8 * (.00147/3) * .1
GEN -4230,3,1, 931,0, 803,1, .8 * (.00415/3) * .8
GEN -4235,3,1, 931,0, 103,1, .8 * (.00287/3) * .2

```

```

C   RADK BETWEEN HONEYCOMB TRAYS
-4240, 920, 940, 1038.5* .098759
-4245, 960, 980, 1038.5* .098759

```

This is the INCLUDE statement mentioned earlier in the text. To change the heat loads that Spartnik is subjected to, simply change the filename.

```

HEADER ARRAY DATA, MAIN
INCLUDE LOW00.HR

```

The DA11MC function linearly interpolates the data from the heat rate files. The first array (A1) contains the values of the time step for one orbit. Each value of time corresponds to a time when heat rates are generated. The arrays A2-A11 contain the heat loads due to solar and albedo radiation. The arrays A12-A21 contain the heat loads due to Earth IR. The arrays (A2-A21) represent the heat load on a side of the spacecraft (10 arrays for solar and albedo loads, and 10 arrays for the Earth IR loads). These heat loads change as the simulated spacecraft changes position in its orbit. This is how the tumble motion of one tumble per half orbit of Spartnik is simulated. Note that the first entry in the function call is the time for one orbit. This will need to change depending on what orbit is used to generate the heat rate file listed in the above INCLUDE statement.

```

HEADER VARIABLES 1, MAIN

```

```

C   THERE ARE 10 DIFF. SURFACES FOR WHICH HEAT RATES WERE GENERATED
C   THERE ARE CURRENTLY 104 EXTERNAL NODES TO WHICH HEAT RATES
C   SHALL BE APPLIED

```

```

F   COMMON/SJS1/QSA(10),QEA(10),NOD(302),AE(2,104)

```

```

CALL DA11MC(5422.1,TIMEM,A1,A2,1.0,QS1)
CALL DA11MC(5422.1,TIMEM,A1,A3,1.0,QS2)
CALL DA11MC(5422.1,TIMEM,A1,A4,1.0,QS3)
CALL DA11MC(5422.1,TIMEM,A1,A5,1.0,QS4)
CALL DA11MC(5422.1,TIMEM,A1,A6,1.0,QS5)
CALL DA11MC(5422.1,TIMEM,A1,A7,1.0,QS6)
CALL DA11MC(5422.1,TIMEM,A1,A8,1.0,QS7)
CALL DA11MC(5422.1,TIMEM,A1,A9,1.0,QS8)
CALL DA11MC(5422.1,TIMEM,A1,A10,1.0,QS9)
CALL DA11MC(5422.1,TIMEM,A1,A11,1.0,QS10)

```

```

CALL DA11MC(5422.1,TIMEM,A1,A12,1.0,QE1)
CALL DA11MC(5422.1,TIMEM,A1,A13,1.0,QE2)
CALL DA11MC(5422.1,TIMEM,A1,A14,1.0,QE3)

```

```

CALL DA11MC(5422.1,TIMEM,A1,A15,1.0,QE4)
CALL DA11MC(5422.1,TIMEM,A1,A16,1.0,QE5)
CALL DA11MC(5422.1,TIMEM,A1,A17,1.0,QE6)
CALL DA11MC(5422.1,TIMEM,A1,A18,1.0,QE7)
CALL DA11MC(5422.1,TIMEM,A1,A19,1.0,QE8)
CALL DA11MC(5422.1,TIMEM,A1,A20,1.0,QE9)
CALL DA11MC(5422.1,TIMEM,A1,A21,1.0,QE10)

```

This code simulates a rapid spin rate for the spacecraft by adding up the total flux on the eight sides of the spacecraft and dividing by the number of sides. In the original TSS file Spartnik was simulated with no spin. Taking the average value simulates a 'fast' spin. This gives an average flux. The original TSS surfaces had A= .069. We ratio the area here to the true A=.0496.

```

C CALC TOTAL INCIDENT FLUX ON SIDES

```

```

  QSOL=(QS1+QS2+QS3+QS4+QS5+QS6+QS7+QS8)/8 * (.0496/.069)

```

```

  QES=(QE1+QE2+QE3+QE4+QE5+QE6+QE7+QE8)/8 * (.0496/.069)

```

```

  QSOLTB=(QS9+QS10)/2 * (.156/.136)

```

```

  QESTB=(QE9+QE10)/2 * (.156/.136)

```

```

C EXT. SIDES ARE AT BEGINING OF NODE ARRAY, SEQUENCE NO.

```

```

C 10-80. TOP BOTTOM ARE SEQUENCE NUMBERS 1010-,1050-

```

This section of code stores the correct value of Q in the space allocated for each exterior node. The original TSS surfaces had alpha=1.0 and e=1.0 to allow us to easily adjust them here in the code.

```

  DO NTEST=1,72

```

```

F   QTEST=QSOL*AE(1,NTEST)+QES*AE(2,NTEST)

```

```

F   NUMB=NOD(NTEST)

```

```

F   Q(NUMB)=QTEST

```

```

  END DO

```

```

  DO NTEST=73,104

```

```

F   QTEST=QSOLTB*AE(1,NTEST)+QESTB*AE(2,NTEST)

```

```

F   NUMB=NOD(NTEST)

```

```

F   Q(NUMB)=QTEST

```

```

  END DO

```

```

HEADER OPERATIONS DATA

```

```

BUILD MODEL, MAIN

```

```

  CALL CALLAE

```

```

  CALL FORWRD

```

```

C   CALL QMAP('MAIN','ALL',0)

```

```

HEADER OUTPUT CALLS, MAIN

```

```
CALL TPRINT('ALL')
C CALL QPRINT('ALL')
```

HEADER SUBROUTINE DATA

```
FSTART
```

```
C *-----*
```

The purpose of this subroutine is to initialize the AE array. AE is a 2 by 104 array, which contains the values of area times emissivity and area times absorbtivity for the external nodes.

SUBROUTINE CALLAE

```
COMMON/SJS1/QSA(10),QEA(10),NOD(302),AE(2,104)
C DECLARE ARRAYS. DONT NEED TO PASS DATA TO OTHER FUNCTIONS
COMMON/SJS2/ISPSA(72)
COMMON/SJS3/ITOPEX(32)
```

```
DATA (ISPSA(N),N=1,72) /10,11,12,13,14,15,16,17,18,20,21,22,
c23,24,25,26,27,28,30,31,32,33,34,35,36,37,38,40,41,42,43,44,45,
c46,47,48,50,51,52,53,54,55,56,57,58,60,61,62,63,64,65,66,67,68,
c70,71,72,73,74,75,76,77,78,80,81,82,83,84,85,86,87,88/
```

```
DATA (ITOPEX(N),N=1,32) /1010,1011,1012,1013,1014,1015,1016,1017,
c1018,1019,1020,1021,1022,1023,1024,1025,1050,1051,1052,1053,1054,
c1055,1056,1057,1058,1059,1060,1061,1062,1063,1064,1065/
```

These are the thermal-optical properties for the exterior of the satellite. They can be varied to simulate the anodizing of the LVA plate or to vary the type of FOSR used.

```
SOLCST=.97
ALFSA = 0.71
ALFEX = 0.8
ALFLVA = .25
C ALFFOSR=.06
EMISSA = 0.8
EMISEX = 0.88
EMISLVA = .04
C EMISFOSR = .80
```

```
DO N=1,72
CALL NODTRN('MAIN',ISPSA(N),NOD(N))
AE(1,N) =ALFSA*SOLCST
AE(2,N) = EMISSA*SOLCST
END DO
```

```
DO N=1,4
CALL NODTRN('MAIN',ITOPEX(N),NOD(N+72))
```

```
AE(1,N+72) = ALFEX*SOLCST
AE(2,N+72) = EMISEX*SOLCST
END DO
```

```
DO N=1,8
  CALL NODTRN('MAIN',ITOPEX(N),NOD(N+76))
  AE(1,N+76) = ALFSP*SOLCST
  AE(2,N+76) = EMISSP*SOLCST
END DO
```

```
DO N=1,4
  CALL NODTRN('MAIN',ITOPEX(N),NOD(N+84))
  AE(1,N+84) = ALFEX*SOLCST
  AE(2,N+84) = EMISEX*SOLCST
END DO
```

```
DO N=1,4
  CALL NODTRN('MAIN',ITOPEX(N),NOD(N+88))
  AE(1,N+88) = ALFEX*SOLCST
  AE(2,N+88) = EMISEX*SOLCST
END DO
```

```
DO N=1,8
  CALL NODTRN('MAIN',ITOPEX(N),NOD(N+92))
  AE(1,N+92) = ALFSP*SOLCST
  AE(2,N+92) = EMISSP*SOLCST
END DO
```

```
DO N=1,4
  CALL NODTRN('MAIN',ITOPEX(N),NOD(N+100))
  AE(1,N+100) = ALFLVA*SOLCST
  AE(2,N+100) = EMISLVA*SOLCST
END DO
```

```
RETURN
END
```

FSTOP

END OF DATA

10.9.4.2 *SINDA Output*

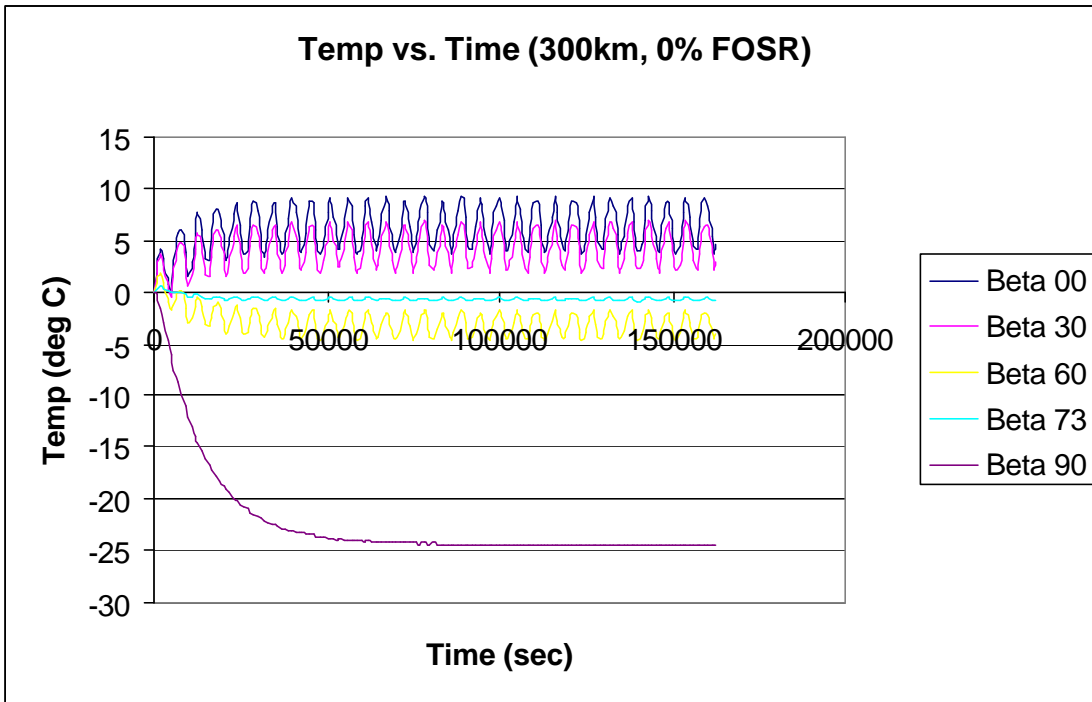


Figure 10.9.23 SINDA Results for Battery Temp Over 30 Orbits

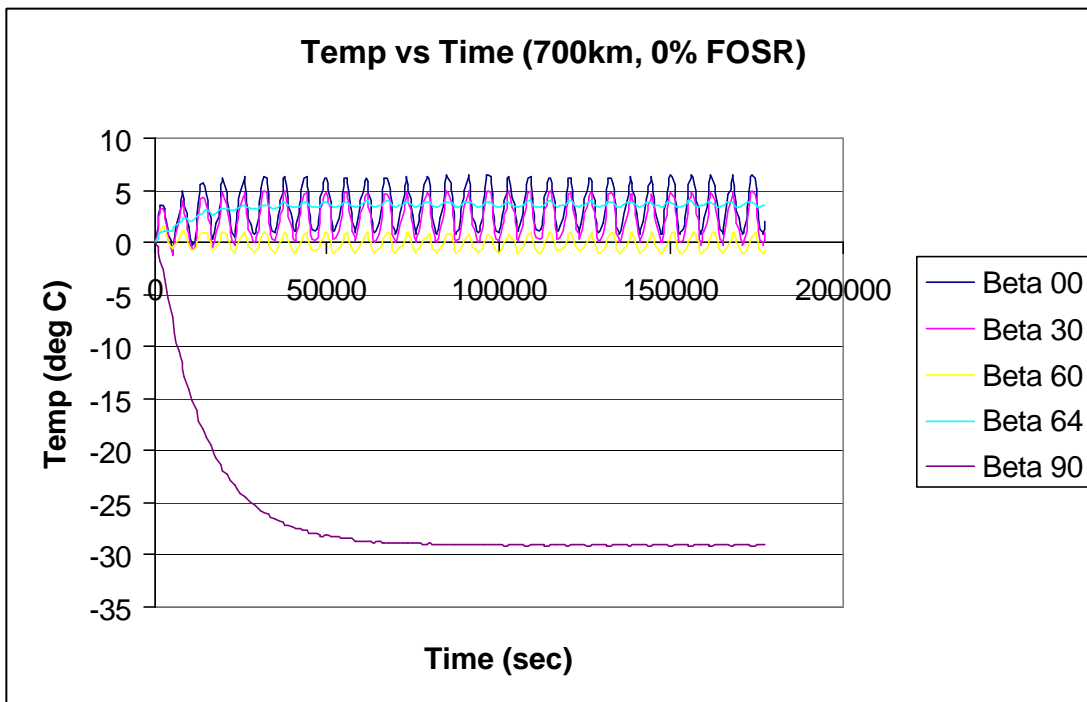


Figure 10.9.24 SINDA Results for Battery Temp Over 30 Orbits

10.9.5 SINDA 3D Analysis

SINDA 3D is a next-generation version of the SINDA program. It shares many of the same features of SINDA, and is capable of integrating geometric information about a thermal model into the solution process. Models generated in SINDA cannot be updated to a 3D-version, as there is no geometric information contained in them. The manufacturer also states that a conversion program or utility is not possible. Preliminary work has been done to create a 3D model of Spartnik, and the significant node locations and model construction techniques will be discussed below.

Some important issues concerning SINDA 3D's operation and limitations should be noted. Firstly, although the version of SINDA 3D in use by the Spartnik team is Windows-compatible and supports long filenames, the Fortran compiler that performs the model processing does not. Thus, model names must adhere to the conventional DOS-style 8.3 file names.

SINDA 3D makes use of property tables, which can be accessed at any time during the assembly and analysis of the thermal model. This enables ease of modification of heat loads and allows for solving the model under different orbital scenarios.

A model is constructed out of elements. Elements include nodes, plates and bricks. Plates are used when the temperature differential across the thickness of an element is not expected to be significant, and bricks are used when it is expected to be significant. In the current Spartnik model, the outer shell is constructed of plates that represent the honeycomb, and bricks for the various internal components. The center of the bottom Z face was used as the datum point, and node locations are referenced from that point. Some dimensions are not exact, as approximations were used for ease of modeling. Most significant is the approximation used for the aluminum spacers. Curved shapes are problematic in SINDA 3D, because in order to get a reasonably accurate model, many nodes must be used. This slows down processing unnecessarily, and is avoided by modeling the spacers as rectangular bricks with the face area obtained from a correlation in Incropera for conduction shape factors (4th edition, P 171). The factor, or area used is $2D$, where D equals the diameter of the spacer shaft.

The interfaces between components were assumed to have a thickness of 0.1 inches for ease of modeling. SINDA 3D treats interfaces as separate elements, and the user must assign a value for the heat transfer coefficient of the interface.

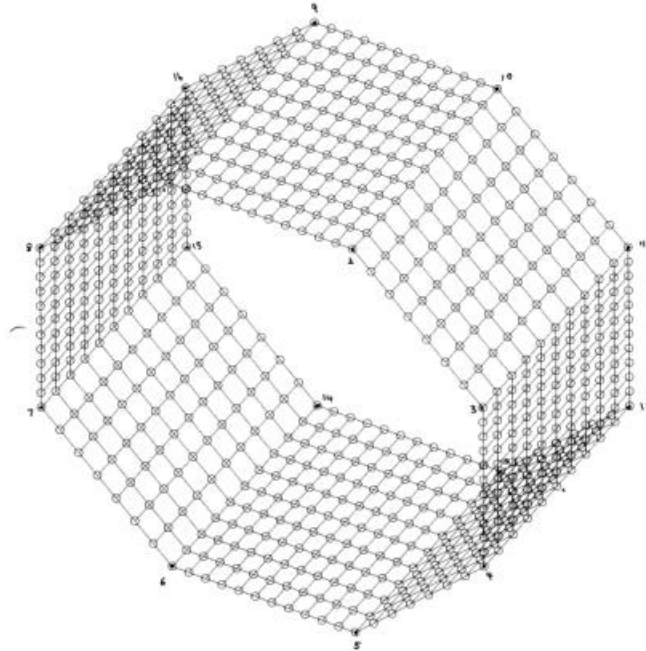
10.9.5.1 Node Locations and Construction Techniques

Bottom Z face	1. Nodes at (6.05,6.05,0) (-6.05,-6.05,0) Add plate diagonal, increment x,y = 11 2. Add nodes at (-3.54,8.55,0) (3.54,8.55,0) Add plate/select nodes. Use these two nodes, plus top left and right nodes of square section. Increment x=11, y=3 Repeat step 2 to complete octagonal shape.
Top Z face	Copy bottom plate with an offset of z=9.40 inches. These structures may need to be rebuilt in order to

	facilitate interfacing with the shell plates. Problems have been encountered with this interface, and have not been resolved by the end of Spring 99 semester.
Payload tray	1. Nodes at (4.95, 4.95, 3.2) (-4.95,-4.95,3.2) Add plate/diagonal, increment x,y = 9
Power tray	Copy payload tray with an offset of z = 3.00 inches
Spacers	1. Nodes at (3.85,3.85,0.1) (2.75,2.75,3.1) Add brick/diagonal, increment x=2, y=2, z=3 2. Rotate copy about z-axis, increment 3, angle 90 This creates bottom set of spacers. To generate top set, copy bottom set with a z offset of 6.2 inches.
Computer box	1. Nodes at (3,-2.5,0.1) (-3,2.5,1.6) Add brick/diagonal, increment x, y = 1 (increment may need to be increased)
Batteries	1. Nodes at (3.9,1.9,3.3) (-3.9,4.7,6.1) Add brick/diagonal, increment x,y = 1 2. Generate second battery by mirroring across x-z plane.
Charge controller	1. Nodes at (5.5,1.8,3.3) (-5.5,-1.8,5.8) Add brick/diagonal, increment x,y = 1
Camera box	1. Nodes at (4.3,4.3,7.60) (-4.3,-4.3,10.25) Add brick/diagonal, increment x,y=1 (increment will probably need to be increased to adequately model the thermal load of the DC converter)
Shell	1. Nodes at (-3.544, 8.555, 0) (3.544, 8.555, 9.843) Add plate/diagonal, increment x=10, y=11 2. Nodes at (8.555, 3.544, 0) (8.555, 3.544, 9.843) Add plate Node 1 -- pt 2 Node 2 – pt 10 Node 3 – pt 11 Node 4 – pt 3 Increment x=10, y=7 3. Nodes at (8.555, -3.544, 0) (8.555, -3.544, 9.843)

	<p>Add plate Node 1 – pt 3 Node 2 – pt 11 Node 3 – pt 12 Node 4 – pt 4 Increment x=10, y=11 4. Nodes at (3.544, -8.555 0) (3.544, -8.555, 9.843)</p> <p>Add plate Node 1 – pt 4 Node 2 – pt 12 Node 3 – pt 13 Node 4 – pt 5 Increment x=7, y=10 5. Nodes at (-3.544, -8.555, 0) (-3.544, -8.555, 9.843)</p> <p>Add plate Node 1 – pt 5 Node 2 – pt 6 Node 3 – pt 14 Node 4 – pt 13 (351) Increment x=11, y=10 6. Nodes at (-8.555, -3.544, 0) (-8.555, -3.544, 9.843)</p> <p>Add plate Node 1 – pt 6 Node 2 – pt 7 Node 3 – pt 15 Node 4 – pt 14 Increment x=7, y=10 7. Nodes at (-8.555, 3.544, 0) (-8.555 3.544, 9.843)</p> <p>Add plate Node 1 – pt 7 Node 2 – pt 8 Node 3 – pt 16 Node 4 – pt 15 Increment x=11, y=10 8. Add plate Node 1 – pt 8 Node 2 – pt 1 Node 3 – pt 9 Node 4 – pt 16 Increment x=7, y=7</p>
--	---

Refer to the following diagram for points that correlate to nodes



All of the above model elements have been generated as separate files, which can be merged into an integrated model to represent Spartnik. These model files are located on the Spartnik laptop in the Thermal directory, as well as on the desktop named Cassini, and are also saved on a Zip Drive disk, labeled Thermal, which is located in the filing cabinet in room E-272.

10.9.6 Thermal Transducer Test Results

Testing of the thermal transducers was performed to document the amount of instrument error inherent in each transducer. The basic procedure consisted of placing the transducers in a thermal test chamber at a given temperature and measuring the output voltage across a resistor of known value. This voltage was then used to calculate transducer output current, which is directly proportional to temperature. Then transducer temperature was compared to chamber temperature, providing a set of correction factors for the operational use of the transducers.

Results obtained show that the transducers, while reasonably accurate, vary somewhat in their output.

Procedure

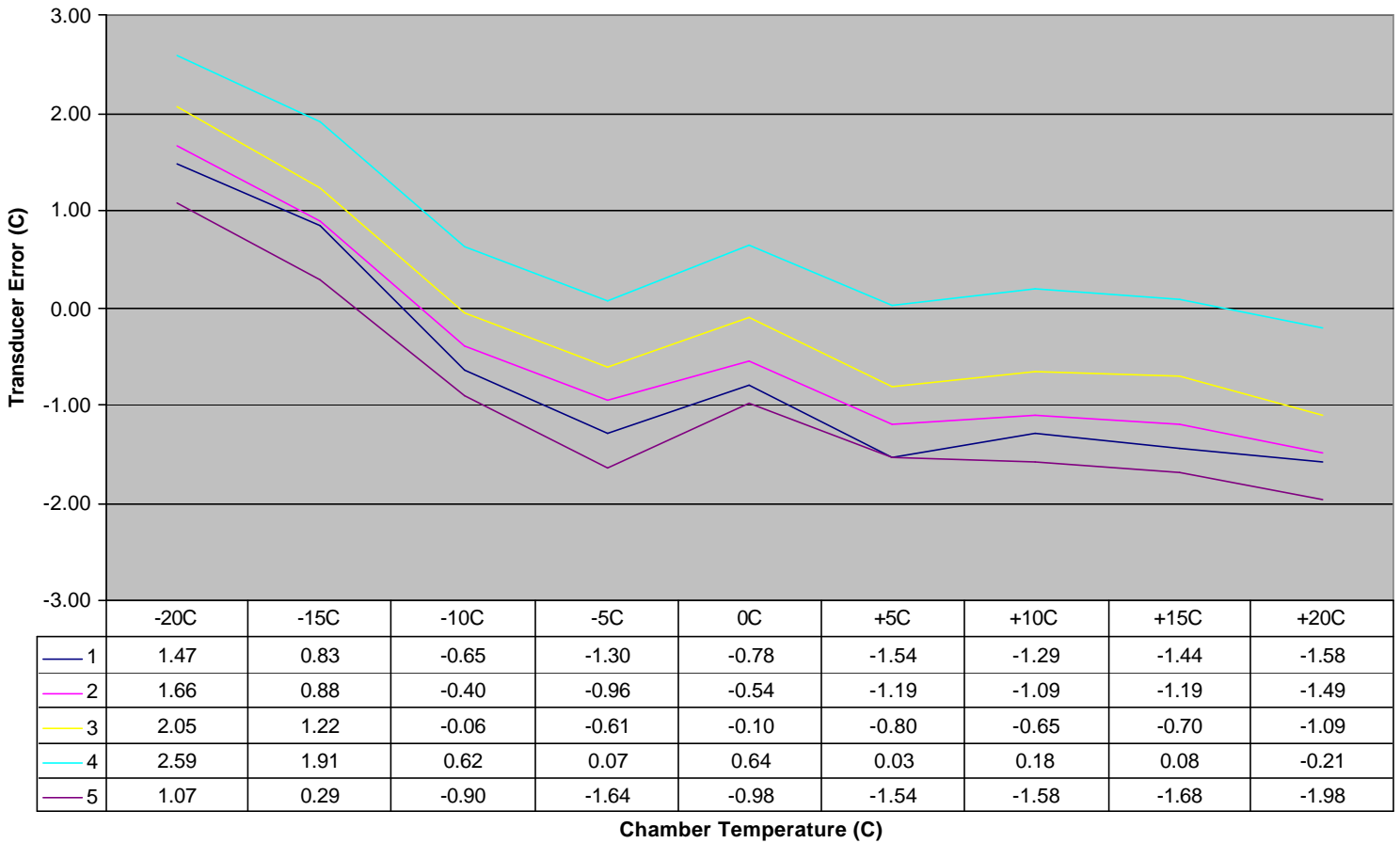
The transducers were placed on a breadboard and wired to a custom built switching circuit containing a precision 1.02K-ohm resistor. 7.2 volts DC was applied to the transducers, to approximate Spartnik bus voltage. The breadboard was placed inside a thermal test chamber, and the chamber was set to a range of temperatures, from -20°C to $+20^{\circ}\text{C}$. The test chamber was allowed to stabilize at each temperature setting until resistor voltage was observed to be constant. A voltage reading was then taken for each transducer. Transducer output current was calculated from this data, and is directly proportional to transducer temperature in degrees Kelvin, in a 1

micro-amp per degree Kelvin relationship. Transducer temperature was compared to chamber temperature and tabulated in both chart and graph form.

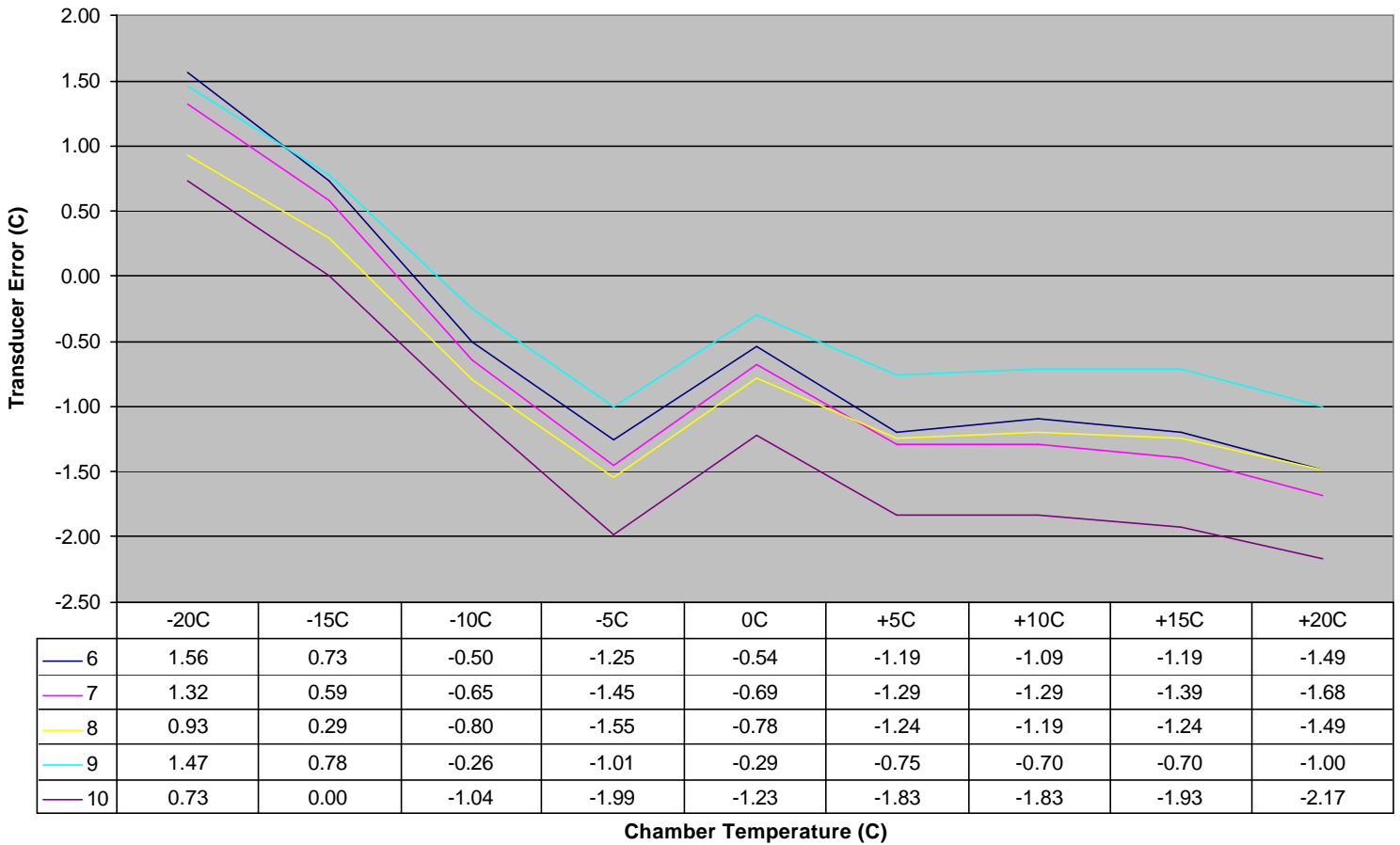
Results

Results are given in graphical and tabular form. Correction factors are obtained directly from either.

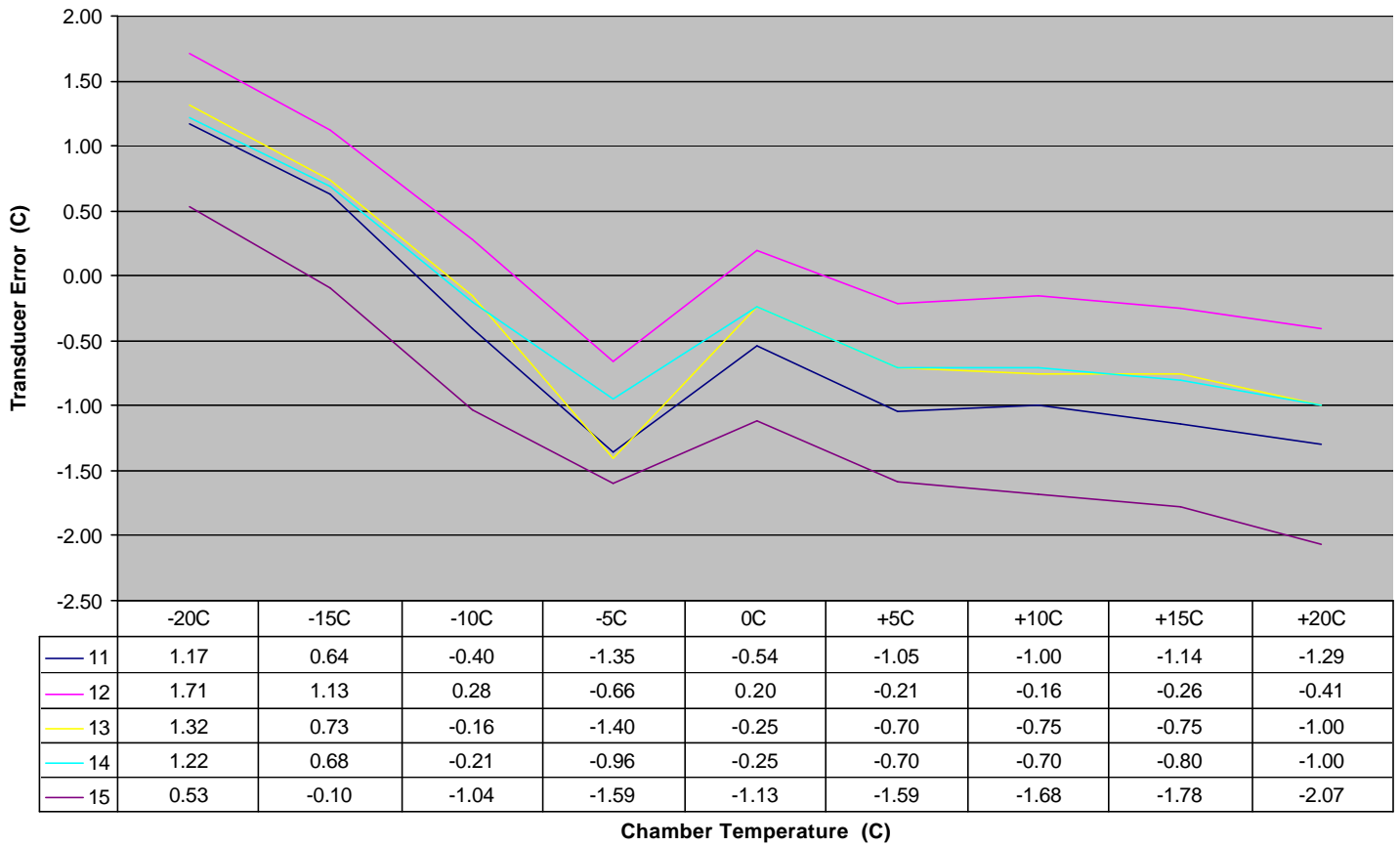
Transducer Error vs. Chamber Temperature (#1-5)



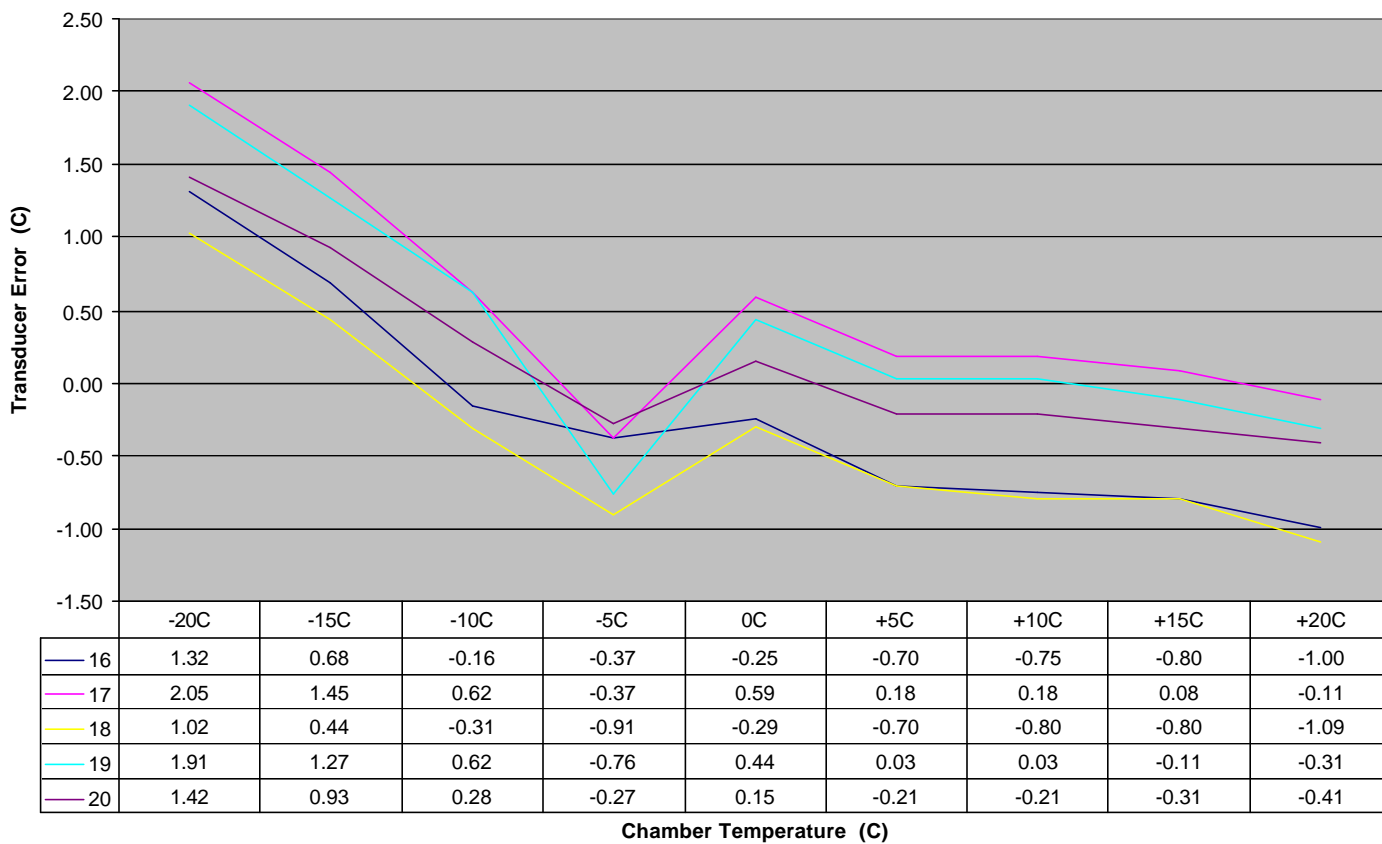
Transducer Error (#6-10)



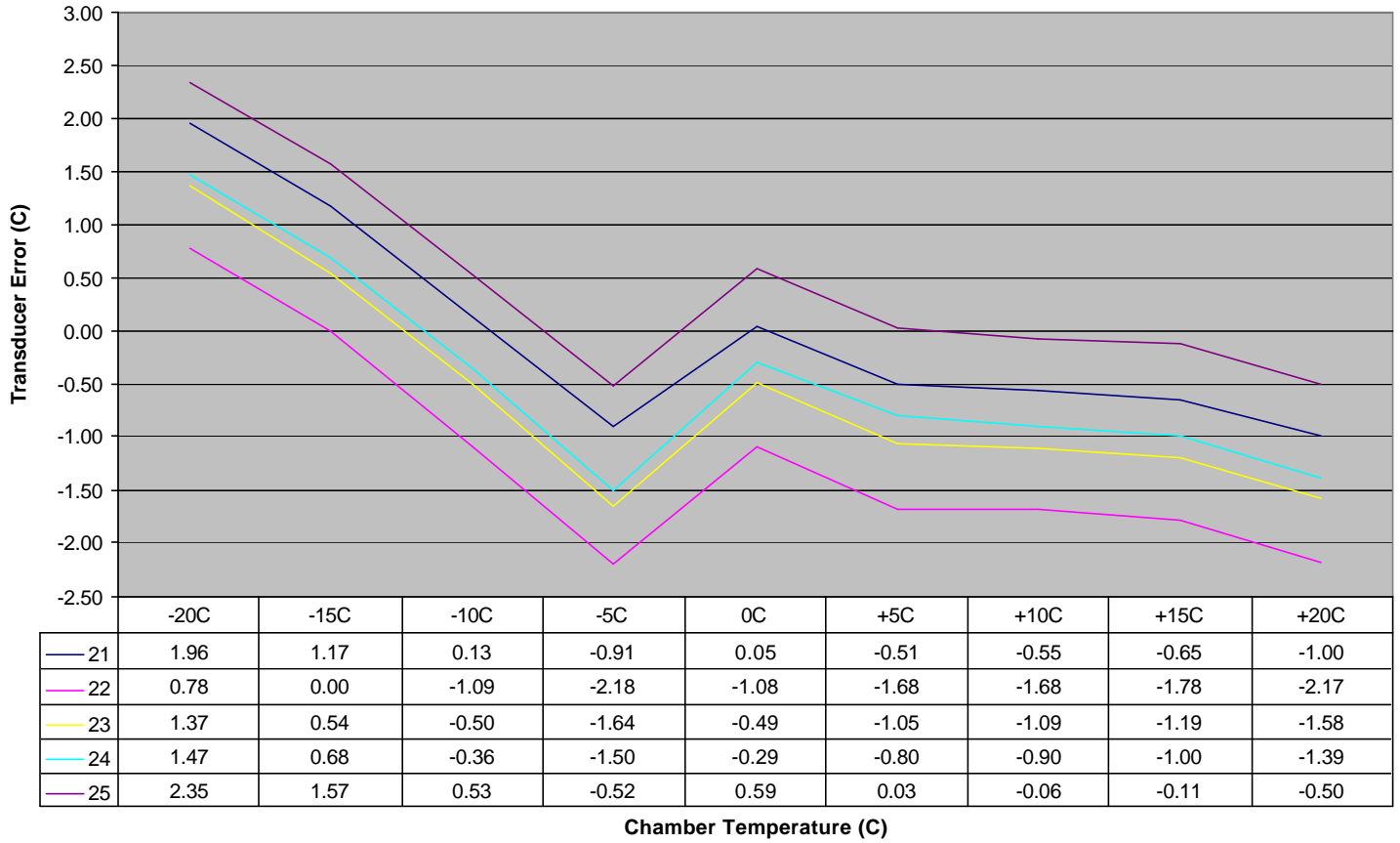
Transducer Error (#11-15)



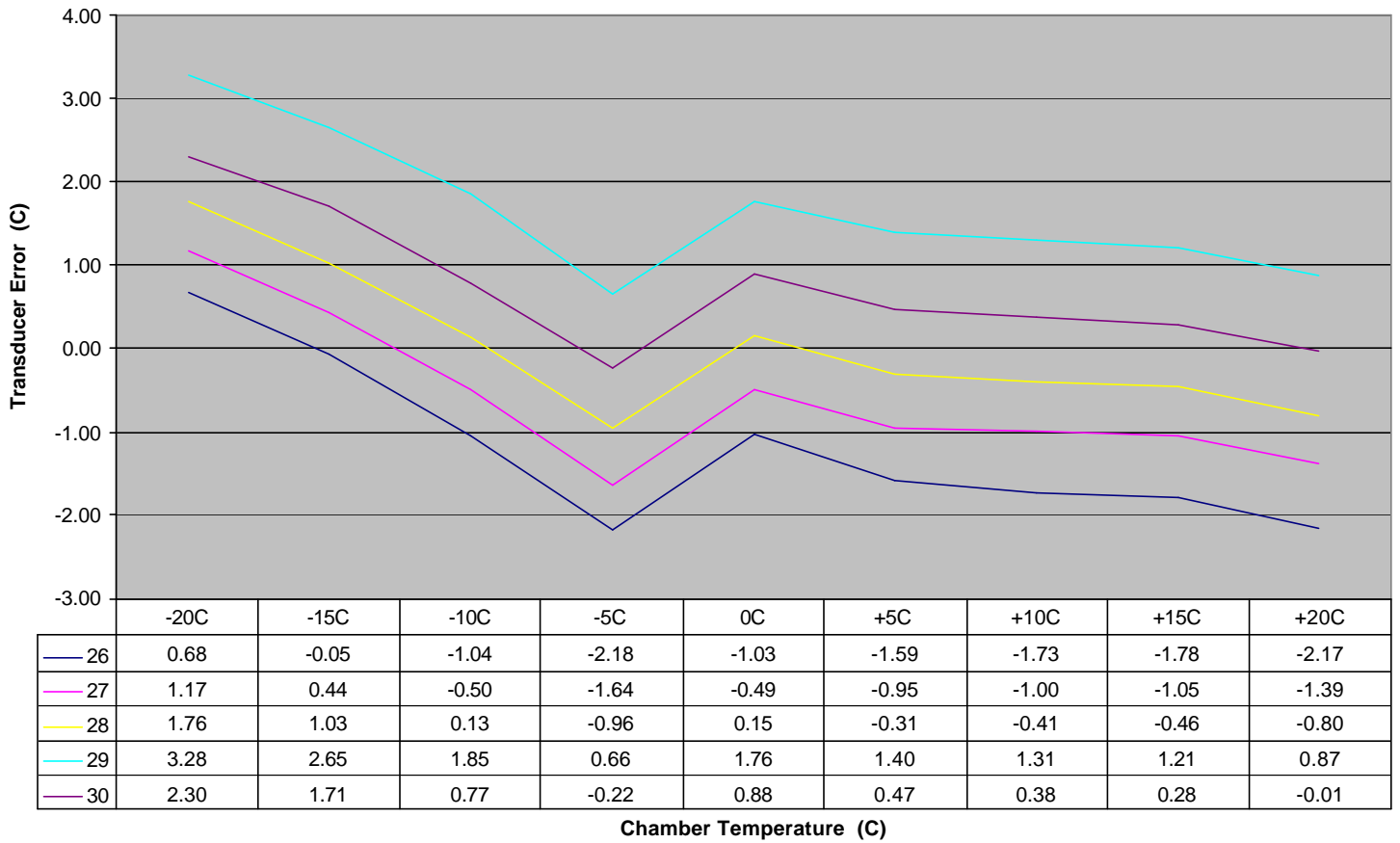
Transducer Error (#16-20)



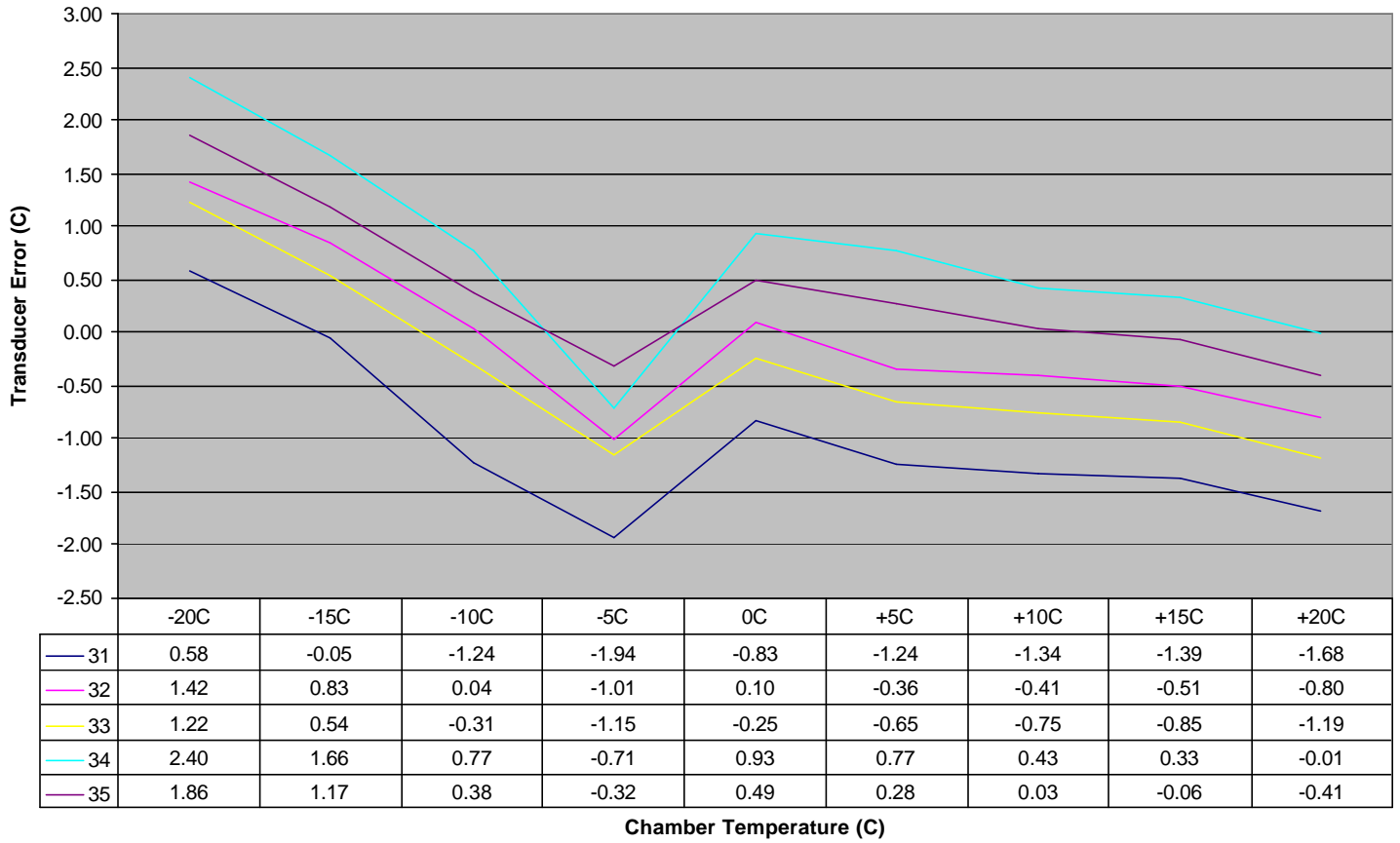
Transducer Error (#21-25)



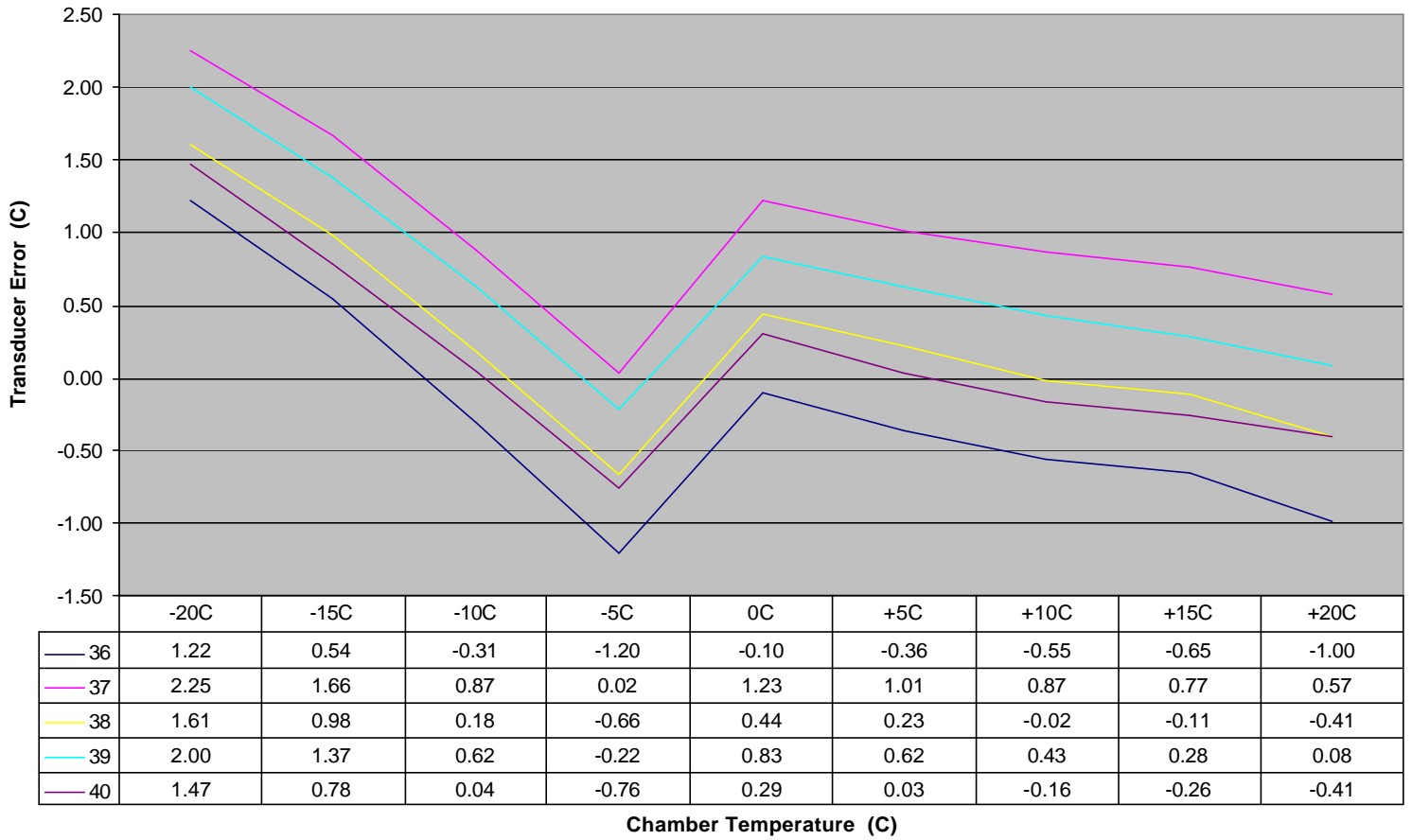
Transducer Error (#26-30)



Transducer Error vs. Chamber Temperature (#31-35)



Transducer Error (#36-40)



Apparatus

Equipment used is listed in the table below.

Equipment	Manufacturer	Model Number	Serial Number	Calibration date
Thermal Test Chamber (Test #1)	Tenney Environmental	T20C-3	25735-06	1/14/99 Due 1/14/00
Thermal Test Chamber (Test #2)	Tenney Environmental	T20C-3	25777-02	1/18/99 Due 1/18/00
Power Supply	Tektronix	TM502A	B017993	N/A
Digital Multimeter	Hewlett-Packard	3466A	1716-05241	N/A
Resistor				
Transducers	Analog Devices	AD590K	N/A	N/A

10.9.7 Glossary of Thermal Control Systems Terms and Acronyms:

The following is an alphabetical listing of all unusual terms and acronyms used in the report. Each item description is given in as close to English as possible.

“Absorbption- The process of converting radiation intercepted by matter to internal thermal energy.”¹³

“Absorbptivity- Fraction of the incident radiation absorbed by matter. ... Modifiers: *directional, hemispherical, spectral, total*”¹⁴

$$\alpha_{\lambda, \theta}(\lambda, \theta, \phi) \equiv \frac{I_{\lambda, i, \text{abs}}(\lambda, \theta, \phi)}{I_{\lambda, i}(\lambda, \theta, \phi)} \quad \text{spectral, directional absorptivity}$$

$$\alpha_{\lambda}(\lambda) \equiv \frac{G_{\lambda, \text{abs}}(\lambda)}{G_{\lambda}(\lambda)} \quad \text{spectral, hemispherical absorptivity}$$

$$\alpha \equiv \frac{G_{\text{abs}}}{G} \quad \text{total, hemispherical absorptivity}$$

Beta Angle- The beta angle of an orbit is defined as the minimum angle measured from the solar vector to the orbit plane. It is of use when determining the Earth-shadowing characteristics of the orbit.

“Blackbody- The ideal emitter and absorber. Modifier referring to ideal behavior. Denoted by the subscript b.”¹⁵

Conduction. Conduction is a mode of heat transfer where heat is moved by molecular interaction within a volume.

“HEAT ENERGY IS TRANSFERRED on a MOLECULAR basis and there is no motion of the MACROSCOPIC parts of the system relative to each other. The basis of all analyses and calculations of heat transfer by this mode is FOURIER’S LAW”¹⁶

Convection. Convection is a mode of heat transfer involving the motion one or more fluids.

“Heat transfer by convection occurs when a temperature difference exists between a solid surface and a moving fluid, with some degree of relative motion between them; the fluid may be either a gas, vapor, or liquid. Within this mode are (1) FORCED CONVECTION where the fluid is moved along by a pump, for example, and (2) NATURAL (or free) CONVECTION where the motion is produced by DENSITY GRADIENTS, which, in turn, are caused by TEMPERATURE GRADIENTS in the fluid. The analysis of convection is rather more complex than conduction as it involves both heat transfer and fluid flow. Fluid properties are important in this mode (density, thermal conductivity, viscosity, flow-velocity, etc.). The Energy Equation, Continuity of Flow Equation, Newton’s Second Law, with Fourier’s Law are involved in heat convection analyses. Heat transfer by convection frequently leads to complex problems.”¹⁷

“Diffuse - Modifier referring to the directional independence of the intensity associated with emitted, reflected, or incident radiation.”¹⁸

“Directional- Modifier referring to a particular direction. Denoted by the subscript θ ”¹⁹

“Directional Distribution- Refers to variation with direction.”²⁰

“Emission- The process of radiation production by matter at a finite temperature. Modifiers: *diffuse, blackbody, spectral*.”²¹

“Emissive power- Rate of radiant energy emitted by a surface in all directions per unit area of the surface, E (W/m^2). Modifiers: *spectral, total, blackbody*.”²²

“**Emissivity**- Ratio of the radiation emitted by a surface to the radiation emitted by a blackbody at the same temperature. ... Modifiers: *directional, hemispherical, spectral, total*”²³

$$\varepsilon_{\lambda, \theta}(\lambda, \theta, \phi, T) \equiv \frac{I_{\lambda, e}(\lambda, \theta, \phi, T)}{I_{\lambda, b}(\lambda, T)} \quad \text{spectral, directional emissivity}$$

$$\varepsilon_{\theta}(\theta, \phi, T) \equiv \frac{I_e(\theta, \phi, T)}{I_b(T)} \quad \text{total directional emissivity}$$

$$\varepsilon_{\lambda}(\lambda, T) \equiv \frac{E_{\lambda}(\lambda, T)}{E_{\lambda, b}(\lambda, T)} \quad \text{spectral, hemispherical emissivity}$$

$$\varepsilon(T) \equiv \frac{E(T)}{E_b(T)} \quad \text{total, hemispherical emissivity}$$

$$\varepsilon(T) \equiv \frac{\int_0^{\infty} \varepsilon_{\lambda}(\lambda, T) \cdot E_{\lambda, b}(\lambda, T) d\lambda}{E_b(T)}$$

Fourier’s Equations. Fourier’s Equations involve govern heat transfer in a solid. In differential form:

$$dQ = -k dA \frac{dT}{dx} \cdot d\theta$$

Where: dQ is the quantity of heat passing through area dA in period of time $d\theta$,
 k is the proportionality constant, thermal conductivity,
 dA is the differential area normal to the direction of heat flow.
 dT/dt is the temperature/length relationship.

“**Gray surface**- A surface for which the spectral absorbtivity and the emissivity are independent of wavelength over the spectral regions of surface irradiation and emission.”²⁴

Heat Transfer. Heat transfer is defined as energy in transit due to a temperature difference. Heat transfer also refers to the science of studying this phenomenon. See also conduction, convection and radiation.

“HEAT is ENERGY in TRANSITION under the influence of a TEMPERATURE DIFFERENCE and HEAT TRANSFER deals with the RATE at which HEAT ENERGY is TRANSFERRED. In THERMODYNAMIC processes TIME is not considered a pertinent factor as many processes involve heat transfer by means of

an infinitesimally small temperature difference, which, of course, implies an infinitely long time for the transfer to occur. In ACTUAL processes large temperature differences are used so that the required heat transfer can be accomplished in a reasonable length of time.

There are THREE MODES of Heat Transfer, (1) Conduction, (2) Convection, and (3) Radiation, but common to all of them is THE REQUIREMENT OF A TEMPERATURE DIFFERENCE”²⁵

“**Hemispherical**- Modifier referring to all directions in the space above a surface.”²⁶

“**Intensity**- Rate of radiant energy propagation in a particular direction, per unit area normal to the direction, per unit solid angle about the direction, I ($\text{W}/\text{m}^2 \text{ sr}$). Modifier: *spectral*”²⁷

Isothermal. A body is said to be isothermal when the temperature everywhere in the body is the same.

“**Irradiation**- Rate at which radiation is incident on a surface from all directions per unit area of the surface, G (W/m^2). Modifiers: *spectral, total, diffuse*.”²⁸

“**Kirchoff’s Law**- relation between emission and absorption properties for surfaces irradiated by a blackbody at the same temperature.”²⁹

Newton’s Law of Cooling. Newton’s Law of Cooling is the fundamental equation used in the calculation of convection heat transfer problems. In basic form:

$$Q = h \cdot dA \cdot \Delta T$$

Where: Q is the heat transfer rate
 h is the film or convection coefficient
 dA is the area of the heat transfer
 ΔT is the difference between the surface temperature and the bulk temperature of the fluid.

“**Plank’s Law**- Spectral distribution of emission from a blackbody.”³⁰

Radiation. Radiation is a heat transfer mode involving electromagnetic transport of thermal energy.

“Heat Transferred by this mode does not depend on any medium between the source and the sink (where the heat is deposited). All substances above zero absolute-temperature emit electro-magnetic radiation (electro-magnetic waves), ordinarily around the infra-red wave-lengths. These waves readily pass through a vacuum. Radiation heat transfer is based on the laws of Kirchoff, Lambert, and Stefan-Boltzmann.”³¹

“**Radiosity**- Rate at which radiation leaves a surface due to emission and reflection in all directions per unit area of the surface, J (W/m^2). Modifiers: *spectral, total*.”³²

“**Reflection**- The process of redirection of radiation incident on a surface. Modifiers: *diffuse, specular*.”³³

“**Reflectivity**- Fraction of the incident radiation reflected by matter. Modifiers: *directional, hemispherical spectral, total*.”³⁴

“**Semitransparent**- Refers to a medium in which radiation absorption is a volumetric process.”³⁵

“**Solid angle**- Region subtended by an element of area on the surface of a sphere with respect to the center of the sphere, ω .”³⁶

“**Spectral**- Modifier referring to a single-wavelength (monochromatic) component. Denoted by the subscript”³⁷

“**Spectral distribution** - Refers to variation with wavelength.”³⁸

“**Specular**- Refers to a surface for which the angle of reflected radiation is equal to the angle of incident radiation.”³⁹

“**Stefan-Boltzmann law** - Emissive power of a blackbody.”⁴⁰

Thermal Contact Resistance. Thermal contact resistance is the resistance to heat flow developed due to an imperfect interface between two objects. It is defined as:

$$R''_{t,c} = (T_A - T_B) / q''_x$$

“**Thermal radiation** - Electromagnetic energy emitted by matter at a finite temperature and concentrated in the spectral region from approximately 0.1 to 100 μm .”⁴¹

“**Total** - Modifier referring to all wavelengths.”⁴²

“**Transmission** - The process of thermal radiation passing through matter.”⁴³

“**Transmissivity** - Fraction of the incident radiation transmitted by matter.”⁴⁴

“**Wien’s Law** - Locus of the wavelength corresponding to peak emission by a blackbody.”⁴⁵

10.9.8 Materials and Company Contact Information

In order to facilitate future contact with suppliers if needed, the following list of materials purchased and the manufacturer contact information is tabulated below.

MATERIAL	MANUFACTURER/ DISTRIBUTOR	ADDRESS	PHONE	CONTACT NAME
Thermally Conductive Grease	Nu-Sil	Carpinteria, CA 9		
Thermally Conductive Epoxy		Hayward, CA 9		
Epoxy for Honeycomb Structure Inserts	Packaging Systems, Inc		(818) 246-5568	Steve Gray
Inserts	Shur-Lock			Robert Skidmore

Additionally, in researching low-outgassing materials, a website maintained by NASA's Goddard Space Flight Center proved invaluable. The address is [HTTP://misspiggy.gsfc.nasa.gov/og](http://misspiggy.gsfc.nasa.gov/og).

¹ Atlas Mission Planner's Guide, General Dynamics Commercial Launch Services, March 1989

² Gilmore, pg. 4-5

-
- ³ Gilmore, pg. 9-8.
 - ⁴ Gilmore, pg. 9-30
 - ⁵ Gilmore, pg. 9-32
 - ⁶ Incropera, pg. 27
 - ⁷ Incropera, pg. 107
 - ⁸ Incropera, pg. 86
 - ⁹ Incropera, pg. 6
 - ¹⁰ Incropera, pg. 7
 - ¹¹ Incropera, pg. 10
 - ¹² Incropera, pg. 711-712
 - ¹³ Incropera, pg. 756
 - ¹⁴ Incropera, pg. 756
 - ¹⁵ Incropera, pg. 756
 - ¹⁶ Clothier, Heat Transfer Handout, pg. 1
 - ¹⁷ Clothier, Heat Transfer Handout, pg. 1
 - ¹⁸ Incropera, pg. 756
 - ¹⁹ Incropera, pg. 756
 - ²⁰ Incropera, pg. 756
 - ²¹ Incropera, pg. 756
 - ²² Incropera, pg. 756
 - ²³ Incropera, pg. 756
 - ²⁴ Incropera, pg. 757
 - ²⁵ Clothier, Heat Transfer Handout, pg. 1
 - ²⁶ Incropera, pg. 757
 - ²⁷ Incropera, pg. 757
 - ²⁸ Incropera, pg. 757
 - ²⁹ Incropera, pg. 757
 - ³⁰ Incropera, pg. 757
 - ³¹ Clothier, Heat Transfer Handout, pg. 1
 - ³² Incropera, pg. 757
 - ³³ Incropera, pg. 757
 - ³⁴ Incropera, pg. 757
 - ³⁵ Incropera, pg. 757
 - ³⁶ Incropera, pg. 757
 - ³⁷ Incropera, pg. 757
 - ³⁸ Incropera, pg. 757
 - ³⁹ Incropera, pg. 757
 - ⁴⁰ Incropera, pg. 757
 - ⁴¹ Incropera, pg. 757
 - ⁴² Incropera, pg. 757
 - ⁴³ Incropera, pg. 757
 - ⁴⁴ Incropera, pg. 757
 - ⁴⁵ Incropera, pg. 757